

1974

Heterogeneous nucleation in the crystallization of isotactic polypropylene from the melt.

Beata J. Abbs

University of Massachusetts Amherst

Follow this and additional works at: <https://scholarworks.umass.edu/theses>

Abbs, Beata J., "Heterogeneous nucleation in the crystallization of isotactic polypropylene from the melt." (1974). *Masters Theses 1911 - February 2014*. 1273.

Retrieved from <https://scholarworks.umass.edu/theses/1273>

This thesis is brought to you for free and open access by ScholarWorks@UMass Amherst. It has been accepted for inclusion in Masters Theses 1911 - February 2014 by an authorized administrator of ScholarWorks@UMass Amherst. For more information, please contact scholarworks@library.umass.edu.

UMASS/AMHERST



312066 0015 7520 9

HETEROGENEOUS NUCLEATION IN THE CRYSTALLIZATION OF
ISOTACTIC POLYPROPYLENE FROM THE MELT

A Thesis Presented By

Beata J. Abbs

Submitted to the Graduate School of the
University of Massachusetts in partial
fulfillment of the requirements for the degree of

MASTER OF SCIENCE

August

1974

Polymer Science and Engineering

HETEROGENEOUS NUCLEATION IN THE CRYSTALLIZATION OF
ISOTACTIC POLYPROPYLENE FROM THE MELT

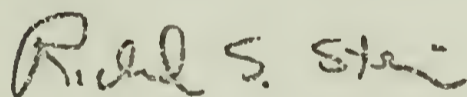
A Thesis Presented By

Beata J. Abbs

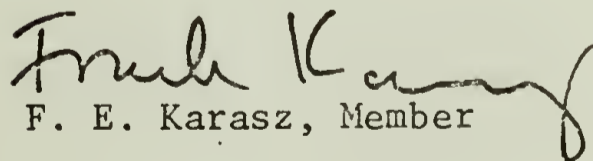
Approved as to style and content by:



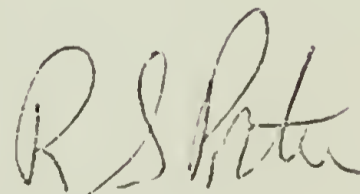
F. P. Price, Chairman of Committee



R. S. Stein, Member



F. E. Karasz, Member



Roger S. Porter, Head of Department

August 1974

Dedicated to D.O.D. and D.O.M.

ACKNOWLEDGEMENTS

My deepest thanks go to my thesis advisor, Professor Fraser P. Price, whose generous share of wisdom and sense of humor made working for him a pleasant and rewarding experience. I am grateful, also, for the ideas and constructive criticism offered by my other committee members, Professors Richard S. Stein and Frank E. Karasz.

Thanks go to Dr. A. M. Chatterjee for the many helpful discussions and to Professor I. C. Sanchez for his thoughts on the probability treatment of Chapter II. I cannot fail to mention Dr. Ashok Misra, Mr. Mark Hoffman, and Mr. Michael Wolkowicz, whose day-to-day help was readily available and often used.

TABLE OF CONTENTS

I. INTRODUCTION 1

II. BACKGROUND 2

III. EXPERIMENTAL PROCEDURE 19

IV. RESULTS 29

V. DISCUSSION 43

VI. CONCLUSIONS 56

VII. SUGGESTIONS FOR FURTHER RESEARCH 58

REFERENCES 59

TABLES 64

FIGURE CAPTIONS 82

FIGURES 86

APPENDIX A 123

CHAPTER I

INTRODUCTION

The spherulitic texture of a polymer greatly influences the physical and mechanical properties of that polymer. A fine, homogeneous texture has been found to result in certain polymers when additives are present which enhance nucleation. Nucleating agents, then, are a means of controlling the nucleation, and hence the texture and final properties, of a polymer. While the process of nucleation is very important, it is poorly understood. It is hoped that this study clarifies some of the mystery surrounding the nucleation process.

In this study the isothermal crystallization of isotactic polypropylene (iPP) in the presence of isotactic polystyrene (iPS) is studied in depth. It has been shown that iPP transcrystallizes against iPS in the crystallization temperature range of 120-130°C.⁴⁵ The temperature range investigated here includes this range in which transcrystallinity results, plus the range 130-140°C, in which a spherulitic morphology results. The temperature-dependence of the nucleation and growth rates is found, which gives information about the surface energies involved. Both amorphous and crystalline iPS substrates were used to determine if nucleating ability correlates with crystallinity of the substrate. In addition, the nucleating power of an oriented substrate was compared to that of an unoriented one. Aside from the influence of the substrate properties, the effect of varying the time and temperature of melting of the iPP was found. Finally, repeated runs were done at certain temperatures to determine if nuclei tended to reappear at the same positions on the substrate or in the same order in time.

C H A P T E R I I

BACKGROUND

Experimental

In the past much effort was expended in deriving theories of homogeneous nucleation in a liquid-solid phase transition. A good deal of evidence was amassed, however, that showed heterogeneous nucleation to be the dominating influence in most bulk crystallizations.^{1,2} It was found that heterogeneous nuclei became activated at much lower supercoolings than the homogeneous variety.^{3,4} The presence, then, of a few heterogeneous nuclei could lead to the transformation of an entire sample before the temperature was even reached at which homogeneous nuclei could come into play. The understanding and even control of these heterogeneous nuclei had wide implications in polymer crystallization and many studies were subsequently devoted to this end. These are reviewed in the following sections.

Nucleating Agents. The effect of various nucleating agents present as a dispersed phase within a crystallizing polymer has been studied quite extensively. Often low molecular weight organic compounds were used as the nucleants. Their effect was generally to reduce the induction time prior to nucleation and to increase the nucleation rate, thus increasing the overall rate of crystallization.⁵ In addition the average spherulite size was reduced, leading to a more homogeneous structure and more desirable mechanical properties.

Last⁶ found that there were three requirements for a good nucleating agent:

- 1) The additive must be crystallizable.
- 2) The melting point of the additive must exceed that of the base polymer.
- 3) The cohesive energy per chain unit of the two should be approximately equal. This governs the dispersibility of the additive in the polymer.

He found, as did Inoue⁵, that the differences in crystallinity and density between nucleated and non-nucleated polymers were slight.

Kargin and coworkers used microscopic and density techniques to study the effect of nucleants on the crystallization kinetics and morphology of various polymers.⁷⁻¹⁵ They found that the size and number of the added nucleants determined the resultant polymer morphology.⁸ The organic solids used had melting points above those of the crystallizing polymer, were insoluble in it, and did not chemically react with it.⁷ Particle shape was shown to exert a great influence on the morphology. That is, when alizarin in the form of acicular crystals was added to polypropylene (PP), the resultant morphology was ribbonlike with high nucleation densities along the alizarin needles.⁷ Although not recognized as such, the structure appeared to be transcrystalline, a phenomenon to be discussed later. Isotactic polystyrene (iPS) was seen to be an active nucleator of PP. This "primer action," as it was called, disappeared, however, when the mixture was heated above the melting point of the iPS.⁷ Mechanical tests revealed that polymers having nucleating agents added exhibited increased mechanical strength and deformability over the entire range of temperatures tested.^{9,11,13,14}

In another study Kargin, et al.¹⁰ attempted to correlate nucleating ability with lattice parameter match, wettability, and dimensions

of the nucleant. They found that a match between neither the lattice parameters nor the crystal structure of the nucleating agent and the polymer were necessary to insure good nucleating ability. It was found to be important, however, that the polymer wet the surface of the nucleant. In addition, the size of the nucleating particle had to be at least some critical dimension before good nucleating action would occur. This critical dimension decreased as the crystallization temperature decreased.

A mechanism was proposed by Kargin and coworkers to explain the preferred nucleation at included particles.¹² The strain about these inclusions could lead to micro-orientation of the polymer chains which in turn could become the primary nuclei for further crystallization, it was hypothesized. Justification was thus given for the nucleating action of gas and liquid bubbles within the polymer. The magnitude of the stresses, and hence the nucleating power, depends on the size of the nucleant particles, the nature of the polymer and the nucleant, and their interaction. A similar orientation mechanism had been proposed earlier by Keller.^{16,17}

Beck and Ledbetter¹⁸ explored the effect of several nucleants on PP crystallization by means of differential thermal analysis (DTA). A system containing an active nucleant was found to crystallize at a lower supercooling than the pure polymer. They found that a broad spectrum of nucleating ability existed and that the process was very selective. They also found that artificial nucleants served to increase the rate of nucleation, but to leave the growth rate of individual spherulites unchanged. The effect, then, is to increase the overall rate of crystallization. In another study using the same technique,

Beck¹⁹ found that the molecular weight of the PP made no difference in the response to addition of nucleating agents. Beck²⁰ later proposed a model compound that would promote PP crystallization. It was composed of two parts: an organic, solubizing group and a polar, insolubizing group. The organocarboxylic acid salts fit this model, but even within this group a large variation in nucleating ability was found to exist. The conclusion drawn was that nucleating ability does not seem to correlate with any one property or structural feature, and is probably a function of many properties acting at once.

Rybnikar²¹ used a variety of techniques (density, x-ray diffraction, microscopic measurements) to compare the structures of normal and nucleated PP. The primary difference between the two was the number of spherulites, the nucleated sample having 100 times as many spherulites as the control sample. The spherulitic growth rate remained the same. It was further determined that both samples exhibited an identical dependence of crystallinity on crystallization temperature. The PP with the additive nucleated at higher temperatures, however, and was thus able to develop a higher degree of crystallinity for the same heat treatment. In a similar manner, the nucleated sample would crystallize much faster than the control sample at the same crystallization temperature. In a further study Rybnikar²² found that different commercial isotactic polypropylenes (iPP) showed different responses to identical nucleating agents. He was unable to make any general correlations between nucleating ability and structure, molecular weight, ash content, or atactic fraction of the iPP. He concluded that the role of nucleating agents was secondary and that they merely activated heterogeneities already present in the

melt by improving the wetting of the heterogeneity by the molten polymer. This idea was carried further²³ when he proposed that minute bubbles of gas or vapor were the real nucleation centers, their existence being promoted by added nucleants or decomposition products.

Binsbergen²⁴ studied the nucleation of polyolefins and found that a good nucleant must have a higher melting point than the polymer and must not be soluble in or react with the polymer. Most good nucleants he studied were crystalline. He was able to rule out epitaxial growth as a possible mechanism because active nucleation was found to occur through an increasing homologous series wherein the lattice dimensions were gradually changing. He, like Beck, proposed a two-part model compound for a good nucleant. It consisted of a non-polar, hydrocarbon portion that was a good solvent for the polymer, plus a polar, insoluble portion. He found that the method of dispersing the nucleant in the polymer had a large effect on its nucleating ability.

Nucleating agents can be used to impart tailor-made morphology and structure to the crystallizing polymer. They allow good control of nucleation density and the resultant homogeneity of the polymer. Spherulitic texture, which can be regulated by nucleants, determines transparency,⁶ opacity,²⁵ and surface gloss.²⁴ Nucleating agents can decrease void formation in injection-molded parts, and increase the rate of crystallization, leading to shorter processing times.²⁴ In addition, various mechanical properties can be improved by a finer spherulitic texture, including impact strength,²⁴ tensile strength,^{9,11,13-15} elongation at break,^{7,9,14,15,26,27} flexural modulus,²⁷ and upper yield point.²⁷

In summary, nucleating agents allow crystallization of polymers at lower supercoolings, thus increasing the overall rate of crystallization. Despite much work in the area, the mechanism of heterogeneous nucleation remains unresolved. It is thought that a good nucleant must be a solid, crystalline material that is wet by the polymer and that does not react with the polymer. The size, shape, and concentration of the nucleant, as well as the melting and crystallization treatment of the polymer, all affect the resultant morphology.

Transcrystallinity. When a polymer melt crystallizes against a surface of strong nucleating ability, a special morphology is seen to develop. It consists of closely-spaced nuclei, whose growth laterally is limited by impingement with neighboring nuclei, but whose growth normal to the surface is unhindered. Such a morphology is transcrystalline, a term first applied to metal grains that grew preferentially away from the mold surface.²⁸ The phenomenon was first reported in polyurethane and polyamide systems by Jenckel, Teege, and Hinrichs.²⁹ It was shown that the structure of the transcrystalline region was spherulitic in character, the structure along a spherulite radius and normal to the surface of a transcrystalline region being the same. The final thickness that this transcrystalline region attained was found to vary inversely with the cooling rate. Soon after, Keller^{16,17} reported a morphology much like the transcrystalline region which he termed "row orientation." He saw it form along cracks, edges, and flow lines in polyethylene (PE), polyamide, and polyethylene terephthalate (PET). The frequency of these row structures was greatest in PE and least in PET.

Like Jenckel, et al. he found the same structure existed along a spherulite radius as perpendicular to the row of nuclei.

Barriault and Gronholz³⁰ introduced the idea that a temperature gradient was necessary to the formation of a transcrystalline region, and that rapid quenching was more apt to produce a temperature gradient, and hence a transcrystalline region. Burnett and McDevit³¹ found that transcrystallinity was the cause of the "gray field" preceding spherulite growth that had evidently confounded polymer microscopists for some time.

X-ray crystallographic analysis of these transcrystalline regions in PE by Keller,¹⁶ and later by Eby,³² Gieniewski and Moore,³³ and Hara and Schonhorn,³⁴ revealed that the long axis, the b axis, of the unit cell was oriented perpendicular to the nucleating surface. The a and c axes were oriented at random in the plane of the nucleating surface. Hence the transcrystalline region was found to consist of lamellae packed with their long dimension normal to the surface. Eby³² found that diffusion through a transcrystalline region was augmented along the lamella direction. He, like Barriault and Gronholz,³⁰ felt that a temperature gradient was the cause of transcrystalline formation.

Up to this point, PE had been made to transcrystallize against high-energy surfaces such as metals, metal oxides, and alkali halide crystals.³⁵⁻³⁷ This led Schonhorn^{26,38} and coworker³⁹ to claim that a high energy surface was necessary to the formation of a transcrystalline region.

Fitchmun and Newman^{40,41} soon showed, however, that neither a high energy surface, nor a temperature gradient at that surface were necessary to the development of transcrystallinity. PP was crystallized

against an aluminum oxide substrate, a high-energy substrate, and the morphology was spherulitic. That same PP when crystallized against PET, a low-energy surface, was transcrystalline. In addition to the nature of the mold surface the melt temperature, crystallization temperature, and the cooling rate all determine the surface morphology, they found. Transcrystallinity was favored by rapid cooling rates and a high crystallization temperature.

Hobbs⁴² has done some interesting work on the heterogeneous nucleation of iPP against graphite fibers. Transcrystallinity was seen to develop against the fibers containing relatively large graphite basal planes which are highly oriented. Regular spherulitic morphology (no preferred nucleation) occurred against the fibers containing much smaller and highly disoriented basal planes. This suggests that some minimum area is necessary for polymer adsorption and enhanced nucleation. In another study⁴³ this delicate dependence on substrate structure was seen for two different carbon films, one amorphous and one replicated directly on an iPP film. The carbon replica induced transcrystallinity, whereas the amorphous carbon film did not. A similar effect was recently demonstrated with etched and unetched copper wire.⁴⁴

Chatterjee⁴⁵ has characterized a number of polymer systems as to their ability to form transcrystalline regions. He confirmed the selectivity of the process and found that a range of nucleating ability exists. The resultant morphology could be transcrystalline, mixed (transcrystalline plus spherulitic) or neither, a case in which spherulitic growth at the surface was actually retarded. Many systems were found to transcrystallize only when quenched to within a certain

crystallization temperature range. Neither similarity in crystal structure of the substrate and nucleating polymer nor surface energy of the substrate correlated with nucleating ability, in agreement with Kargin, et al.¹⁵ Crystallinity of the substrate was found to be a necessary but not sufficient condition for inducing transcrystallinity. Chatterjee also concluded that a fixed number of nucleation sites exist on the surface of the nucleating substrate, which can become active in succession and lead to nucleation having both homogeneous and heterogeneous character.

Because of the oriented, lamellar structure, the physical properties of the transcrystalline region differ greatly from those of the bulk. Several studies of the mechanical response of transcrystalline PE have been carried out.⁴⁶⁻⁴⁸ It was found that the dynamic Young's moduli, as well as $\tan \delta$, each increased with increasing transcrystallinity at all temperatures tested. The response of transcrystalline PE has been successfully modelled by Wang.⁴⁹

In a further study⁵⁰ of transcrystalline PE the improved mechanical properties were confirmed over the temperature range $-160^{\circ}\text{C} - 120^{\circ}\text{C}$. It was found that the crystallinity of the bulk exceeded that of the transcrystalline region. Kwei, et al.⁴⁷ had previously found no difference in the crystallinity between the transcrystalline and normal regions, and Hara and Schonhorn³⁴ subsequently found the opposite.

The surface properties, as one would expect, have been shown to change upon transcrystallization. Thus transcrystalline PE has a higher adhesion,³⁵ as do certain polymer-fiber bonds in composites.⁵¹ Transcrystalline films have also been shown to exhibit lower contact angles

with various liquids, that is, they are more wettable.^{26,52,53}

Schonhorn⁵² has attributed this to a difference in density at the surface and has developed a modified Fowkes-Young equation to explain the behavior.

In summary, transcrystallinity is a result of enhanced nucleation at a substrate, leading to spherulitic lamellae packed normal to the substrate plane. Transcrystalline regions offer improved mechanical and physical properties. The occurrence of transcrystallinity in a polymer-substrate pair is very selective and depends on crystallization temperature and cooling rate, as well as the nature of the pair. It has not been found to correlate with surface energy or crystal structure.

Theoretical

Heterogeneous Nucleation. The Turnbull-Fisher equation⁵⁴ for homogeneous nucleation of a daughter phase, β , in a mother phase, α , is

$$I = \frac{NkT}{h} \exp[-(\Delta F^* + \Delta f^*)/kT] \quad (1)$$

where I = nucleation rate in nuclei/mole/second

Δf^* = free energy barrier to short-range diffusion across the α - β interface

ΔF^* = free energy of formation of a critical-sized primary nucleus.

When modified for heterogeneous nucleation^{55,56} the form of the equation remains the same, although the pre-exponential factor changes, as does ΔF^* .

To determine ΔF^* consider a length of polymer chain nucleating against a substrate, S. The model is shown in Figure 1. Let σ_e be the fold surface energy, σ be the side surface energy in contact with the melt, σ_c be the substrate-polymer interfacial energy, and σ_m be the substrate-melt interfacial energy. The free energy of formation for incoherent nucleation is given by

$$\Delta F = -abl \Delta F_v + 2ab\sigma_e + 2bl\sigma + al\Delta\sigma \quad (2)$$

where $\Delta\sigma = \sigma + \sigma_c - \sigma_m$

Differentiating with respect to a, b, and l, setting the derivatives equal to zero, and solving yields the following dimensions of the critical-sized nucleus:

$$a^* = \frac{4\sigma}{\Delta F_v}$$

$$b^* = \frac{2\Delta\sigma}{\Delta F_v}$$

$$l^* = \frac{4\sigma_e}{\Delta F_v}$$

When used in Equation 2, above, these dimensions give:

$$\Delta F^* = \frac{16\sigma\sigma_e \Delta\sigma}{(\Delta F_v)^2}$$

Using Equation 1 and the relation $\Delta F_v = \frac{\Delta H_v \Delta T}{T_m}$ yields:

$$I = \frac{NkT}{h} \exp\left(-\frac{\Delta f^*}{kT}\right) \exp\left[\frac{-16\sigma\sigma_e \Delta\sigma T_m^2}{kT(\Delta T)^2 (\Delta H_v)^2}\right] \quad (3)$$

The temperature dependence lies primarily in the last exponential term. Thus a plot of the logarithm of the nucleation rate versus $\frac{1}{T(\Delta T)^2}$ will have a slope that is related to the product $\sigma\sigma_e \Delta\sigma$.

Probability Treatment. It has been proposed that heterogeneous nuclei are discrete. In order to investigate this as well as the heirarchy of activity of heterogeneous nuclei, consider four successive crystallizations of iPP against the same iPS substrate. Individual sites were identified and the order of appearance of the nuclei in each run was recorded. By random nucleation one would expect that a nucleus might reappear at the same site in subsequent runs if the number of nuclei were large with respect to the number of sites. What then is the random probability for reoccurrence of a nucleus at the same site? Also, the order of appearance at a given site might be the same in two runs, and the random probability for this will be calculated.

Consider a surface with x total nucleation sites on it. During the first run, n of these sites become nuclei. During the second and successive runs a different set of n sites become nuclei. What is the random probability that a site will become a nucleus every time? What is the random probability that a site will become a nucleus every time except once, and so on?

For a completely random situation the probability that a site will become a nucleus is $\frac{n}{x}$. The probability that it will not is $1 - \frac{n}{x}$. The

probability that it will become a nucleus in the second run is $(\frac{n}{x})^2$, since the two events are considered independent. By extending this the probability that a given site will be a nucleus four times in a row is:

$$P_4 = (\frac{n}{x})^4$$

The probability that a given site will become a nucleus three out of four times is the probability that it will be a nucleus three times multiplied by the probability that it will not be a nucleus once. There is a multiplicity of four since it does not matter in which of the four runs the site does not nucleate:

By analogy:

$$P_3 = 4(\frac{n}{x})^3 (1 - \frac{n}{x})$$

$$P_2 = 6(\frac{n}{x})^2 (1 - \frac{n}{x})^2$$

$$P_1 = 4(\frac{n}{x})^1 (1 - \frac{n}{x})^3$$

$$P_0 = (\frac{n}{x})^0 (1 - \frac{n}{x})^4 = (1 - \frac{n}{x})^4$$

$$P_4 + P_3 + P_2 + P_1 + P_0 = 1$$

We do not recognize a site unless a nucleus forms at that point at least once. Therefore, P_0 is zero. The total probability must still equal one.

$$P_1' + P_2' + P_3' + P_4' = 1$$

where:

$$P_1' = \frac{P_1}{P} = \text{Probability that a site nucleates once out of four runs.}$$

$$P_2' = \frac{P_2}{P} = \text{Probability that a site nucleates twice out of four runs.}$$

$$P_3' = \frac{P_3}{P} = \text{Probability that a site nucleates three times out of four runs.}$$

$$P_4' = \frac{P_4}{P} = \text{Probability that a site nucleates four times out of four runs.}$$

and:

$$\begin{aligned} P &= P_1 + P_2 + P_3 + P_4 \\ &= 1 - P_0 \\ &= 1 - \left(1 - \frac{n}{x}\right)^4 \\ &= \frac{4n}{x} - \frac{6n^2}{x^2} + \frac{4n^3}{x^3} - \frac{n^4}{x^4} \end{aligned}$$

Now let us consider the order in which these nuclei appear. During each run the n nuclei appear in a given order from 1 to n . Consider a particular site. In one run a nucleus formed at that site after $i-1$ nuclei had already formed. The site under consideration had the i^{th} nucleus. In another run a nucleus formed at that same site after $j-1$ nuclei had already formed. The site under consideration now had the j^{th} nucleus. What is the random probability that $i = j$?

To determine this probability consider one site that has become a nucleus during each of four successive runs. Call it Site A. During the first run, Site A nucleated i^{th} , during the second run the site nucleated j^{th} , and so on.

First Run	i^{th}
Second Run	j^{th}
Third Run	k^{th}
Fourth Run	l^{th}

If any two of these i , j , k , or l are equal, it will be considered a match. The total number of possible pairs is $6n^2$. That is, there are n^2 possible pairs for each of the following combinations: ij , ik , il , jk , jl , and lk with $1 \leq i, j, k, l \leq n$. The number of pairs that match is $6n$: $i = j$, $i = k$, $i = l$, $j = k$, $j = l$, $k = l$, for $1 \leq i, j, k, l \leq n$. Thus, the random probability that site nucleates with the same order number in any two of four runs is:

$$p = \frac{6n}{6n^2} = \frac{1}{n}$$

This can be visualized in the following way. Consider an $n \times n$ matrix whose elements are pairs of numbers. Each member of the pair can range from 1 to n . The matrix looks like this:

$$\begin{pmatrix} 1,1 & 1,2 & \dots & 1,i & \dots & 1,n \\ 2,1 & 2,2 & \dots & 2,i & \dots & 2,n \\ \vdots & \vdots & & \vdots & & \vdots \\ j,1 & j,2 & \dots & j,i & \dots & j,n \\ \vdots & \vdots & & \vdots & & \vdots \\ n,1 & n,2 & \dots & n,i & \dots & n,n \end{pmatrix}$$

Let the first member of each pair represent the order number of appearance of a nucleus at a site in one run. Let the second member of each pair represent the order number of appearance of a nucleus in another run. Exact matches in order numbers occur along the main diagonal of the matrix. The probability of a match is therefore:

$$P = \frac{n}{n^2} = \frac{1}{n}$$

Since an entirely new nucleus might become activated and completely change the ordering of a run, a margin of error should be introduced. Consider a match to be a site renucleating in the same order, or one site earlier or later, that is $i = j \pm 1$. With regard to the matrix this means counting the terms lying just off the diagonal as matches, as well as the diagonal terms. Thus:

$$\begin{aligned} P &= \frac{n + 2(n - 1)}{n^2} \\ &= \frac{1}{n} + \frac{2}{n} - \frac{2}{n^2} \\ &\approx \frac{3}{n}, \text{ for large } n \end{aligned}$$

In summary the actual reoccurrence of nuclei in particular sites will be compared to the random probability expectation. In addition the order in which these nuclei reappear will be correlated as a function of "matches" between runs. This will also be compared with the random probability to see if a correlation does, in fact, exist. This treatment

assumes that the same number of nuclei reappear each run. This, of course, is an oversimplification, but the error incurred is probably small when compared to the error in the counting of nuclei.

C H A P T E R I I I

EXPERIMENTAL PROCEDURE

Materials

The polymer-polymer system under investigation consisted of isotactic polypropylene (iPP) crystallizing in the presence of an isotactic polystyrene (iPS) substrate. The iPP used was Hercules Profax 6323. Data from the manufacturer indicated that the isotactic content was 96-97% and that the intrinsic viscosity was 1.8 dl/gm in decalin at 135°C. This yielded a viscosity-average molecular weight of 209,000 grams per mole when used in the Mark-Houwink equation. These viscosity measurements were the same within experimental error for both the as-received iPP and one that had been severely heat-treated. The suspicion that the polymer might thermally degrade while being tested was thus eliminated. The ash content of the iPP, consisting mostly of metal oxides, was 3.57% as determined by the Microanalytical Laboratory of the Department of Chemistry, University of Massachusetts.⁴⁵ The melting temperature of the iPP was determined by slowly heating the polymer on the Mettler hot stage and observing it between crossed polars. The disappearance of birefringence was taken to indicate that the melting point had been reached. The value thus found for the melting point was 172.0°C.

The iPS used was Dow EP1340-128. Data from the supplier showed that its isotactic content was 85%, and its titanium and aluminum contents were less than 1 ppm each. Its ash content was found to be 0.025%. The high purity of this iPS made it a logical choice for a substrate material. The

viscosity-average molecular weight was 515,000 grams per mole. The maximum degree of crystallinity attained was 30-35% after a four-hour anneal at 135°C. The melting temperature was found by observation in the Mettler hot stage to be 130.2°C.

The data for these two materials is summarized in Table I.

Equipment

A photograph of the equipment used is shown in Figure 2. It consists of the following:

- 1) a Zeiss polarizing microscope, equipped with a long-working distance objective and a beam splitter
- 2) a Mettler FP-2 hot stage and corresponding control unit
- 3) a Bolex 16 mm movie camera
- 4) a McLaughlin Research Corporation Intervalometer, which drives the movie camera at prescribed intervals.

The light intensity to the camera was regulated by means of a transformer with settings ranging from 8 watts to 2.5 watts. The optimum wattage for the film used was found by trial and error to be 3.5 watts.

A Zeiss UD 6.3X (NA = .12) lens was used for normal runs. No ocular lens was used in the optical train. The magnification obtained was thus relatively low (8.5X at the film plane) so that a larger portion of each sample was included in the film record. This, of course, made the resolution poorer, but it did improve the statistics of the problem. Focus was achieved by means of the beam splitter, whereby the optical distance to the eye was identical with the optical distance to the film

plane. Both the intervalometer and the camera were equipped with frame-counters, which were extremely useful for record-keeping purposes.

The equipment, when linked in this manner, comprised a very useful, semi-automatic device. Microscopic examination could be made over a wide range of temperatures, or over a wide range of temperature scanning rates, or both. In addition, a film record could be made that ranged from 64 frames per second to one frame per twelve hours.

Procedure

Sample Preparation. Both the polymers used were in the form of films. These were prepared in the Carver press. The as-received polymer was placed on a piece of aluminum foil and surrounded by shims approximately 5 mils thick. Another piece of foil was placed on top of this and the whole assembly was then placed in between a pair of steel plates, forming a sandwich. This sandwich was then placed in the Carver press which had been pre-heated to 15°C above the melting point of the polymer. The platens were brought together until they were in contact with both of the steel plates and were maintained in this position for 5 minutes. At the end of that time the pressure between the platens was increased to 5000 psi and maintained for an additional 5 minutes. The platens were then separated and the polymer film was quickly transferred to an ice water bath where it was allowed to cool. The films were easily separated from the aluminum foil and were stored in a dessicator until ready for use.

In some cases an additional treatment was given to the iPS substrate films which rendered their properties different from the amorphous, unoriented, as-pressed film. The first of these treatments was to increase

the crystallinity of the sample by annealing it above the glass transition temperature (T_g). This was accomplished by placing the as-pressed film in an aluminum weighing pan and annealing it in an oven for two hours at 150°C. Its crystallinity was determined by density measurements as summarized in Table II.

Orientation was imparted to several samples by placing a small piece of the as-pressed film, approximately 1 cm x 3 cm in size, in a stretching apparatus. A 1 cm gauge mark was placed on the film and the whole apparatus was placed in a silicone oil bath maintained at 115°C. After one minute the film was stretched rapidly and transferred to an ice water bath. The stretched film was then removed from the stretcher and washed carefully in a solution of soap and water to remove any traces of the silicone oil. The birefringence of the sample was determined by means of a Babinet compensator.

Melting and Crystallization. A small rectangle of each of the two polymers under consideration was cut using a scissors cleaned in carbon tetrachloride. The scissors were used only for this purpose and were cleaned regularly to reduce the possibility of contamination of the nucleating substrate. The two polymer rectangles were overlapped approximately 2 mm and placed on a glass slide, the iPP film being on the top. A cover slip was placed over the films and the slide was then put in the Mettler hot stage. This configuration is shown in Figure 3. The hot stage was clamped to the stage of the microscope and the image of the two overlapped films was focused. The edge of the iPS against which the iPP would subsequently crystallize was aligned diagonally across the field of view by rotation of the microscope stage. This put the maximum area

of the substrate into view. A photomicrograph of a typical iPS substrate prior to nucleation is shown in Figure 4.

The temperature of the sample was raised quickly to some temperature T_1 , above the melting point of the iPP. This melting temperature was varied over a wide range, but in most cases it was 200.0°C. After the control unit of the hot stage indicated that temperature equilibrium had been established, the timing was begun for the melt treatment. Again, this time was varied, but the typical time for melting was 5 minutes. At the end of the melt time, the temperature was dropped rapidly to the crystallization temperature, T_c , below T_m . This was in the range of 120-140°C. The actual quench time using the Mettler took approximately 50 seconds and an additional 2 minutes until the temperature equilibrated. The time at which equilibration occurred was termed the zero in time. All movies begin at this point, regardless of the framing rate employed. Pictures were taken at appropriate intervals until the substrate had been filled with spherulites. At this point the sample was quenched to room temperature and removed, or it was left in place and remelted prior to another crystallization. Care was taken in this case so that the sample was not moved. At the end of the experiment, the thickness of the iPS portion of the sample was measured using a micrometer.

Analysis. The 16 mm film used was Kodak 4-X Reversal Film 7277, and it was developed in a rack-and-tank apparatus as recommended in Kodak Technical Bulletin D-9. Each run was identified, and within each run every tenth frame was numbered. This allowed individual frames to be easily identified. The film was then analyzed in a Craig Film Editor or on a specially designed light table. The latter was preferred as it

enlarged the image to an 8" x 11" size in a horizontal plane, as opposed to the vertical, 5" x 7" image produced by the film editor.

The number of iPP nuclei at the surface of the iPS were counted as a function of the frame number. The substrate as it appeared in the first frame was traced and used as a template for subsequent frames. When a nucleus appeared at the surface, it was counted and marked off so it would not be recounted. Thus, implicit in this analysis of the data, is that no nuclei could appear prior to temperature equilibration of the system (the first frame). All new nuclei were counted in this fashion until the surface had become filled, at which point no more surface nuclei could possibly appear. The length of the iPS substrate in the last frame was measured and reduced to real dimensions by dividing by the magnification produced by the light table.

For each run this counting procedure was repeated four separate times. Attempts were made to eliminate bias in the counts resulting from memory of previous counts. Each count was made long after previous counts, and data from previous counts was not visible. Such precautions were necessary since the counting procedure is one of judgement and can be very subjective. The temptation is great to "count" the same as earlier counts because this reduces the standard deviation, and hence the error in the measurement, and it is immensely easier. It is believed that this pitfall has been successfully avoided, and, if the nucleation data has large errors associated with it, that at least reflects the actual situation.

A computer program was written that averaged the four counts of number of nuclei (Appendix A). The average was then normalized to some arbitrary area, one square centimeter in this case. This normalization

was necessary since film thicknesses differed slightly, as did the length of each IPS surface observed. The standard deviation was calculated as well as the error in the area determination. The total limiting error was calculated as follows:

$$N_N = \frac{N_A}{lw} = \frac{\text{Average number of nuclei counted}}{\text{actual area}}$$

$$\text{Total Limiting Error} = \frac{1}{lw} \delta_{N_A} + \frac{N_A}{lw^2} \delta_w + \frac{N_A}{wl^2} \delta_l$$

where δ_{N_A} = standard deviation of N_A

δ_l, δ_w = experimental errors in length and width determinations, respectively.

But $\frac{\delta_w}{w} \approx .08$ in all cases

and $\frac{\delta_l}{l} \approx .02$

$$\text{Therefore T.L.E.} = \frac{1}{wl} [\delta_{N_A} + .08N + .02N] = \frac{1}{wl} [\delta_{N_A} + .10N]$$

Probable Error = .6745 (T.L.E.)

Further analysis of the data was made by identifying individual nucleation sites on a given substrate. Then, by observing subsequent crystallizations against this substrate one can determine whether or not a particular site again acts as a nucleation site. For this analysis each nucleus is marked as it appears just as in the previous analysis. What is important here, however, is the order in which the nuclei appear and where they form on the surface. This was done for several cases.

The number of times a particular site nucleated was recorded, as well as the order in which nuclei appeared on that site in different runs.

Special Techniques

Crystallinity Measurements. To determine the crystallinity of the iPS substrates used, densities were determined by means of a density gradient column. The column was constructed from 2 solutions of potassium iodide in the density range of 1.02 - 1.08 g/cc. It was calibrated using multi-colored standard density beads. Small pieces of the as-quenched and annealed iPS films were placed in the column and the level to which they sank was a function of their density. The percent crystallinity was determined from the following relation:

$$X = \frac{\frac{1}{\rho} - \frac{1}{\rho_a}}{\frac{1}{\rho_c} - \frac{1}{\rho_a}}$$

where X = percent crystallinity

ρ_a = amorphous density

ρ_c = crystalline density

The density of an iPS film that had been quenched to 0°C from above the melt temperature was found to be 1.56 g/cc. This was taken as ρ_a . The crystalline density⁵⁷ was taken as $\rho_c = 1.11$ g/cc. The densities of the iPS in various states are summarized in Table II.

Orientation Measurement. Two iPS films were stretched above their T_g to impart orientation to their structure. The birefringence of these

films was measured in the Babinet compensator both prior to their use and after they had served as substrates for nucleation. The Babinet compensator consists of a quartz wedge mounted on a calibrated screw so that it can be moved in and out of a light beam. Without any sample in the path of the light the wedge is adjusted so that the zeroth order interference fringe is aligned with the compensator crosshair and a reading is taken. The sample is then placed in the light beam and the fringe can be seen to shift by some amount. The quartz wedge is then readjusted to compensate for the added retardation of the sample. Another reading is taken, and the difference between the first and second readings is related by a calibration constant to the retardation of the sample. The birefringence can be determined from the retardation by using the following relation:

$$\Delta = \frac{R\lambda}{d}$$

where Δ = birefringence

R = retardation

λ = wavelength of incident light

d = thickness of sample

The birefringence can be used to obtain the orientation function using the following relation assuming free rotation of the benzene ring about the chain backbone⁵⁸:

$$\Delta = \Delta_{am}^{\circ} f_e$$

where $\Delta_{am}^{\circ} = -.161$.

The results of the orientation determination are summarized in Table XI.

Molecular Weight Determination. Intrinsic viscosity measurements were carried out on two iPP samples, one that was in the as-received condition and one that had been heat-treated for 2 1/2 hours at 135°C. The measurements were carried out according to the standard procedure⁵⁹ with successive dilutions in an Ubbelohde viscometer. The solvent was decalin at 135°C. The reduced viscosity, η_{red} , was plotted as a function of concentration.

$$\eta_{red} = \frac{\eta_r - 1}{c}$$

where η_r = relative viscosity = $\frac{\text{flow time of solution}}{\text{flow time of solvent}}$

The intrinsic viscosity, $[\eta]$, was found by extrapolating the reduced viscosity to zero concentration:

$$[\eta] = \lim_{c \rightarrow 0} \eta_{red}$$

The intrinsic viscosity was then used in the Mark-Houwink equation to determine the viscosity-average molecular weight:

$$[\eta] = KM_v^a$$

where⁶⁰ $K = 10.0 \times 10^{-5}$

$$a = 0.80$$

C H A P T E R I V

RESULTS

Data Treatment

For this study of the heterogeneous nucleation of iPP against an iPS substrate the raw data taken was the number of iPP nuclei at the substrate versus time. Each crystallization was analyzed four separate times, and in some cases, five. The curves of number of nuclei versus time are averages of these four readings that have been normalized with respect to area. In the cases where error bars are not shown, the error in the number of nuclei amounts to 20% of the reading or less, as outlined in Chapter III. The error in the time readings is taken to be zero.

All of the curves of the number of nuclei versus time display the same shape: an induction period before any nuclei appear at the surface, an initial "foot" of gradually increasing nucleation rate, a linear portion of constant nucleation rate, with a levelling off to a portion of zero nucleation rate, where nucleation has ceased. Because of the uniform character of these curves, it was convenient to describe them by three parameters:

1. the least-square slope of the linear portion, I .
2. the so-called induction period, τ , the value at which the straight line portion crosses the time axis.
3. the final nucleation density attained, N_f .

A least-squares analysis was done on the linear portion of each curve to determine the best-fitting straight line through the points. In fitting a straight line through an S-shaped curve, a certain amount

of error is incurred due to the selection of just what points are to be included in the least-squares analysis. Unfortunately, this cannot be avoided. The deviations from the straight line fit are negative at low points on the curve near the foot and positive at the top when the level region is approached. The induction period, τ , was taken as the time-intercept of the linear portion of the curve as determined by the least-squares analysis. The reason for the choice of this parameter over the actual time when a nucleus first appears is that the former indicates the onset of the constant nucleation rate portion of the curve. The placement in time of the linear portion of the curve is important in the model of the crystal growth presented in Chapter V.

Temperature Dependence

While it is secondary to the main purpose of this thesis, growth rate data is included at this point because it will be useful later. The spherulitic growth rate, G , was measured as a function of T_c for the samples with unannealed substrates, and the results are summarized in Table III. The growth rate is plotted in Figure 5 as a function of T_c . From the figure it can be seen that the growth rate begins to increase greatly as T_c is dropped below 125°C. This will be discussed in Chapter V.

The straight line plot in Figure 6 shows $\ln G$ versus the quantity $\frac{1}{T(\Delta T)}$. The slope of this curve is equal to $\frac{-4b\sigma e T_m}{k(\Delta H_v)}$ since

$$G = G_0 \exp(-\Delta G_t/kT) \exp\left[\frac{-4b\sigma e T_m}{T(\Delta T)k(\Delta H_v)}\right]$$

where H_v is the enthalpy of fusion per unit volume. The least-square slope and deviation are included in Table III and are equal to $-6.351 \times 10^4 (\text{°K})^2 \pm 1.086 \times 10^4$. Several values for the enthalpy of fusion of PP have been quoted⁶¹, so an intermediate value of 2.1 kcal/mole of monomer units was chosen. This is equivalent to 4.36×10^{-2} kcal/cc if the density of iPP is taken⁶² to be 0.853 g/cc. This leads to a value of $\sigma\sigma_e$ of $180 (\text{ergs/cm})^2 \pm 30$, when a value of 5 Å is assumed for b , the thickness of the polymer chain.

Figures 7-19 show the dependence of nucleation rate on temperature. The substrate for all these runs was an as-pressed iPS of low crystallinity. The determination of percent crystallinity is given in Chapter III, and the results are summarized in Table II. The melt treatment given to each iPP sample was five minutes at 200°C and was identical for all the runs. The only variable, then, was the crystallization temperature, T_c , which was varied over the range 120-140°C. This includes the range where iPP transcrystallizes against iPS and also a range where regular spherulitic growth occurs.

The three curve parameters, I , τ , and N_f , for nucleation against the as-pressed iPS are given in Table IV. The nucleation curves from which they are taken are shown in Figures 7-19. The nucleation rate is seen to decrease dramatically as the crystallization temperature is raised from 120°C to 140°C. The induction period, on the other hand, increases with crystallization temperature. The final nucleation density, though its variation is much more irregular, first increases with T_c and then decreases as T_c is raised above about 134°C. Repeated runs were done against the same area of the substrate for $T_c = 120, 125, 135, 139$, and

140°C. The results are shown in Figures 7-11. Figures 12-19 show data for only single runs at each T_c . If the nucleation rates, induction periods, and nucleation densities are averaged for each temperature at which multiple runs were done, a representative nucleation curve is obtained. The curve parameters for these representative curves are also given in Table IV. These average curves can be compared to the single curves obtained for $T_c = 130-134^\circ\text{C}$ and $136-138^\circ\text{C}$, as shown in Figure 20. Figure 21 demonstrates the dramatic dependence of nucleation rate on supercooling. A drop in the nucleation rate over three orders of magnitude occurs for a decrease in the supercooling of only 20°C . A plot of $\ln I$ versus $\frac{1}{T(\Delta T)}$ is shown in Figure 22. Figure 23 shows a plot of $\ln I$ versus the quantity $\frac{1}{T(\Delta T)^2}$, a plot that is used in obtaining the quantity $\sigma\sigma_e\Delta\sigma$. The slope of this plot as determined by a least-squares analysis was $-4.77 \times 10^6 (\text{°K})^3$ with a standard deviation of $1.05 \times 10^6 (\text{°K})^3$. The least-square slopes and deviations for Figures 22 and 23 are summarized in Tables V and VI.

A plot of $\log \tau$ versus $\log \Delta T$ is shown in Figure 24. Its least-square slope is -9.18×10^{-2} with a standard deviation of 2.62×10^{-2} . The inverse of the slope is equal to ϵ , a parameter useful in fitting the data. In this case, ϵ is equal to 10.87 ± 3.1 . Figure 25 shows a plot of τ versus the inverse of the nucleation rate. The induction period is seen to increase rapidly for very small differences in $\frac{1}{I}$ and then to level off at small values of I .

Figure 26 is a plot of nucleation density versus supercooling. The maximum nucleation density occurs at a supercooling of 38°C , or $T_c = 134^\circ\text{C}$. A second-order least-square fit to this data was done, and

the best fit to the data is given by the following equation:

$$N_f = -800(\Delta T)^2 + 68,500(\Delta T) - 1,353,000$$

This is shown as the solid line in Figure 26.

Figures 7-11 show data for successive runs against the same substrate. The curves are not exactly reproducible from one run to the next. Within each set the curves do seem to maintain the same general character. That is, the error bars of the three curve parameters overlap for most runs. The reproducibility from one run to the next can be seen to get poorer as T_c is increased. This is shown in Table IV by the increased percent standard deviation of the nucleation rate and the induction period for the five representative curves as T_c is raised from 120 to 140°C. The counting error does not change substantially over the entire range of temperatures tested. It remains about 10% of the number of nuclei counted. The increase in the standard deviation of the nucleation rate from 15% to 30% and of the induction period from 13% to 47% must then be due to the stochastic nature of the process. So few nuclei are generated at higher crystallization temperatures that the nucleation rate can be easily affected by the appearance or disappearance of only one nucleus.

Intrinsic viscosity measurements of the as-received iPP resulted in $[\eta] = 1.60 \pm .05$ dl/g, yielding $\bar{M}_v = 181,000 \pm 20,000$. The same technique applied to a sample annealed for 2 1/2 hours at 150°C gave $[\eta] = 1.76 \pm .12$ dl/g and $\bar{M}_v = 203,000 \pm 20,000$. The molecular weight of the iPP, then, did not change over the course of any one experiment, since most were completed in less than 2 hours.

No systematic variation in any of the curve parameters is noted as the sample is remelted and recrystallized. That is, for $T_c = 120^\circ\text{C}$ the first run has a lower nucleation rate than subsequent runs at the same T_c , as shown in Figure 7 and Table IV. For $T_c = 140^\circ\text{C}$ this trend is reversed. The first run has the highest nucleation rate, and the subsequent runs have progressively lower rates, as seen in Figure 11. The nucleation rates at other crystallization temperatures show no trends whatsoever. There seems to be no correlation between a high nucleation rate and a high nucleation density or a short induction period for runs at one crystallization temperature. The variations, then, appear to be random rather than systematic. This is evidence, along with viscosity data presented above, that the molecular weight of the crystallizing iPP remains unchanged throughout the experiment. Were serious degradation of the iPP to occur, one would expect the curve parameters to change consistently in one direction or the other, depending on the effect of increasingly smaller molecular weight. The assumption will thus be made that the iPP is unchanged with respect to molecular weight and melting point over the course of the experiment.

It should be noted here that a dramatic decrease in nucleation rate was noted for an early series of runs. Each time the sample was melted and recrystallized, the nucleation rate was lower than the previous run. It was expected at that time that the effect would be general and that degradation of the iPP was to blame. As just set forth above, neither expectation proved to be warranted. Nevertheless, the deactivation in this early instance was real, and is demonstrated in Figure 27. The series of six photomicrographs consists of the frame at 18 1/3 minutes

after temperature equilibration from each of six successive runs at $T_c = 135^\circ\text{C}$. The progressive decrease in number of spherulites both at the surface of the substrate and in the bulk is obvious.

Effect of Substrate Crystallinity

To determine the effect of the substrate crystallinity on the heterogeneous nucleation kinetics, an iPS sample that had been annealed was used as a substrate instead of the as-pressed iPS film. The annealing treatment was 2 hours at 150°C , a temperature well above the T_g of the iPS. This treatment allowed crystallization to occur, increasing the crystallinity of the iPS substrate from 0% to 27%, as determined by density measurements. A series of runs were done for crystallization temperatures of 120, 125, 130, 135, and 140°C . The melt treatment was identical to that for the unannealed samples: five minutes at 200°C .

Figures 28-32 show the curves of number of nuclei versus time for the various crystallization temperatures used. The curve parameters are summarized in Table VII. Figure 33 shows the five nucleation curves plotted on the same time axis. These five curves are the representative curves obtained by averaging the curve parameters for the set of runs at each crystallization temperature. The shape of the curves is the same as for the unannealed samples. The nucleation rate drops over three orders of magnitude for an increase in T_c of 20°C . The induction period increases over two orders of magnitude for this same temperature range. The variation of the nucleation density with temperature is not so clear-cut as before. A second-order fit to this data yields the following:

$$N_f = -200(\Delta T)^2 + 16,600(\Delta T) - 318,000$$

If both the annealed and unannealed data are fit together the result is:

$$N_f = -600(\Delta T)^2 + 53,100(\Delta T) - 1,036,600$$

These are both shown in Figure 26. It reaches a maximum for $T_c = 130^\circ\text{C}$.

The standard deviations of the average values of nucleation rate, induction period, and nucleation density are approximately equal to those for the samples with unannealed substrates. The run-to-run reproducibility was thus not affected by the heat treatment of the substrate. The standard deviation of the average nucleation rate increases as T_c increases. This was noted for the samples with unannealed substrates, and the same rationale is applicable here. The reproducibility between runs becomes poorer as T_c increases due to the small numbers of nuclei involved and to the random nature of the nucleation process. No progressive drop in the nucleation rate was noted as runs were repeated, except for the series run at $T_c = 125^\circ\text{C}$, shown in Figure 29. In this case the first three slopes agreed within experimental error, while the fourth was much lower.

The average nucleation rates for these runs are included in Figure 21, the plot of I versus T_c . The temperature dependence for these samples with semi-crystalline substrates does not differ significantly from that of the samples with amorphous substrates. This can also be seen in Figures 22 and 23 in which the natural logarithms of nucleation rate are plotted versus the quantities $\frac{1}{T(\Delta T)}$ and $\frac{1}{T(\Delta)^2}$ respectively. Three least-square straight lines are shown on each plot. One was calculated for only the amorphous samples, one for only the semi-crystalline samples,

and one for both sets of data. The slopes and intercepts are summarized in Tables V and VI. The slopes all agree well within experimental error. Thus, the pre-annealing does not affect the temperature dependence of the nucleation rate.

The slope of $\ln I$ versus $\frac{1}{T(\Delta T)^2}$ using both the annealed and unannealed substrate data is $-4.662 \times 10^6 (\text{°K})^3$. This is equal to $\frac{-16\sigma\sigma_e \Delta\sigma T_m^2}{k(\Delta H_v)^2}$, according to Equation 3. This yields 676 ± 150 $(\text{ergs/cm}^2)^2$ for the quantity $\sigma\sigma_e \Delta\sigma$.

In the same manner, the temperature dependence of the induction period for the samples with annealed substrates is included in Figure 24, the plot of $\log \tau$ versus $\log \Delta T$. The least-square analysis indicates that the same straight line can describe the data for the annealed as well as the unannealed samples, as shown by the least-square parameters summarized in Table VIII. The value of ϵ for both sets of data is 10.8 ± 1.3 . The induction periods for these annealed samples are also shown in Figure 25 as a function of the inverse of the nucleation rate. Here again no significant deviation from the behavior of the unannealed samples is noted.

The final nucleation densities of the samples with annealed substrates are plotted versus supercooling in Figure 26. In this case the dependence of nucleation density on supercooling may be different for the two types of samples. There are few points and the correlation is poor, however. The nucleation density initially increases with decreased T_c and then levels off or falls for crystallization temperatures above 134°C approximately.

Effect of Melting Treatment

The melting treatment used for the samples mentioned above has been five minutes at 200°C. This will be considered the standard, or control, melting treatment. For this series of experiments the melting time and temperature were varied, and the effect on the nucleation kinetics was noted.

Melting Time. Melting times of "zero" and fifteen minutes were used for two samples in this set of experiments. A melting time of zero means simply that as soon as the hot stage had equilibrated at the melt temperature, the sample was quenched to the crystallization temperature. Thus, although the sample was melted, it spent zero time at the melt temperature, by definition. The melt temperature used was 200°C. The substrate crystallinity effects, if any, would be minimal due to an absence of secondary crystallization over various melt times. The samples were all quenched to a crystallization temperature of 135°C.

The results are plotted in Figure 34 for the two samples with different melt times. The control curve is Curve 1 from Figure 31, the nucleation curve for an annealed sample that had been melted for five minutes at 200°C prior to quenching to 135°C. The curve parameters are summarized in Table IX. The nucleation rate is seen to increase from 5.45×10^3 nuclei/cm²/min. for zero melting time to 6.44×10^3 nuclei/cm²/min. for a fifteen minute melting time, an increase of 16%. This is a variation just outside the experimental limits afforded by the standard deviation. In addition the induction period decreases for longer melt times. It falls from 5.83 minutes for zero melt time to 5.32 minutes for 15 minutes of melting, a decrease of 8%. This deviation also falls

outside the probable error set by the standard deviation of the least-squares analysis. The nucleation density is lowest for the intermediate melt treatment, highest for the longest melt time, and intermediate for zero melt time.

Melt Temperature. Samples were melted for five minutes at three temperatures other than the control temperature of 200°C. These were 180, 220 and 250°C. The lowest temperature was just above the melting point of the iPP, and the highest was above the melting point of the iPS substrate. The iPS substrate used for these runs had been annealed prior to use. Here again, the hope was to begin with a substrate that had already achieved an equilibrium degree of crystallinity and that would not be changing with time at temperatures above T_g . The crystallization temperature was 135°C so that the control curve was again Curve 1 of Figure 31. The plots of number of nuclei versus time are shown in Figure 35. The three curve parameters are summarized in Table X.

The nucleation density falls off sharply as the melt temperature is increased. The nucleation density remains high for the lower three melt temperatures. For the sample in which the substrate was melted, however, the nucleation density dropped to almost zero. The induction period tended to increase with melting temperature. A single frame from the run in which the substrate was melted is shown in Figure 36 to demonstrate the retarded nucleation at the substrate. A frame from the run with a 200°C melt temperature is included for comparison.

Effect of Substrate Orientation

Two iPS films were stretched above T_g and subsequently used as

substrates to determine what effect, if any, substrate orientation had on the nucleation kinetics. It was necessary to use two films since the stretching apparatus held only enough material for one substrate. Unfortunately, the precision of the stretcher was poor, and each film was stretched by different amounts, as determined by 1 cm gauge marks placed on the film prior to stretching. One film was stretched 120% and was used with the stretching direction parallel to the substrate plane. The other film was stretched only 60% and was used with the stretching direction perpendicular to the substrate plane. The calculation of the orientation functions for these films is shown in Table XI. The substrates were exposed to glass slides prior to their use, in the hope that complete relaxation would not occur.

The curves of number of nuclei versus time for the two oriented substrates and the appropriate unoriented substrate are shown in Figure 37. The control sample was one with an unannealed substrate that was quenched to a crystallization temperature of 135°C, Curve 1 of Figure 9. The crystallinity of the stretched iPS samples was found to be negligible, and the unannealed substrate most closely approximated this condition. The curve parameters are summarized in Table XII.

The nucleation rate is highest against the unoriented substrate and lowest against the most highly-oriented substrate with the stretching direction parallel to the nucleating substrate. The induction periods are all the same within experimental error. The final nucleation density is highest for the unoriented substrate.

Repetition of Sites

Seven sets of four successive runs were studied with respect to the

individual nucleation sites on the iPS substrate. Individual sites were identified and categorized as to how many times nuclei formed at the site during the four runs. The distributions for the seven series are given in Table XIII. Also given are the theoretical probabilities which were calculated as described in Chapter II.

Examination of Table XIII shows that in every case the actual frequency of a site being a nucleus each of four times exceeds the theoretical probability. In all but two cases the actual frequency was at least twice, and often five or six times, that expected for a random nucleation process. In five out of the seven cases, the probability that a site became a nucleus three times exceeded the theoretical probability. The probability for a two-fold appearance of a nucleus at a site always was less than the theoretical calculation. Single appearances of nuclei were favored over the calculated probability somewhat in four out of the seven cases.

Order Correlation

In order to determine whether or not the nuclei tend to reappear in the same, or close to the same, order, three sets of four successive runs were studied in detail. During each run the order of appearance of nuclei at individual sites was recorded. Successive runs were compared and the number of matches between runs were totalled. The results are summarized in Table XIV. The crystallization temperatures are all high. This was deliberate. At lower crystallization temperatures so many nuclei appear that the record-keeping becomes very difficult. Thus, order determinations were restricted to runs done at high T_c .

Table XIV gives the total number of sites generated in each series and also the total number of sites at which nuclei form in more than one run. Of these the matches in order number are shown. The ratio of the number of matches to the number of sites at which nuclei form in more than one run gives the probability of a match in order number. The theoretical probability, as shown in Chapter II is $\frac{3}{n}$, which for these runs is about 0.15. The actual frequency of matches is thus seen to exceed the theoretical probability by about a factor of two, being about 0.30.

CHAPTER V

DISCUSSION

Shape of the Nucleation Curve

As reported in Chapter IV the curves of number of nuclei versus time all share the same shape. This shape has four distinctive features:

1. an induction period before any observable nucleation occurs;
2. a small "foot" of gradually increasing nucleation rate;
3. a linear portion of constant nucleation rate;
4. a flat portion where nucleation has ceased.

This shape has been reported previously^{45,63,64} for various polymers and seems to be fairly general. It has been termed pseudohomogeneous⁶⁵ due to the mix of heterogeneous and homogeneous characters involved. That is, heterogeneous nucleation generally occurs after some induction period, but all the nuclei are activated at once. This leads to a nucleation curve of the shape demonstrated in Figure 38a. Homogeneous nucleation, on the other hand, is characterized by a constant, finite nucleation rate with no induction period. A schematic diagram depicting a homogeneous nucleation curve is shown in Figure 38b. The observed shape for the nucleation curve is shown in Figure 38c.

Such pseudohomogeneous behavior is thought to result from heterogeneities that do not interact strongly with the polymer melt. That is, a range of activity may exist for the heterogeneities, which become sites for nuclei as a function of time, leading to a portion of the nucleation curve with a finite slope. The induction period prior to the onset of any observable nucleation has been explained by Turnbull⁶⁶ in terms of the time necessary to approach a steady state number of

embryos. This approach to steady state is necessarily slow in condensed systems due to the low rate of diffusion. It may be, too, that the induction period results from an imperceptible nucleation rate. The decrease and levelling off of the nucleation rate are due to the completion of the phase transformation. Some authors^{45,63} have reported that the nucleation rate levels off prior to the completion of crystallization. This can be explained in terms of the impurities which are rejected to the growth fronts and which slow the crystallization process, even before the untransformed material is used up.

The induction period, the constant and finite nucleation rate, and the zero nucleation rate portions of the nucleation curves have all been satisfactorily explained. What of the initial portion of the curve of increasing nucleation rate? Flory and McIntyre⁶⁴ and Sharples⁶³ claim it is due to the finite, but reproducible, size at which nuclei become visible in the optical microscope. If the size is reproducible, why should there be any effect on the nucleation curve except a longer induction period due to the time necessary for each nucleus to grow to a visible size? A more probable explanation is one that parallels Turnbull's argument for an induction period.⁶⁶ That is, the approach to equilibrium is very slow in condensed systems and might give rise to a transient in nucleation rate following the induction period.

Proposed Model for the Nucleation Curve

Measurements of the nucleation kinetics at a substrate were made in projection. That is, the nuclei appeared as ever-widening semi-circles along a line. The following model has been developed to describe the nucleation kinetics for such a one-dimensional case.

Assume the area of the substrate is lh and that h is the dimension through which the observations are made. Thus, l is the length available for nucleation. Assume numerous and random nucleation centers are generated on the area lh . If \dot{N}_0 is the number of real and fictitious nuclei appearing per unit time per unit area in the absence of impingement, then the total number of nuclei that would appear in area lh is $\dot{N}_0 lh$. The number of nuclei that could appear per unit time per unit length is $\dot{N}_0 lh/l = \dot{N}_0 h$. The total length of diameters along l at time t in the absence of impingement⁶⁷ is thus:

$$\dot{N}_0 h \int_0^t 2G(t - \tau) d\tau = \dot{N}_0 hGt^2$$

where G is the spherulitic growth rate. Therefore, the fraction of length l that is not occupied by a spherulite at time t is:

$$e^{-\dot{N}_0 hGt^2}$$

Now, the number of real nuclei actually found per unit time per unit length, \dot{n}/l , is equal to the number of nuclei that would have formed in the absence of impingement times the available area, the fraction of the area not already covered:

$$\frac{\dot{n}}{l} = \dot{N}_0 h e^{-\dot{N}_0 hGt^2}$$

(4)

$$\frac{\dot{n}}{lh} = \bar{I} = \dot{N}_0 e^{-\dot{N}_0 hGt^2}$$

\bar{I} is the measured nucleation rate in nuclei/cm²-min.

Measured values of I , G , and h were used to test the validity of the above equation and to find the magnitude of the nucleation rate that would result if no impingement were to occur. Runs at $T_c = 125$, 135 , and 139°C were studied. For the three cases examined, the non-impingement value of the nucleation rate remained within 10% of the measured value over the first 25% of the crystallization time. \dot{N}_0 was within 50% of I up to approximately 50% of the crystallization time. Beyond 50% the model invariably broke down and no value of \dot{N}_0 would satisfy Equation 4.

The failure of the model early in the crystallization is due to the assumption that the centers were numerous and generated at random on the surface of the substrate. Certainly at higher crystallization temperatures the number of nuclei counted were not numerous, and even at $T_c = 125^\circ\text{C}$ the total number of nuclei counted only amounted to about 80 nuclei/ $.001\text{ cm}^2$. This is not a large number by statistical standards. The deviation from random centers results in further distortion of the ideal, random behavior, so that the model only works for a short time after the beginning of the crystallization, despite the adjustable parameter, \dot{N}_0 . It is encouraging, however, that \dot{N}_0 does not deviate markedly from I for at least the first half of the crystallization. This is further justification for the approximation of each nucleation curve by a straight line portion, the slope of which does not differ tremendously from that of the free-growth approximation.

Temperature Dependence

Nucleation and Growth Rates. The temperature-dependence of $\ln G$

and $\ln I$ yield values of $\sigma\sigma_e$ and $\sigma\sigma_e\Delta\sigma$, respectively. These, when divided, yield a value for $\Delta\sigma = \sigma + \sigma_c - \sigma_m = 3.75 \pm 0.05$ ergs/cm².

Here σ is the surface energy of all faces of the polymer nucleus except the fold surface, σ_c is the substrate-crystal interfacial energy, and σ_m is the substrate-melt interfacial energy. Assuming a value of 5 ergs/cm² for the side surface energy of iPP,⁴⁵ $\sigma_m - \sigma_c = 1.25$ ergs/cm². The larger this value, the better the nucleating ability. The value obtained is somewhat smaller than those found by Chatterjee⁴⁵ for the crystallization of poly-butene-1 against iPP and iPS substrates. The value is probably in the intermediate range. This confirms the conclusion drawn previously that the substrate does not interact strongly with the polymer, and pseudohomogeneous behavior results.

Both the nucleation and growth rates are seen to increase with increased supercooling, as shown in Figure 5. The growth rate takes a more dramatic up-swing in the temperature range studied, and may be responsible for the lower nucleation densities observed at high supercoolings. This will be discussed later.

Induction Period. An induction period, τ , was defined in Chapter IV as the time-intercept of the linear part of the nucleation curve. This was seen to increase as the crystallization temperature increased, as shown in Figure 24. The plot of $\log \tau$ versus $\log \Delta T$ is linear with a slope of -9.30×10^{-2} and a standard deviation 1.1×10^{-2} . Buchdahl, Miller, and Newman⁶⁸ found that the temperature-dependence of the induction period for polyethylene crystallization was of the form:

$$\tau \propto \Delta T^{-\epsilon}$$

where ϵ varies between 2.5 and 4. Mandelkern⁶⁹ has found a value of 9 for ϵ for PE, while Hoshino, et al.⁷⁰ found a value of about 5 for several PP fractions of varying tacticity. Magill⁷¹ found the behavior to be similar, except that at crystallization temperatures below 115°C a new, much lower, value of ϵ fit the data. The data of this study confirms the temperature-dependence of the induction period, as set forth in Equation 5. The value of ϵ found, 10.75 ± 1.3 , agrees most closely with the values of Mandelkern, being much higher than other quoted values. The observed higher-order temperature dependence may depend upon the fact that the temperature-range investigated is one over which the nucleation kinetics change drastically. At $T_c = 140^\circ\text{C}$ the nucleation rate is low and the resultant morphology is spherulitic. At $T_c = 120^\circ\text{C}$ the nucleation rate is 3 orders of magnitude higher resulting in a transcrystalline morphology. The fact that a drop in ϵ was noted by Magill at $T_c = 115^\circ\text{C}$ supports this hypothesis.

Other workers^{64,72} have found that the induction period is proportional to the inverse of the nucleation rate. Examination of Figure 25 shows that while this may be true for small values of $\frac{1}{I}$, it certainly does not hold true over the entire range of nucleation rates tested. The induction period seems to saturate at a value of 35 minutes for nucleation rates less than $120 \text{ nuclei/cm}^2\text{-min}$. Admittedly, the error is large in this region of the curve. Still, the deviations from linearity are too great to be explained away by experimental error.

Nucleation Density. Sharples⁶³ found a steady decrease in the nucleation density of poly(decamethylene terephthalate) as the crystallization temperature was increased. This has been observed by other

researchers as well.⁷³⁻⁷⁵ Figure 26 shows a plot of the nucleation density versus the supercooling for the present study. Initially as ΔT is increased, N_f does tend to increase, as noted by previous authors. Above $\Delta T = 42^\circ\text{C}$, however, the nucleation density no longer increases, but tends to fall instead. At such high supercoolings the nucleation process is very rapid, and the nuclei are numerous. Counting errors were undoubtedly made which rendered the experimental value of the nucleation density lower than the actual value. Despite this, a possible explanation might lie in the temperature-dependence of the growth rate. As seen in Figure 5, the growth rate was extremely high at $T_c = 120^\circ\text{C}$. The available area on the surface of the substrate might have been used up too quickly to allow a high nucleation density to be attained. In fact, the spherulitic growth rate at $T_c = 120^\circ\text{C}$ is 70 times the growth rate at $T_c = 140^\circ\text{C}$, and six times the growth rate at $T_c = 125^\circ\text{C}$. It seems possible, then, that the high growth rate, coupled with the tendency to overlook nuclei at high nucleation densities, could cause a decrease in the nucleation rate at crystallization temperatures below 130°C .

Chatterjee⁴⁵ found that transcrystalline surface morphology formed at crystallization temperatures in the range $120\text{--}130^\circ\text{C}$. This was confirmed in this study. At $T_c = 131\text{--}136^\circ\text{C}$, the surface morphology was partially transcrystalline and partially spherulitic. At still higher crystallization temperatures ($T_c = 137\text{--}140^\circ\text{C}$), the surface morphology was totally spherulitic. Chatterjee has used a nucleation density of 10^6 nuclei/cm² as an arbitrary cut-off point between transcrystalline and normal spherulitic morphology. The data presented here, however, indicates that nucleation density alone is insufficient to characterize the surface morphology. At

$T_c = 120^\circ\text{C}$, the nucleation density is no higher than the average for certain mixed morphologies, yet the morphology is transcrystalline. The nucleation rate is so much higher at $T_c = 120^\circ\text{C}$ however, that virtually all the nuclei are injected onto the surface at once. This, coupled with the extremely high growth rate at this crystallization temperature, means that lateral impingement occurs rapidly and columnar growth away from the surface ensues. The morphology is thus typically transcrystalline. Since the nucleation and growth rates are lower at higher crystallization temperatures, the initial nuclei can grow in a normal spherulitic fashion before impingement occurs, leading to mixed or spherulitic morphologies. Thus, as long as the nucleation rate, nucleation density, and spherulitic growth rate are moderately high, a transcrystalline morphology can develop, even though the final nucleation density is not extremely high.

Substrate Crystallinity

The crystallinity of the substrate, within the limits 0-30%, does not affect the nucleation kinetics. This is shown by Figures 21-25. In no case is the temperature behavior of the plotted parameters of the sample with the crystalline substrate different from those of the samples with amorphous substrates. Only in Figure 26, the plot of nucleation density versus supercooling, is it possible to discern any effect of the annealing of the substrate. The difference in this case may very well be without significance, due to the large uncertainties involved in the nucleation density data. It seems, therefore, that the annealing of the iPS substrate prior to use had no effect whatsoever on the activity of the substrate as a heterogeneous nucleant.

It should be noted here that the crystallinity of the iPS substrate can and did change over the course of the experiment. As shown in Table II, an unannealed substrate that was initially amorphous had a final degree of crystallinity after four runs of 34%, regardless of T_c . This is nearly the same value found for annealed samples both before and after use. Thus, an initially amorphous sample when used at $T_c = 120^\circ\text{C}$, changes from 0 to 34% crystallinity. If used at $T_c = 140^\circ\text{C}$, the same change occurs, though probably at a somewhat accelerated rate. A pre-annealed sample, however, starts with about 27% crystallinity and changes only very little, to about 35% crystallinity, over the course of the experiment. This holds at all crystallization temperatures.

After heating at 200°C for five minutes, the standard melt treatment for the iPP, the crystallinity of the iPS substrate was still 0%. Depending on the rate of crystallization, then, the only runs that began with substrates of undetectable crystallinity were the first runs of samples with unannealed substrates. Even these, however, when compared to the averages of the annealed samples, behave no differently. The conclusion must be drawn that the degree of crystallinity of the substrate plays no significant role in the activity of an iPS substrate to iPP nucleation.

Chatterjee⁴⁵ has found that atactic polystyrene did not induce transcrystallinity, while iPS did. He attributed this lack of enhanced nucleation to the lack of crystallinity in the amorphous substrates, concluding that a crystalline substrate was a necessary, but not sufficient, criterion for inducing transcrystallinity. The fact that the degree of crystallinity of the iPS substrate had no apparent effect on the nucleation

kinetics of the iPP in this investigation indicates that it is not the degree of crystallinity of the substrate that yields the different behavior of the atactic PS from that of the iPS. Instead, other differences in the substrates must be suspected, such as the inherent molecular structure. Perhaps the atactic nature of the one PS does not readily permit adsorption of iPP chains at the surface of the PS, regardless of the crystallinity. If so, then a substrate need only be crystallizable to be an active nucleator. At any rate, a high degree of crystallinity of the substrate is neither a necessary nor a sufficient criterion for inducing transcrystallinity in iPP.

Melting Treatment

The crystallization kinetics of polymers have been shown to be strongly dependent on the melt treatment, both the time and temperature of melting.^{55,76,77} This study has confirmed the strong dependence on melt temperature. The higher the melt temperature, the lower the nucleation rate and final nucleation density. Turnbull⁵⁵ has proposed that small patches of crystal may be retained above the melting point in crevices and other surface imperfections, due to favorable energy balances. These retained patches may serve as nuclei in the subsequent crystallization. If the melting treatment is severe enough to destroy any such patches, the subsequent nucleation rate is diminished. This is in fact what is observed. Collier and Neal⁷⁷ have proposed three temperature regimes above the melting point of the polymer. In order of increasing melt temperature, they result in:

1. partial melting and gross self-nucleation

2. insensitivity to melting temperature

3. deactivation of nuclei

If such a classification is applied to the data of this study, it would seem that melt temperatures equal to 180 and 200°C are already in the insensitive range, as they are nearly equal. At 220°C and higher, however, deactivation sets in, leading to much lower nucleation rates and longer induction times.

As already mentioned in Chapter IV when a melting temperature of 250°C was used, the nucleation rate was reduced to nearly zero. The question that comes to mind here is what condition the substrate is in when melted for 5 minutes and quenched to 135°C, still above its glass transition temperature. Why is nucleation so retarded at this substrate compared to the other iPS substrates? Physically, the melted substrate is probably much like many of the other iPS substrates used -- leathery and low in crystallinity. Could the severe melting treatment destroy every niche on the surface where a growing iPP might have gained a foothold? Or was the roughness of the iPS substrate, imparted during cutting, merely the reason for the enhanced nucleation, which disappeared on melting? An insufficient amount of data exists at this point to draw any conclusions, but this might be an area for further study.

The variation of the nucleation rate with melt time is certainly not large, being only about 16%. The range of times examined (0-15 minutes) was rather narrow and may be the cause for the small variations found. If, as one would expect, the longer melt time would destroy more retained nuclei, the nucleation rate should be lower for longer melt times. This is the opposite of what was observed. By the same token

the induction period should be longer for longer melt times. It was longest, however, for the 0 melt time. The variations in τ and I fall just outside the error limits, and in view of this, it seems likely that over the range of times studied, the kinetics of nucleation were unaffected by the time of melting.

Substrate Orientation

The oriented iPS films were used in two perpendicular orientations in the hope of observing a difference in the nucleation kinetics, as Hobbs^{42,43} did with graphite fibers. A variation was noted, but certainly not as conclusive a one as Hobbs'. Both oriented iPS films showed nucleation rates lower than the unoriented substrate. Of the oriented films, the one with its stretching direction perpendicular to the substrate plane gave the higher nucleation rate. Again, the variations, though they fall outside the experimental error, are not great enough to conclude that substrate orientation had any effect on the nucleation rate. The induction periods all agreed within experimental error.

The oriented iPS substrates did relax over the course of the experiments. The retardation colors changed as the temperature was increased over the glass transition temperature. The birefringence of the samples was found to be zero after two runs had been run with them as substrates. Depending on how rapid the relaxation was, then, it may be in error to say that the films were unlike. In that case, no variation in their nucleation kinetics would be expected.

Nature of Heterogeneous Nuclei

It has been proposed that heterogeneous nuclei are discrete^{3,4,45,5} and that these sites can vary in their activity as nuclei.^{42,78} Both of these proposals have been confirmed by this study. It was shown in Chapter IV that there is a tendency for nuclei to reappear at particular sites. If the entire area of the substrate were of equal nucleating ability, no one site would ever be favored over another. This is not the case. Certain individual sites are favored more than random statistics would permit. Therefore, these sites are discrete.

It was also shown that particular sites tend to appear in the same order time after time. That is, if Site A appeared early in Run 1 it would tend to appear early in subsequent runs also. This is confirmation of the proposal that a spectrum of nucleating activity exists. Strong nucleators will renucleate early and in every run. Weak nucleators will tend to appear later, and perhaps not every time. Therefore, sites vary in their activity as nuclei.

CHAPTER VI

Conclusions

1. The nucleation curve consists of four regions: an induction period, a "foot" of gradually increasing nucleation rate, a linear portion of constant slope, and a levelling off to zero nucleation rate.
2. The reproducibility between runs becomes poorer as the crystallization temperature is raised.
3. Both the growth and nucleation rates increase greatly with supercooling.
4. The induction period increases as the supercooling decreases.
5. The final nucleation density reaches a maximum at about $T_c = 130^\circ\text{C}$ due to the high growth rate at lower crystallization temperatures.
6. The temperature coefficients for the growth and nucleation rates lead to an intermediate value for the difference between the substrate-melt and substrate-crystal interfacial energies. The interaction between the substrate and the polymer crystal is thus intermediate, leading to pseudohomogeneous nucleation behavior.
7. The degree of crystallinity of an iPS substrate, within the limits 0-35%, does not affect the nucleation kinetics of iPP.
8. The melting time of the iPP does not affect the nucleation kinetics, at least over the range 0-15 minutes.
9. The melting temperature greatly affects the nucleation rate and induction period. High melting temperatures lead to low nucleation rates and long induction periods.

10. Effects of substrate orientation on iPP nucleation were inconclusive.
11. Heterogeneous nuclei appear to be discrete and to vary in nucleating activity.

CHAPTER VII

SUGGESTIONS FOR FURTHER RESEARCH

While information has been gained about the activity and permanence of heterogeneous nuclei, their exact nature still remains a mystery. More insight may be gained by examining in a scanning electron microscope an iPS substrate which had been transcrystallized against. By scanning across the substrate and performing energy dispersive analysis, it may be possible to identify certain heterogeneities which share the same periodicity as the iPP nuclei. At the same time, a more accurate value of the nucleation density may be found using electron microscopy.

The dependence of the nucleation kinetics on the surface treatment of the substrate needs to be explored. All substrates in this study were prepared by cutting the film to the desired size. The cutting process itself might have introduced cracks and surface imperfections in which retained nuclei could readily form, enhancing nucleation. Other means of surface preparation should be employed, such as polishing or using free surfaces. It would be advisable in this case to use a more easily characterizable surface than iPS, such as a metal. The surface properties of iPS are not well-defined, and conclusive evidence is hard to gain with its use.

REFERENCES

1. B. J. Vonnegut, *J. Colloid Sci.*, 3, 563 (1948).
2. W. J. Barnes, W. G. Luetzel, and F. P. Price, *J. Phys. Chem.*, 65, 1742 (1961).
3. F. P. Price, *J. Am. Chem. Soc.*, 74, 311 (1952).
4. R. L. Cormia, F. P. Price, and D. Turnbull, *J. Chem. Phys.*, 37, 1333 (1962).
5. J. Inoue, *J. Poly. Sci., A*, 1, 2013 (1963).
6. A. G. M. Last, *J. Poly. Sci.*, 39, 543 (1959).
7. V. A. Kargin, T. I. Sogolova, and T. K. Shaposhnikova, *Dokl. Phys. Chem.*, 156, 612 (1964).
8. V. A. Kargin, T. I. Sogolova, and N. Ya. Rapoport-Molodtsova, *Poly. Sci. USSR*, 6, 2318 (1964).
9. V. A. Kargin, T. I. Sogolova, I. I. Kurbanova, *Dokl. Phys. Chem.*, 162, 467 (1965).
10. V. A. Kargin, T. I. Sogolova, and N. Ya. Rapoport-Molodtsova, *Dokl. Phys. Chem.*, 163, 600 (1965).
11. V. A. Kargin, T. I. Sogolova, and T. K. Shaposhnikova, *Poly. Sci. USSR*, 7, 250 (1965).
12. V. A. Kargin, T. I. Sogolova, and T. K. Shaposhnikova, *Poly. Sci. USSR*, 7, 423 (1965).
13. V. A. Kargin, T. I. Sogolova, and N. Ya. Rapoport-Molodtsova, *Poly. Sci. USSR*, 7, 631 (1965).
14. V. A. Kargin, T. I. Sogolova, and I. I. Kurbanova, *Poly. Sci. USSR*, 7, 2308 (1965).

15. V. A. Kargin, T. I. Sogolova, N. Ya. Rapoport, and I. I. Kurbanova, *J. Poly. Sci., C*, 16, 1609 (1967).
16. A. Keller, *J. Poly. Sci.*, 15, 31 (1955).
17. A. Keller, *J. Poly. Sci.*, 21, 363 (1956).
18. H. N. Beck and H. D. Ledbetter, *J. Appl. Poly. Sci.*, 9, 2131 (1965).
19. H. N. Beck, *J. Poly. Sci., A-2*, 4, 631 (1966).
20. H. N. Beck, *J. Appl. Poly. Sci.*, 11, 673 (1967).
21. F. Rybnikar, *Kunststoffe*, 58, 515 (1968).
22. F. Rybnikar, *J. Appl. Poly. Sci.*, 13, 827 (1969).
23. F. Rybnikar, *Polymer*, 10, 747 (1969).
24. F. L. Binsbergen, *Polymer*, 11, 253 (1970).
25. B. Levy, *J. Appl. Poly. Sci.*, 5, 408 (1961).
26. H. Schonhorn, *J. Poly. Sci., B*, 5, 919 (1967).
27. H. W. Starkweather and R. E. Brooks, *J. Appl. Poly. Sci.*, 1, 236 (1959).
28. C. S. Barrett and T. B. Massalski, Structure of Metals, McGraw-Hill: New York, 1966, pp. 535-8.
29. E. Jenckel, E. Teege, and W. Hinrichs, *Kolloid - Z. z. Polym.*, 129, 19 (1952).
30. R. J. Barriault and L. F. Gronholz, *J. Poly. Sci.*, 18, 393 (1955).
31. B. B. Burnett and W. F. McDevit, *J. Poly. Sci.*, 20, 211 (1956).
32. R. K. Eby, *J. Appl. Phys.*, 35, 2720 (1964).
33. C. Gieniewski and R. S. Moore, *Macromolecules*, 2, 385 (1969).
34. K. Hara and H. Schonhorn, *J. Appl. Phys.*, 42, 4549 (1971).
35. H. Schonhorn, *J. Poly. Sci., B*, 2, 465 (1964).
36. J. A. Koutsky, A. G. Walton, and E. Baer, *J. Poly. Sci., B*, 5, 185 (1967).

37. H. Schonhorn and F. W. Ryan, *J. Poly. Sci.*, A-2, 6, 231 (1968).
38. H. Schonhorn, *Macromolecules*, 1, 145 (1968).
39. J. P. Luongo and H. Schonhorn, *J. Poly. Sci.*, A-2, 6, 1649 (1968).
40. D. Fitchmun and S. Newman, *J. Poly. Sci.*, B, 7, 301 (1969).
41. D. Fitchmun and S. Newman, *J. Poly. Sci.*, A-2, 8, 1545 (1970).
42. S. Y. Hobbs, *Nature: Phys. Sci.*, 234, (44), 12 (1971).
43. S. Y. Hobbs, *Nature: Phys. Sci.*, 239, (89), 28 (1972).
44. J. R. Shaner and R. D. Corneliussen, *J. Poly. Sci.*, A-2, 10, 1611 (1972).
45. A. M. Chatterjee, *Heterogeneous Nucleation in the Crystallization of High Polymers From the Melt*, Ph.D. Dissertation, University of Massachusetts, 1974.
46. R. K. Eby and J. P. Colson, *J. Acoust. Soc. Am.*, 39, 506 (1966).
47. T. K. Kwei, H. Schonhorn, and H. L. Frisch, *J. Appl. Phys.*, 38, 2512 (1967).
48. M. Takayanagi, *Mem. Fac. Eng. Kyushu Univ.*, 23, 1 (1963).
49. T. T. Wang, *J. Appl. Phys.*, 44, 2218 (1973).
50. S. Matsuoko, J. H. Daane, H. E. Bair, and T. K. Kwei, *J. Poly. Sci.*, B, 6, 87 (1968).
51. F. S. Cheng, J. L. Kardos, and T. L. Tolbert, *SPE J.*, 26, 62 (1970).
52. H. Schonhorn and F. W. Ryan, *J. Phys. Chem.*, 70, 3811 (1966).
53. K. Hara and H. Schonhorn, *J. Appl. Poly. Sci.*, 16, 1103 (1972).
54. D. Turnbull and J. C. Fisher, *J. Chem. Phys.*, 17, 71 (1949).
55. D. Turnbull, *J. Chem. Phys.*, 18, 198 (1950).
56. D. Turnbull, *J. Chem. Phys.*, 20, 411 (1952).
57. J. Brandrup and E. H. Immergut, eds., Polymer Handbook, Interscience: New York, 1966, p. VI-75.

58. R. S. Stein, *J. Appl. Phys.*, 32, 1280 (1961).
59. D. Margerison and G. C. East, Introduction to Polymer Chemistry, Pergamon Press: Oxford, 1967, pp. 101-118.
60. J. Brandrup and E. H. Immergut, eds., Polymer Handbook, Interscience: New York, 1966, p. IV-9.
61. *Ibid.*, p. III-6.
62. *Ibid.*, p. III-6.
63. A. Sharples, *Polymer*, 3, 250 (1962).
64. P. J. Flory and A. D. McIntyre, *J. Poly. Sci.*, 18, 592 (1955).
65. F. P. Price, Nucleation, ed. by A. C. Zettlemoyer, Marcel Dekker: New York, 1969, pp. 405-488.
66. D. Turnbull, *Trans. Am. Inst. Min. Met. Engrs.*, 175, 774 (1948).
67. L. Mandelkern, Crystallization of Polymers, McGraw-Hill, Inc.: New York, 1964, p. 226-8.
68. R. Buchdahl, R. L. Miller, and S. Newman, *J. Poly. Sci.*, 36, 215 (1959).
69. L. Mandelkern, *Chem. Revs.*, 56, 903 (1956).
70. S. Hoshino, E. Meinecke, J. Powers, R. S. Stein, and S. Newman, *J. Poly. Sci., A*, 3, 3041 (1965).
71. J. H. Magill, *Polymer*, 3, 35 (1962).
72. A. Packter and K. A. Sharif, *J. Poly. Sci., B*, 9, 435 (1971).
73. F. P. Price, *J. Am. Chem. Soc.*, 74, 311 (1952).
74. J. N. Hay, *J. Poly. Sci., A*, 3, 433 (1965).
75. W. Banks, M. Gordon and A. Sharples, *Polymer*, 4, 189 (1963).
76. F. J. Limbert and E. Baer, *J. Poly. Sci., A*, 1, 3317 (1963).
77. J. R. Collier and L. M. Neal, *Poly. Sci. and Eng.*, 9, 182 (1969).

78. A. I. Bykhovskii in Solid State Transformations, N. N. Sirota, F. K. Gorskii, and V. M. Varikash, eds., Consultants Bureau: New York, 1966, pp. 105-111.

TABLE I

CHARACTERIZATION DATA OF MATERIALS

Isotactic Polypropylene (Hercules Profax 6323)

Isotactic Content = 96 - 97%

Ash Content = 3.57%

Intrinsic Viscosity = 1.8 dl/gm in decalin at 135°C

\bar{M}_v = 209,000

T_m = 172.0 ± .2°C

Isotactic Polystyrene (Dow EP1340-128)

Isotactic Content = 85%

Ash Content = 0.025%

Ti Content < 1 ppm

Al Content < 1 ppm

\bar{M}_v = 515,000

T_m = 230.2 ± .2°C

TABLE II

DENSITY OF ISOTACTIC POLYSTYRENE SUBSTRATES

$\rho_a = 1.056$

$\rho_c = 1.11$

<u>iPS Sample</u>	<u>Density (g/cc)</u>	<u>Degree of Crystallinity (%)</u>
Film, pressed at 240°C and quenched to 0°C	1.056	0
Film, annealed for 2 hours at 150°C	1.070	27
Film, stretched at 115°C and quenched to 0°C	1.056	0
Amorphous Substrate, after 4 runs at $T_c = 120^\circ\text{C}$	1.071	34
Amorphous Substrate, after 4 runs at $T_c = 140^\circ\text{C}$	1.074	34
Annealed Substrate, after 4 runs at $T_c = 120^\circ\text{C}$	1.075	36
Annealed Substrate, after 4 runs at $T_c = 140^\circ\text{C}$	1.074	34
Amorphous Substrate, annealed for 5 minutes at 200°C and quenched	1.056	0

TABLE IIISPHERULITIC GROWTH RATE VERSUS T_c

T_c (°C)	G (cm/min $\times 10^4$)
120	67.3
125	10.9
130	8.3
131	6.6
132	5.8
133	5.3
134	2.7
135	2.6
136	2.3
137	1.7
138	1.4
139	1.05
140	0.97

$\ln G$ vs. $\frac{1}{T\Delta T}$

Least-square slope = -6.351×10^4 (°K)²

$\pm 1.086 \times 10^4$

TABLE IV

NUCLEATION RATE, INDUCTION PERIOD, AND NUCLEATION DENSITY FOR NUCLEATION OF IPP
AGAINST AN AS-PRESSED AMORPHOUS IPS SUBSTRATE (0% CRYSTALLINE)

Melt Treatment = 5 minutes at 200°C

T_c (°C)	RUN	I (nuclei/cm ² /min $\times 10^{-3}$)	Standard Deviation (%)	τ (min.)	Standard Deviation (%)	N_f^2 (nuclei/cm ² $\times 10^{-3}$)	Probable Error (nuclei/cm ² $\times 10^{-3}$)
120	1	163.4	5.1	0.134	2.4	43.7	4.6
	2	188.9	16.4	0.120	15.9	54.1	5.1
	3	221.6	9.1	0.155	7.6	55.3	6.4
	Representative Curve	191.3	15.2	0.136	13.0	50.6	4.5
125	1	133.2	6.8	0.593	2.7	87.2	11.7
	2	99.5	6.8	0.585	3.7	91.1	9.5
	3	108.3	4.2	0.604	1.7	85.0	9.8
	4	90.3	5.7	0.567	2.5	83.4	7.7
	Representative Curve	107.8	17.1	0.587	2.6	86.5	2.3

TABLE IV (cont.)

T_c (°C)	RUN	I (nuclei/cm ² /min $\times 10^{-3}$)	Standard Deviation (%)	τ (min.)	Standard Deviation (%)	N_f^2 (nuclei/cm ² $\times 10^{-3}$)	Probable Error (nuclei/cm ² $\times 10^{-3}$)
135	1	10.47	14.1	4.43	9.1	73.7	7.8
	2	8.77	9.6	5.43	5.7	73.1	9.7
	3	7.31	7.7	6.90	3.7	67.3	8.6
	4	9.76	12.0	7.85	4.0	70.9	9.6
	Representative	Curve	15.1	6.15	2.5	71.2	2.1
139	1	0.862	3.2	11.33	4.7	36.1	4.8
	2	1.071	9.1	18.69	7.6	39.0	6.2
	3	0.596	10.6	7.56	25.2	33.1	4.6
	4	0.790	8.8	17.68	6.4	25.7	3.4
	Representative	Curve	23.7	13.82	38.4	33.5	3.8
140	1	0.166	7.0	35.06	8.7	17.1	2.4
	2	0.131	17.6	13.37	17.0	8.5	0.8
	3	0.102	18.1	34.45	15.3	9.7	1.9
	4	0.079	11.5	52.65	15.6	13.4	2.0
	Representative	Curve	31.7	33.88	47.4	12.2	2.4
130	1	68.0	12.2	2.05	3.3	99.1	9.8

TABLE IV (cont.)

T_c (°C)	RUN	I (nuclei/cm ² /min $\times 10^{-3}$)	Standard Deviation (%)	τ (min.)	Standard Deviation (%)	N_f^2 (nuclei/cm ² $\times 10^{-3}$)	Probable Error (nuclei/cm ² $\times 10^{-3}$)
131	1	47.5	11.3	2.10	5.4	103.5	9.2
132	1	20.3	11.8	2.77	7.5	90.9	8.5
133	1	34.3	6.7	3.38	2.1	106.0	3.8
134	1	35.2	8.1	3.67	4.3	147.9	13.8
135	1	7.11	10.2	8.58	6.1	83.0	8.7
136	1	3.27	6.5	10.0	6.2	71.4	8.8
137	1	3.94	5.3	19.1	2.0	61.7	5.8
138	1	2.73	4.3	10.9	2.0	47.9	5.1

TABLE V

LEAST-SQUARE PARAMETERS FOR PLOT OF $\ln I$ vs $\frac{1}{T\Delta T}$

(Figure 22)

	Slope (°K) ⁺² x 10 ⁻⁵	Standard Deviation (°K) ⁺² x 10 ⁻⁵	Y-Intercept	Standard Deviation
Samples with Unannealed Substrates	-2.51	0.7	25.5	0.8
Samples with Annealed Substrates	-2.49	0.3	24.9	0.5
Samples with Annealed or Unannealed Substrates	-2.45	0.6	25.0	0.7

TABLE VI

LEAST-SQUARE PARAMETERS FOR PLOT OF $\ln I$ vs $\frac{1}{T(\Delta T)^2}$
 (Figure 23)

	Slope (°K) ⁺³ x 10 ⁻⁶	Standard Deviation (°K) ⁺³ x 10 ⁻⁶	Y-Intercept	Standard Deviation
Samples with Unannealed Substrates	-4.77	1.05	17.52	0.69
Samples with Annealed Substrates	-4.69	0.41	16.96	0.34
Samples with Annealed or Unannealed Substrates	-4.66	0.88	17.22	0.62

TABLE VII

NUCLEATION RATE, INDUCTION PERIOD, AND NUCLEATION DENSITY FOR NUCLEATION OF iPP
AGAINST AN ANNEALED iPS SUBSTRATE (27% CRYSTALLINE)

Melt Treatment = 5 minutes at 200°C

T _c	RUN	I (nuclei/cm ² /min x 10 ⁻³)	Standard Deviation (%)	τ (min.)	Standard Deviation (%)	N _f (nuclei/cm ² x 10 ⁻³)	Probable Error (nuclei/cm ² x 10 ⁻³)
120	1	302.1	15.6	0.158	6.8	65.7	6.8
	2	215.3	3.8	0.174	2.2	50.2	12.2
	3	275.3	4.4	0.103	4.0	62.2	9.3
	4	245.1	2.5	0.159	13.9	69.7	6.9
Representative Curve		259.5	14.5	0.148	21.0	61.8	5.7
125	1	111.7	2.5	0.492	1.0	54.4	6.8
	2	110.5	10.8	0.540	3.7	52.2	6.9
	3	102.8	10.8	0.493	4.3	51.0	5.7
	4	67.0	12.5	0.584	5.0	34.9	3.6
Representative Curve		97.98	21.5	0.527	8.4	48.0	5.9

TABLE VII (cont.)

T_c	RUN	I (nuclei/cm ² /min $\times 10^{-3}$)	Standard Deviation (%)	τ (min.)	Standard Deviation (%)	N_f (nuclei/cm ² $\times 10^{-3}$)	Probable Error (nuclei/cm ² $\times 10^{-3}$)
130	1	34.26	9.0	1.512	3.7	71.4	11.8
	2	36.00	11.3	1.693	5.3	62.2	7.5
	4	24.99	7.2	1.947	3.7	61.8	5.7
	Representative Curve		31.75	18.6	1.717	12.8	65.0
135	1	5.93	6.0	5.40	3.8	48.3	5.7
	2	10.59	7.0	5.31	2.6	57.4	5.1
	3	9.66	7.8	5.76	3.2	57.8	4.6
	4	8.56	14.6	5.55	7.6	62.5	5.9
Representative Curve		8.68	23.3	5.51	3.9	56.2	4.0
140	1	0.374	5.3	22.70	7.9	29.9	3.7
	2	0.207	8.6	22.56	13.1	22.1	3.7
	3	0.237	20.6	33.55	19.8	18.5	2.8
	4	0.256	6.6	24.51	10.6	23.5	2.8
Representative Curve		0.269	27.2	25.83	20.2	23.5	3.2

TABLE VIII

LEAST-SQUARE PARAMETERS FOR THE PLOT OF LOG τ vs LOG ΔT

(Figure 24)

$[\tau \alpha \Delta T^{-\epsilon}]$

	Slope, $\frac{1}{\epsilon}$	Standard Deviation	ϵ	Standard Deviation
Samples with Unannealed Substrates	-9.2×10^{-2}	2.6×10^{-2}	10.87	3.08
Samples with Annealed Substrates	-9.57×10^{-2}	0.4×10^{-2}	10.45	0.46
Samples with Annealed or Unannealed Substrates	-9.30×10^{-2}	1.1×10^{-2}	10.75	1.27

TABLE IX

NUCLEATION RATE, INDUCTION PERIOD, AND NUCLEATION DENSITY FOR
 NUCLEATION OF IPP AGAINST AN ANNEALED IPS SUBSTRATE

Melt Temperature = 200°C

Crystallization Temperature = 135°C

Melt Time (min.)	I (nuclei/cm ² /min. x 10 ⁻³)	Standard Deviation (%)	τ (min.)	Standard Deviation (%)	N _f (nuclei/cm ²) x 10 ⁻³	Probable Error (nuclei/cm ²) x 10 ⁻³
0	5.45	9.6	5.83	6.8	53.6	6.1
5	5.93	6.0	5.40	3.8	48.3	5.7
1.5	6.44	7.3	5.32	5.5	65.1	7.8

TABLE X

NUCLEATION RATE, INDUCTION PERIOD, AND NUCLEATION DENSITY FOR

NUCLEATION OF IPP AGAINST AN ANNEALED IPS SUBSTRATE

Melt Time = 5 minutes

Crystallization Temperature = 135°C

Melt Temperature (°C)	I (nuclei/cm ² /min x 10 ⁻³)	Standard Deviation (%)	τ (min.)	Standard Deviation (%)	N _f (nuclei/cm ²) x 10 ⁻³	Probable Error (nuclei/cm ²) x 10 ⁻³
180	7.67	18.5	3.93	18.8	67.5	7.0
200	5.93	6.0	5.40	3.8	48.3	5.7
220	3.86	8.3	14.05	4.0	71.6	5.3
250	0.212	11.7	8.10	11.7	4.4	0.7

TABLE XI

ORIENTATION FUNCTIONS OF STRETCHED FILMS

$$\Delta = \Delta_{am}^{\circ} f_{\epsilon}$$

$$f_{\epsilon} = \frac{\Delta}{\Delta_{am}^{\circ}} = \frac{\Delta}{-.161}$$

	Elongation	Birefringence	f_{ϵ}
Film #1	120%	-5.27×10^{-3}	3.28×10^{-2}
Film #2	60%	-1.17×10^{-3}	0.73×10^{-2}

TABLE XII

NUCLEATION RATE, INDUCTION PERIOD, AND NUCLEATION DENSITY FOR

NUCLEATION OF iPP AGAINST AN AMORPHOUS iPS SUBSTRATE

Melt Treatment = 5 minutes at 200°C

Crystallization Temperature = 135°C

Elongation of iPS Substrate	Stretching Direction Orientation With Respect to Surface	I (nuclei/cm ² /min x 10 ⁻³)	Standard Deviation (%)	τ (min.)	Standard Deviation (%)	N _f (nuclei/cm ² x 10 ⁻³)	Probable Error (nuclei/cm ² x 10 ⁻³)
0%		10.47	14.1	4.43	9.1	73.7	7.8
120%	Parallel	3.56	5.9	4.07	9.5	68.8	11.8
60%	Perpendicular	7.20	7.5	4.46	3.9	50.4	4.8

TABLE XIII

REPETITION OF NUCLEATION AT SITES

T_c (°C)	Total Sites, x	Sites Nucleating Per Run, n	No. of Repeats	Frequency	Probability	Theoretical Probability
125	67	31	1	12	.179	.313
			2	11	.164	.405
			3	24	.358	.232
			4	20	.299	.050
130	85	53	1	14	.164	.136
			2	22	.259	.337
			3	32	.377	.372
			4	17	.200	.154
130	65	36	1	19	.291	.205
			2	18	.277	.381
			3	14	.216	.316
			4	14	.216	.098
135	71	25	1	38	.534	.465
			2	18	.254	.379
			3	8	.113	.137
			4	7	.099	.019
138	54	15	1	31	.573	.575
			2	15	.278	.332
			3	7	.130	.085
			4	1	.019	.008

TABLE XIII (cont.)

T_c (°C)	Total Sites, x	Sites Nucleating Per Run, n	No. of Repeats	Frequency	Probability	Theoretical Probability
139	45	12	1	28	.622	.592
			2	11	.244	.323
			3	4	.089	.078
			4	2	.045	.007
140	18	9	1	2	.111	.267
			2	6	.333	.400
			3	8	.445	.267
			4	2	.111	.067

FIGURE CAPTIONS

1. Model for the incoherent nucleation of a polymer against a substrate.
2. Photograph of time-lapse equipment:
 - a. Zeiss polarizing microscope
 - b. Mettler hot stage
 - c. Beam splitter
 - d. Bolex 16 mm movie camera
 - e. McLaughlin Intervalometer
 - f. Mettler control unit
3. Configuration of sample
4. Photomicrograph of typical iPS substrate with molten iPP against it.
5. Spherulitic growth rate and nucleation rate versus crystallization temperature.
6. Natural logarithm of the growth rate versus the quantity $\frac{1}{T(\Delta T)}$
7. Number of nuclei versus time for three consecutive runs at $T_c = 120^\circ\text{C}$, unannealed substrate.
8. Number of nuclei versus time for four consecutive runs at $T_c = 125^\circ\text{C}$, unannealed substrate.
9. Number of nuclei versus time for four consecutive runs at $T_c = 135^\circ\text{C}$, unannealed substrate.
10. Number of nuclei versus time for four consecutive runs at $T_c = 139^\circ\text{C}$, unannealed substrate.
11. Number of nuclei versus time for four consecutive runs at $T_c = 140^\circ\text{C}$, unannealed substrate.
12. Number of nuclei versus time for first run only at $T_c = 130^\circ\text{C}$, unannealed substrate.

13. Number of nuclei versus time for first run only at $T_c = 131^\circ\text{C}$, unannealed substrate.
14. Number of nuclei versus time for first run only at $T_c = 132^\circ\text{C}$, unannealed substrate.
15. Number of nuclei versus time for first run only at $T_c = 133^\circ\text{C}$, unannealed substrate.
16. Number of nuclei versus time for first run only at $T_c = 134^\circ\text{C}$, unannealed substrate.
17. Number of nuclei versus time for first runs only of two separate samples at $T_c = 136^\circ\text{C}$, unannealed substrates.
18. Number of nuclei versus time for first run only at $T_c = 137^\circ\text{C}$, unannealed substrate.
19. Number of nuclei versus time for first run only at $T_c = 138^\circ\text{C}$, unannealed substrate.
20. Representative curves of number of nuclei versus time of unannealed substrates for $T_c = 125, 130, 133, 135, 136, 137, 138, 139,$ and 140°C .
21. Nucleation rate versus crystallization temperature, annealed and unannealed substrates.
22. Natural logarithm of the nucleation rate versus the quantity $\frac{1}{T(\Delta T)}$ for unannealed and annealed substrates.
23. Natural logarithm of the nucleation rate versus the quantity $\frac{1}{T(\Delta T)^2}$ for unannealed and annealed substrates.
24. Logarithm of the supercooling, ΔT , versus the logarithm of the induction period, τ , for unannealed and annealed substrates.
25. The induction period versus the inverse of the nucleation rate.
26. Nucleation density, N_f , versus supercooling, ΔT , for annealed and unannealed substrates.

27. Photomicrographs of iPP crystallizing in contact with iPS at $T_c = 135^\circ\text{C}$ and 18 1/3 minutes after temperature equilibration. a) first run; b) second run; c) third run; d) fifth run; e) sixth run; f) seventh run.
28. Number of nuclei versus time for four consecutive runs at $T_c = 120^\circ\text{C}$, annealed substrate.
29. Number of nuclei versus time for four consecutive runs at $T_c = 125^\circ\text{C}$, annealed substrate.
30. Number of nuclei versus time for three consecutive runs at $T_c = 130^\circ\text{C}$, annealed substrate.
31. Number of nuclei versus time for four consecutive runs at $T_c = 135^\circ\text{C}$, annealed substrate.
32. Number of nuclei versus time for four consecutive runs at $T_c = 140^\circ\text{C}$, annealed substrate.
33. Representative curves of number of nuclei versus time of annealed substrates for $T_c = 120, 125, 130, 135$ and 140°C .
34. Number of nuclei versus time for three samples melted at 200°C for various times and crystallized at $T_c = 135^\circ\text{C}$. Melt times were 0 minutes (o), 5 minutes ([]), and 15 minutes (Δ).
35. Number of nuclei versus time for three samples melted for 5 minutes at various temperatures and crystallized at $T_c = 135^\circ\text{C}$. Melt temperatures were 180°C (o), 200°C ([]), 220°C (Δ), and 250°C (\bullet).
36. Photomicrographs showing the effect of melting temperature on the heterogeneous nucleation at the substrate. Photomicrograph (a) shows a sample that was melted at 200°C and quenched to $T_c = 135^\circ\text{C}$. The enhanced nucleation at the substrate is obvious. Photomicrograph (b) shows a similar sample that had been melted at $T_c = 250^\circ\text{C}$ and quenched to the same crystallization temperature, $T_c = 135^\circ\text{C}$. Few nuclei appear at the substrate.

37. Number of nuclei versus time for three samples with substrates of varying degrees of orientation. The melt treatments were identical: 5 minutes at 200°C. Orientations of the substrates were: 1) 120% elongation, stretching direction parallel to the plane against which the iPP nucleated ([]); 2) 60% elongation, stretching direction perpendicular to the plane against which the iPP nucleated (Δ); and 3) unoriented substrate (o).
38. Schematic diagram showing number of nuclei versus time for a) heterogeneous nucleation; b) homogeneous nucleation; and c) pseudo-homogeneous nucleation.

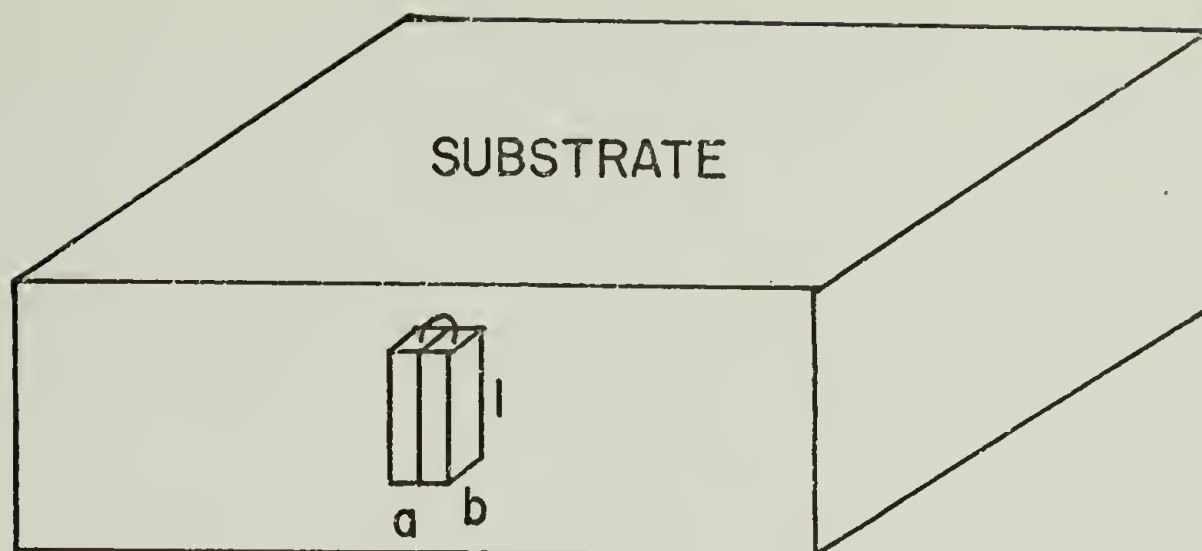


FIGURE 1

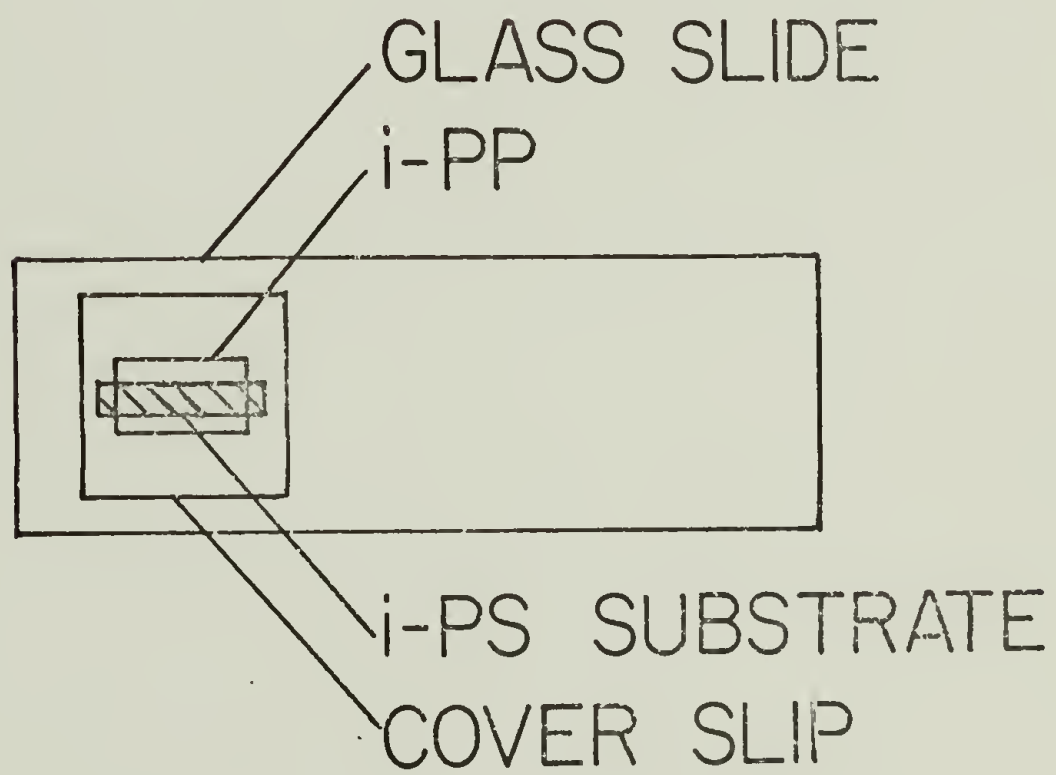


FIGURE 3

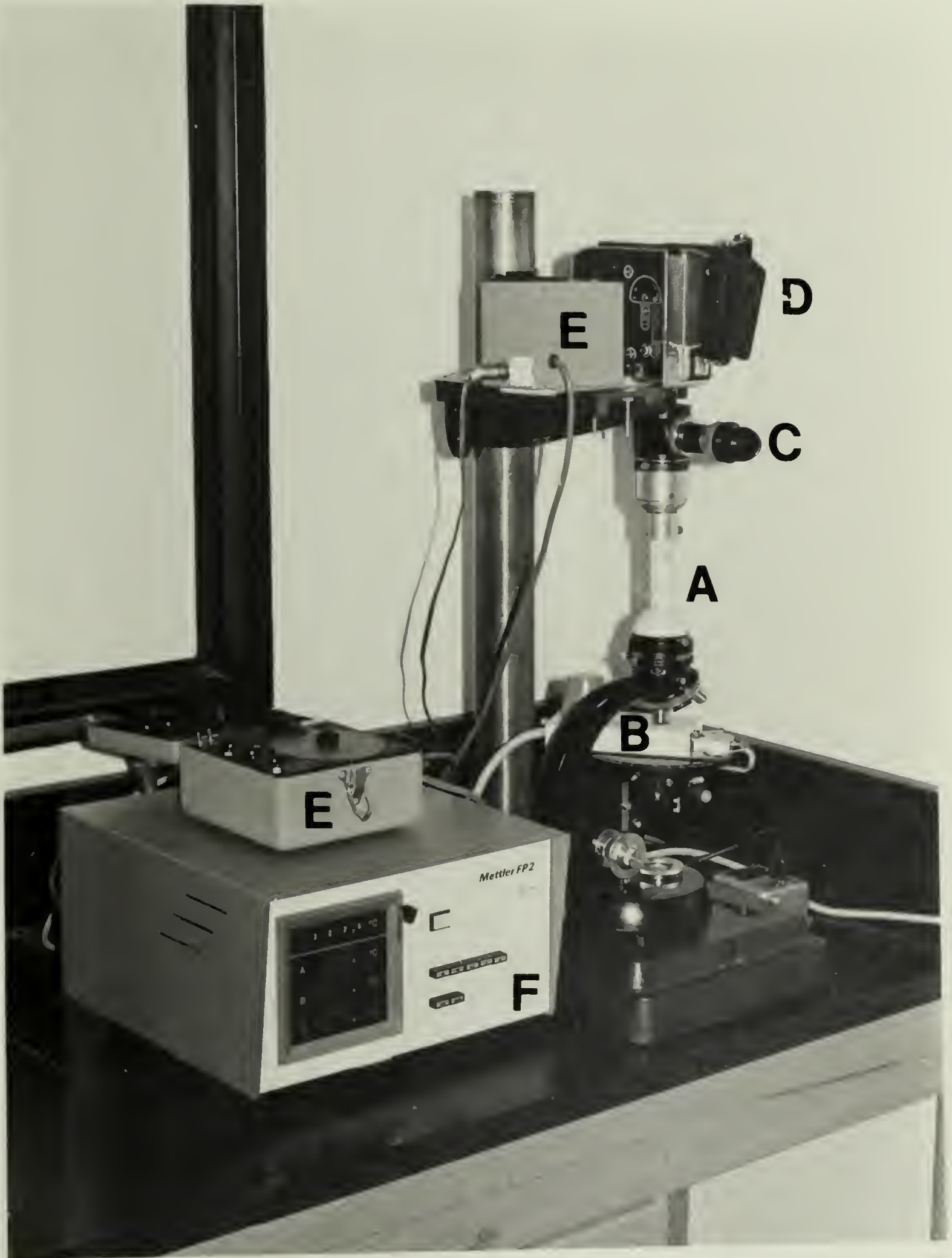


FIGURE 2

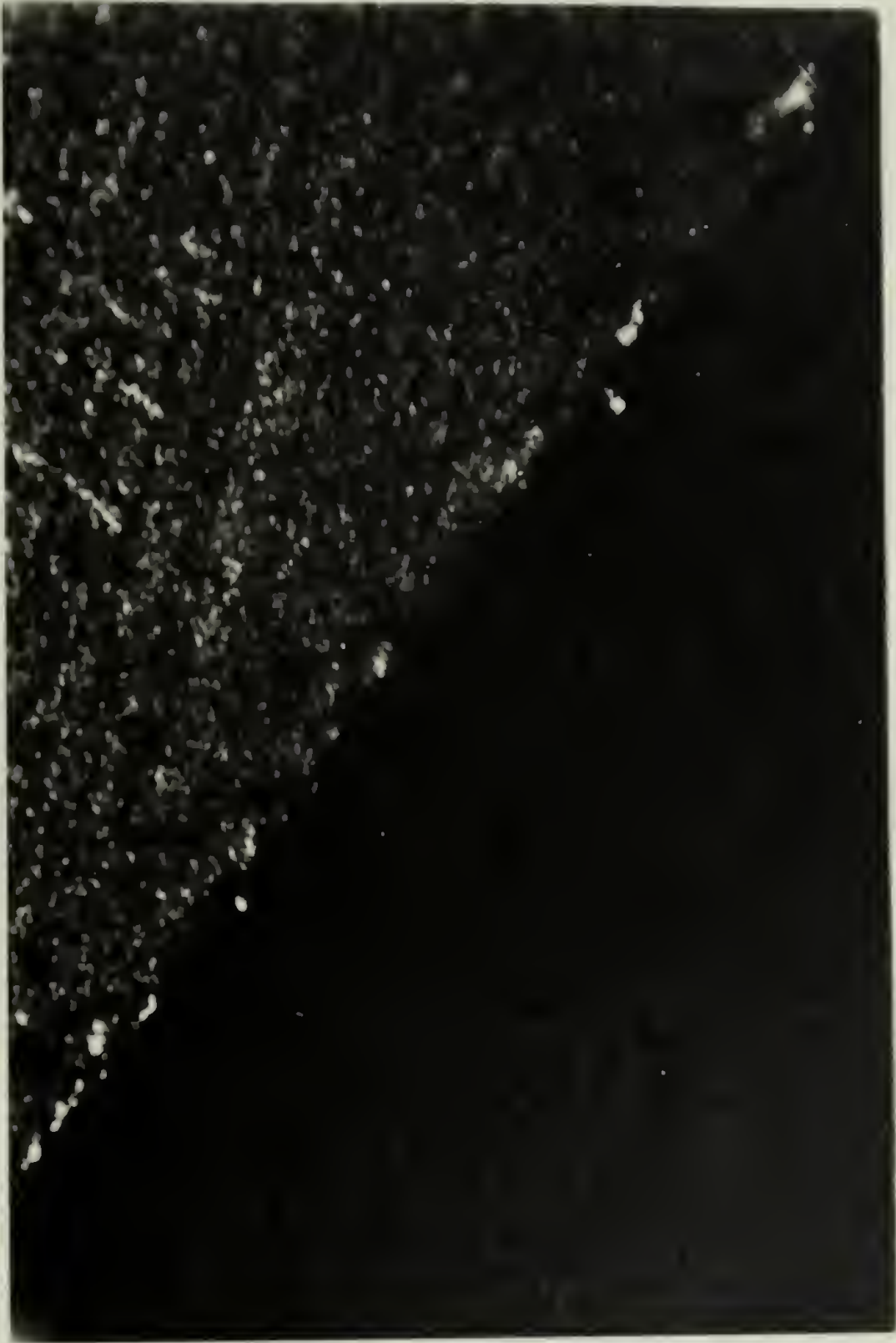


FIGURE 4

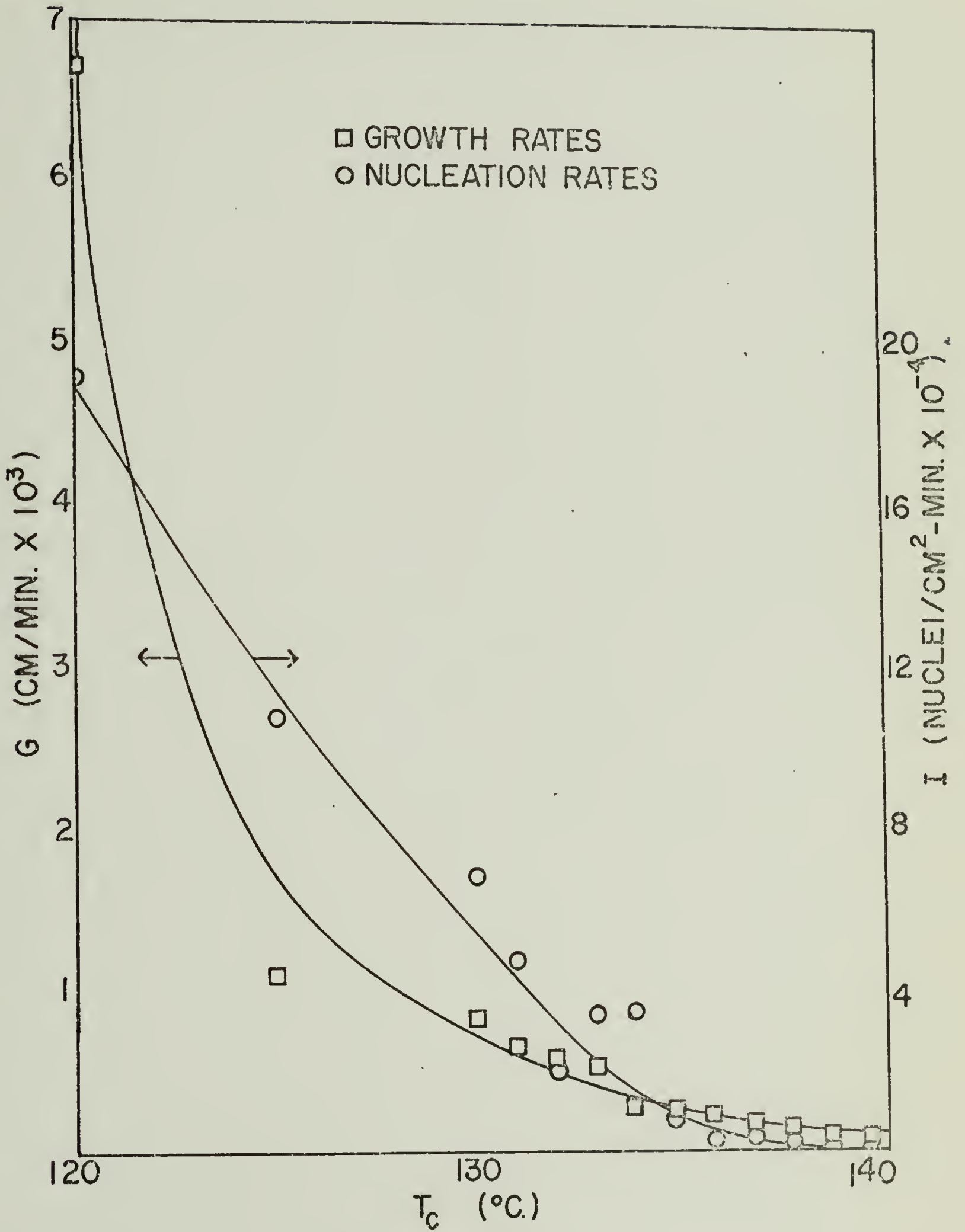


FIGURE 5

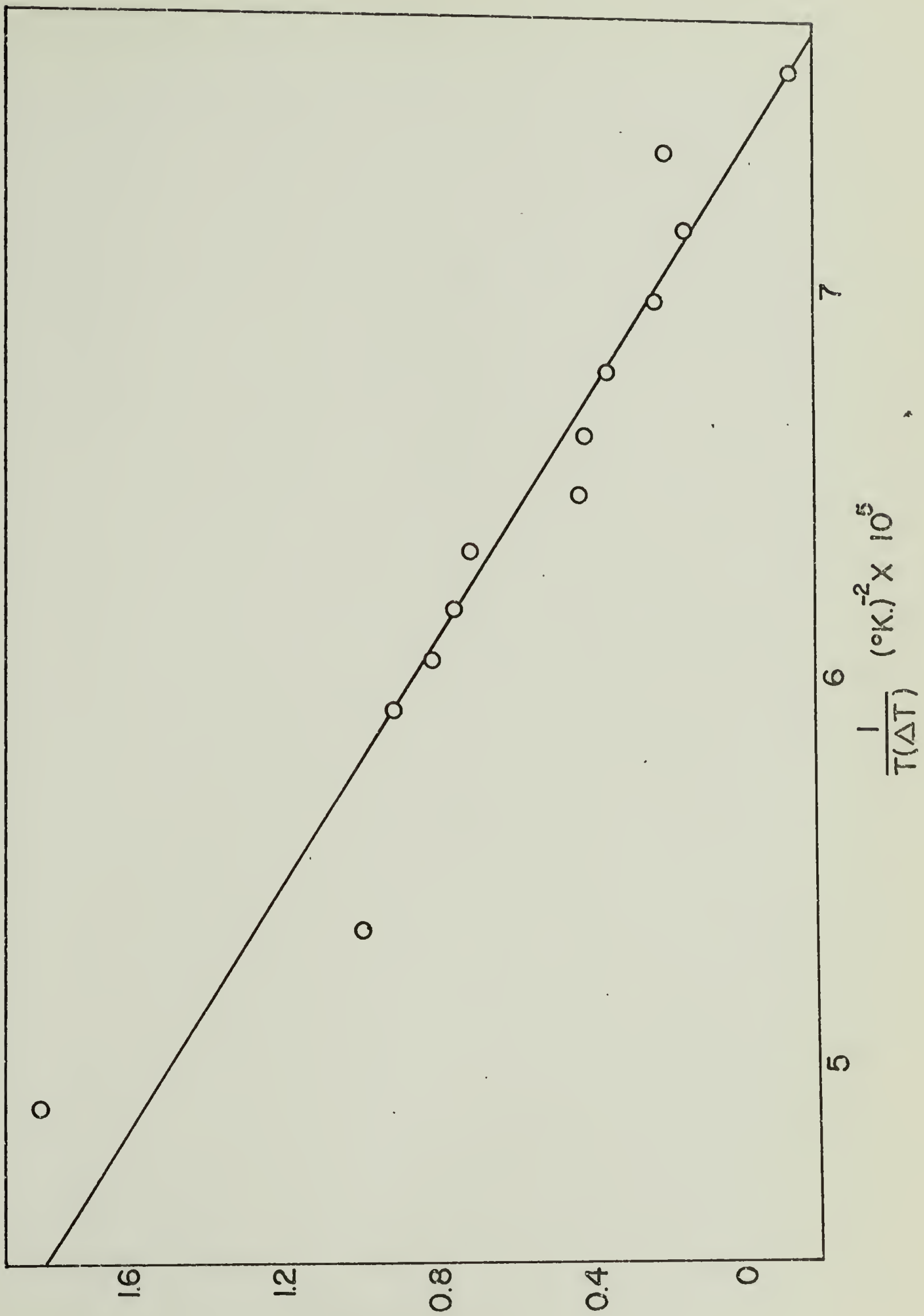
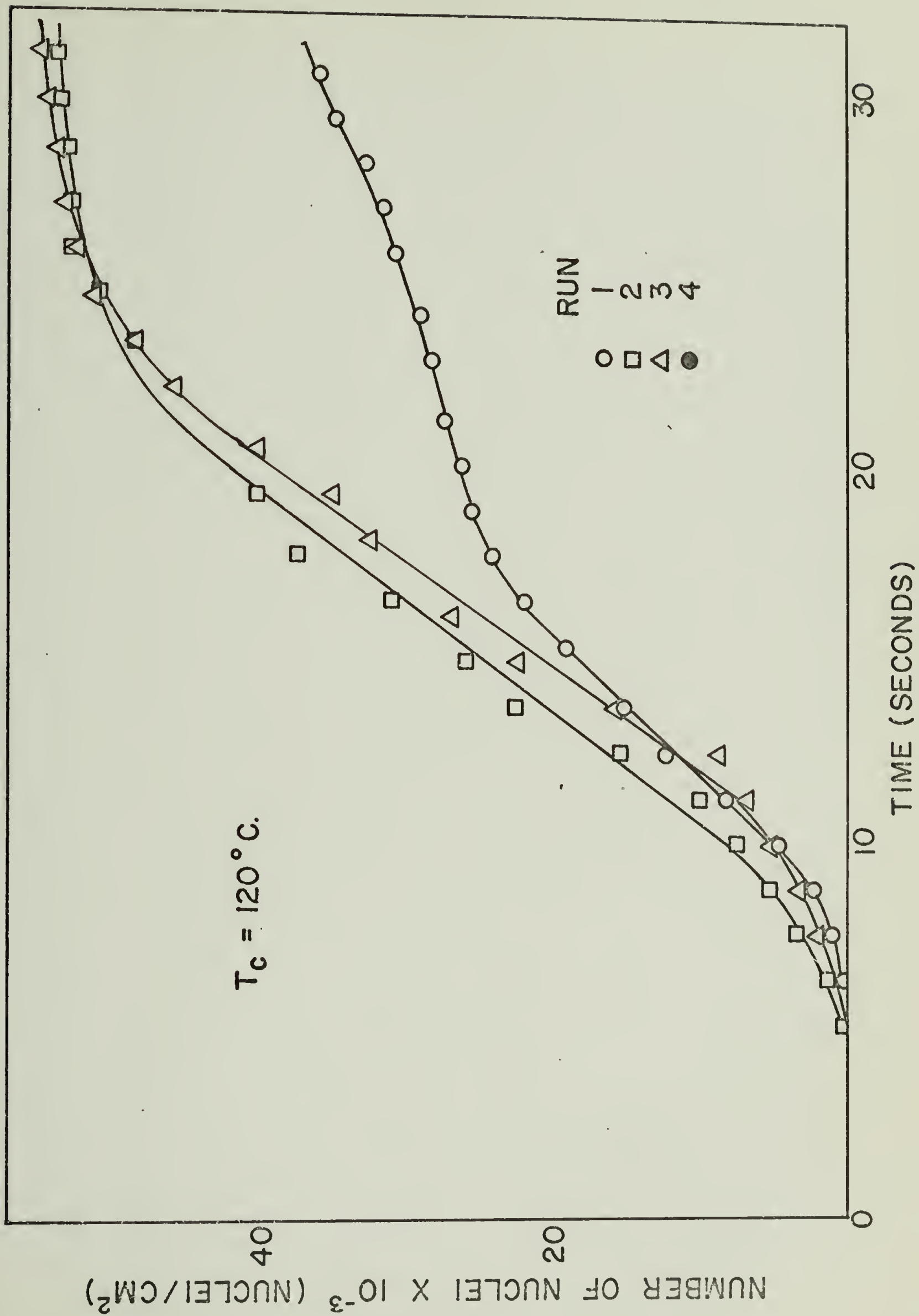


FIGURE 6
(ΔT)² × 10⁴



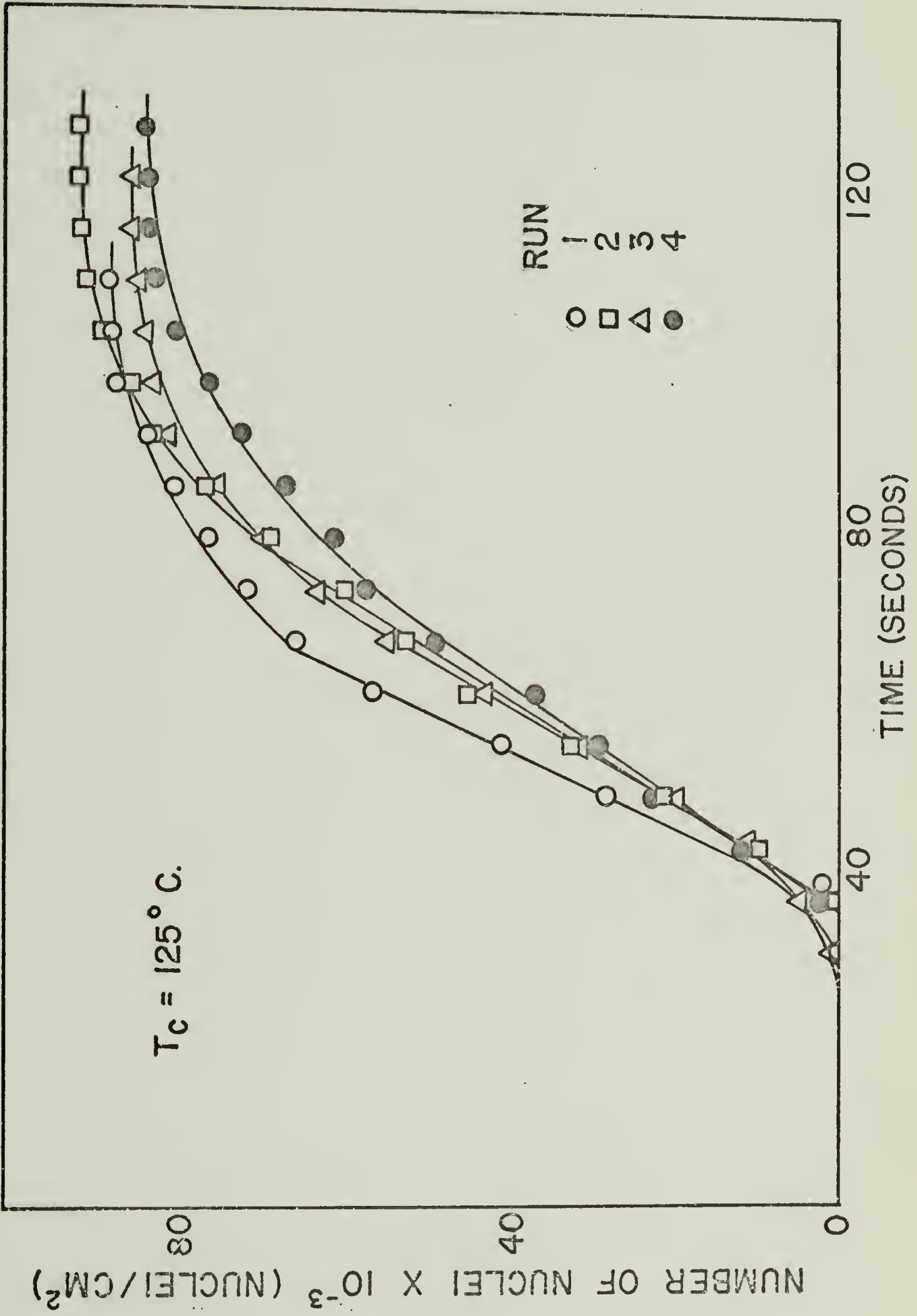


FIGURE 8

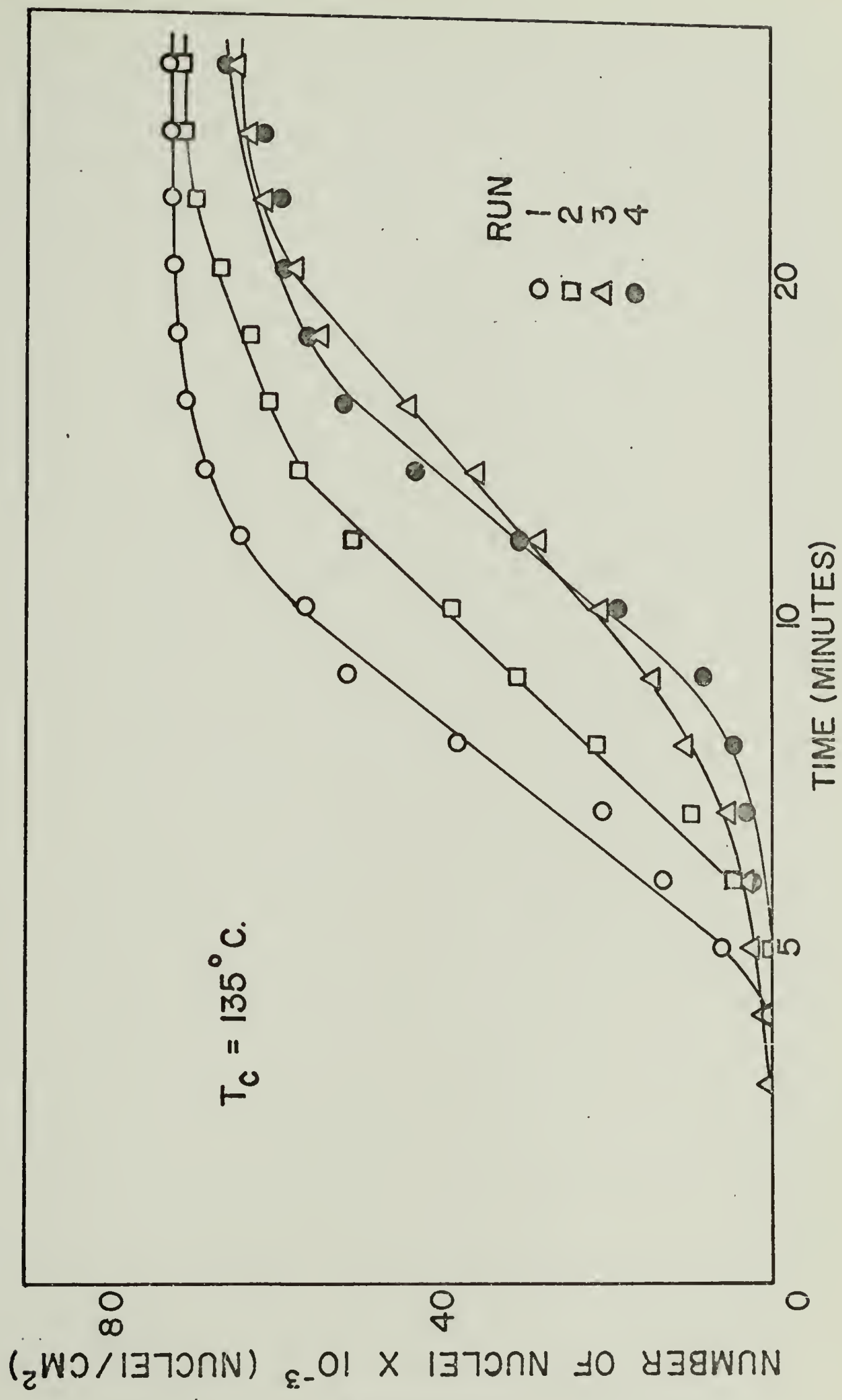


FIGURE 9

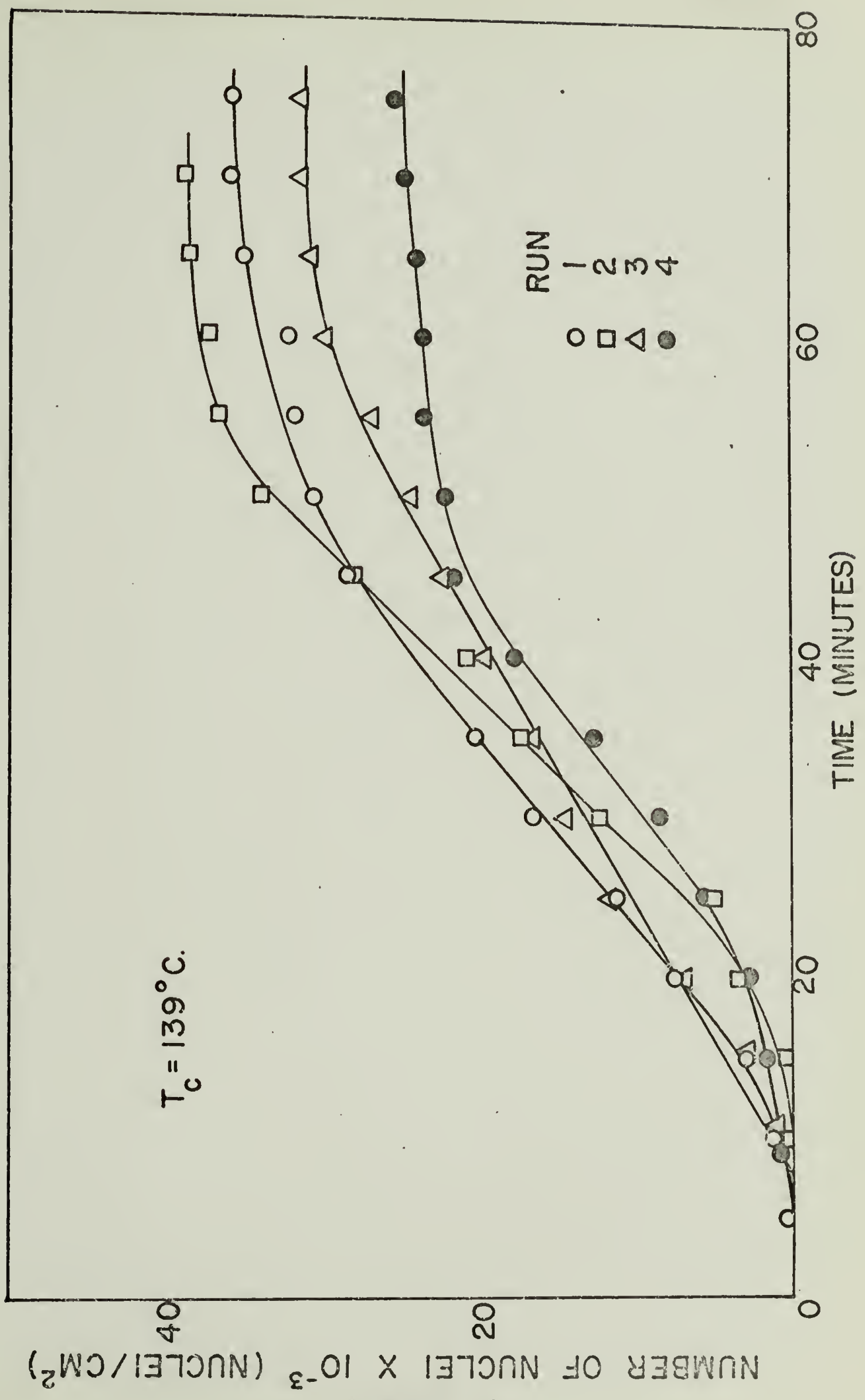


FIGURE 10

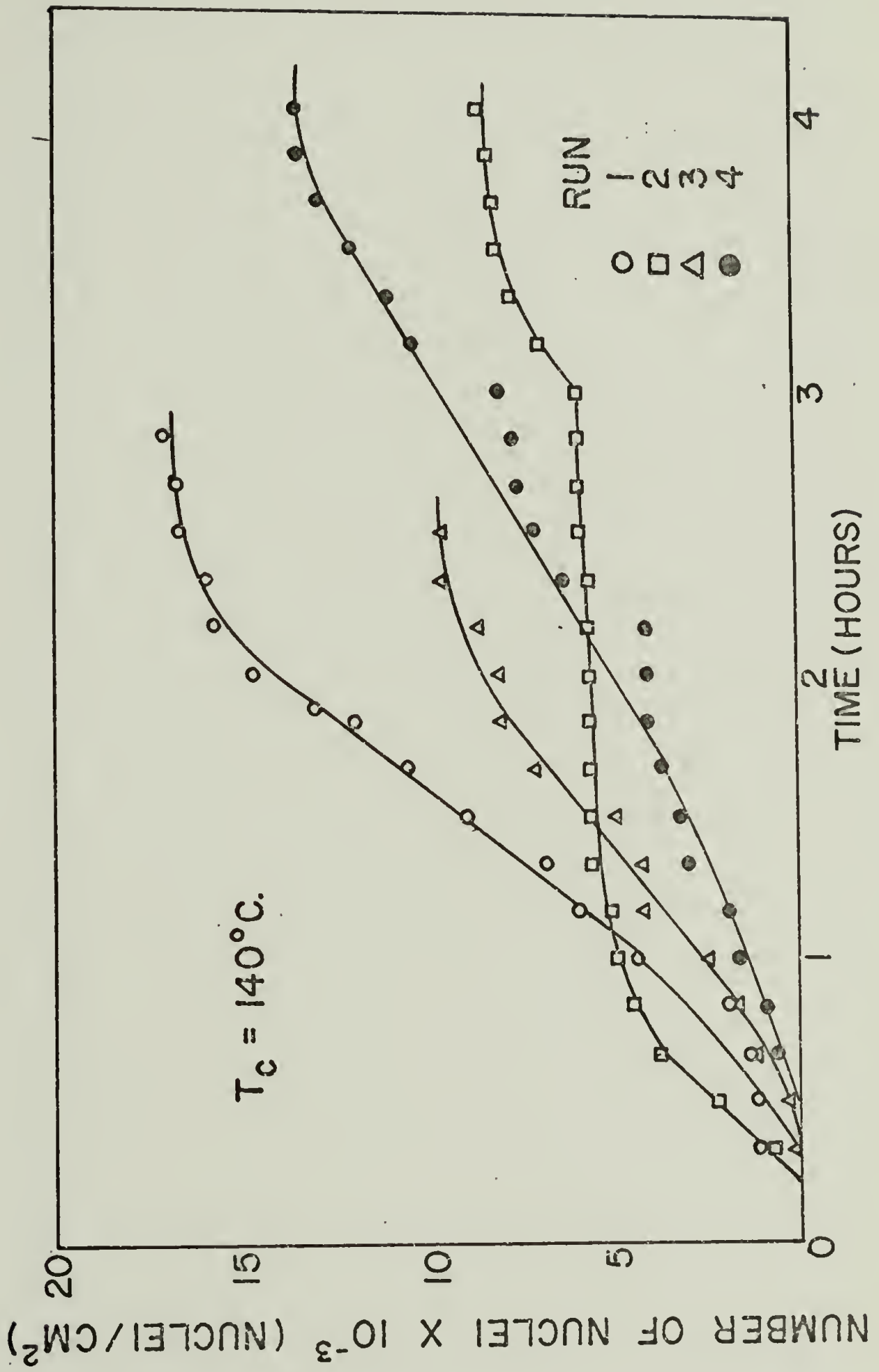


FIGURE II

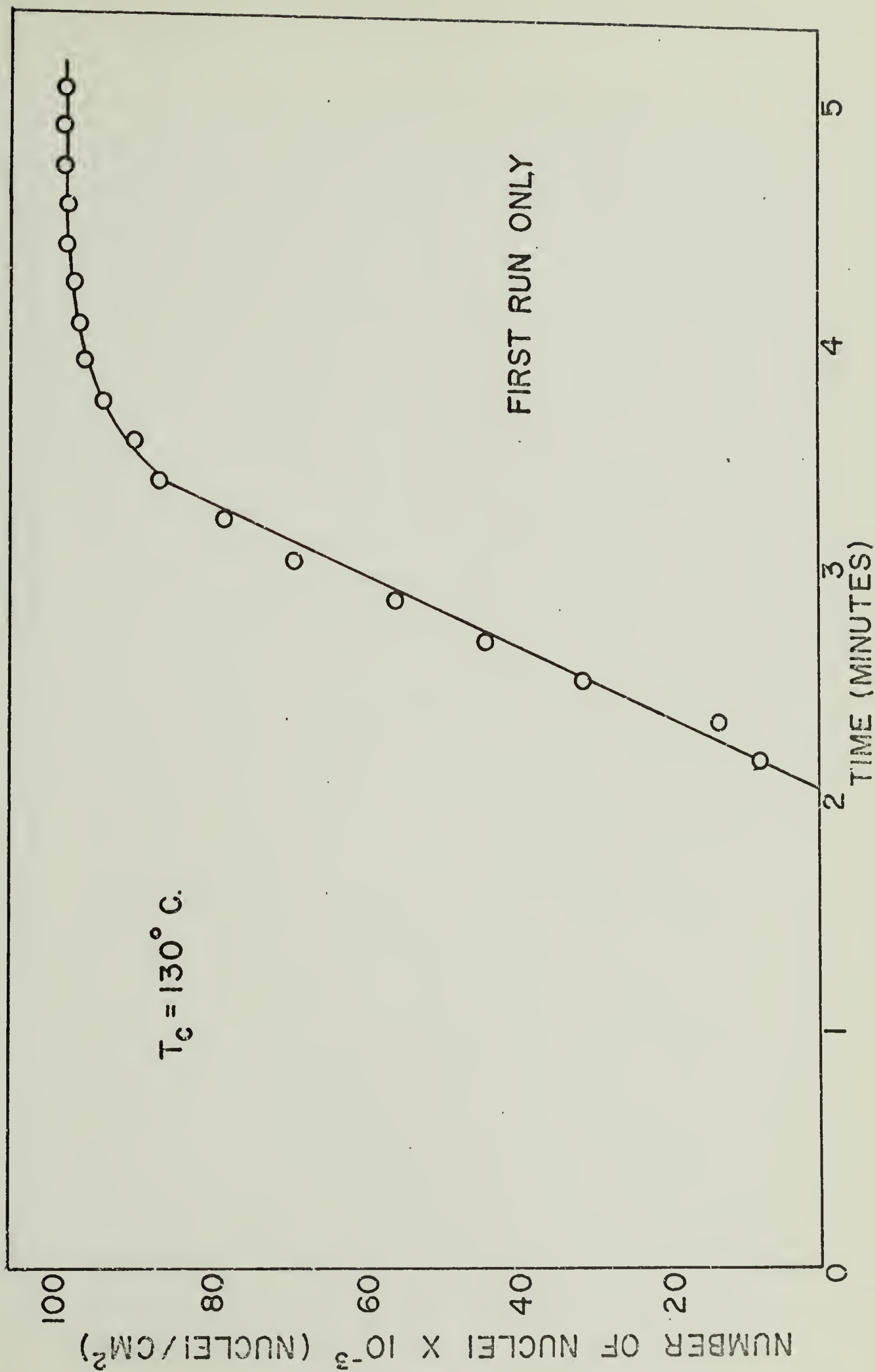


FIGURE 12

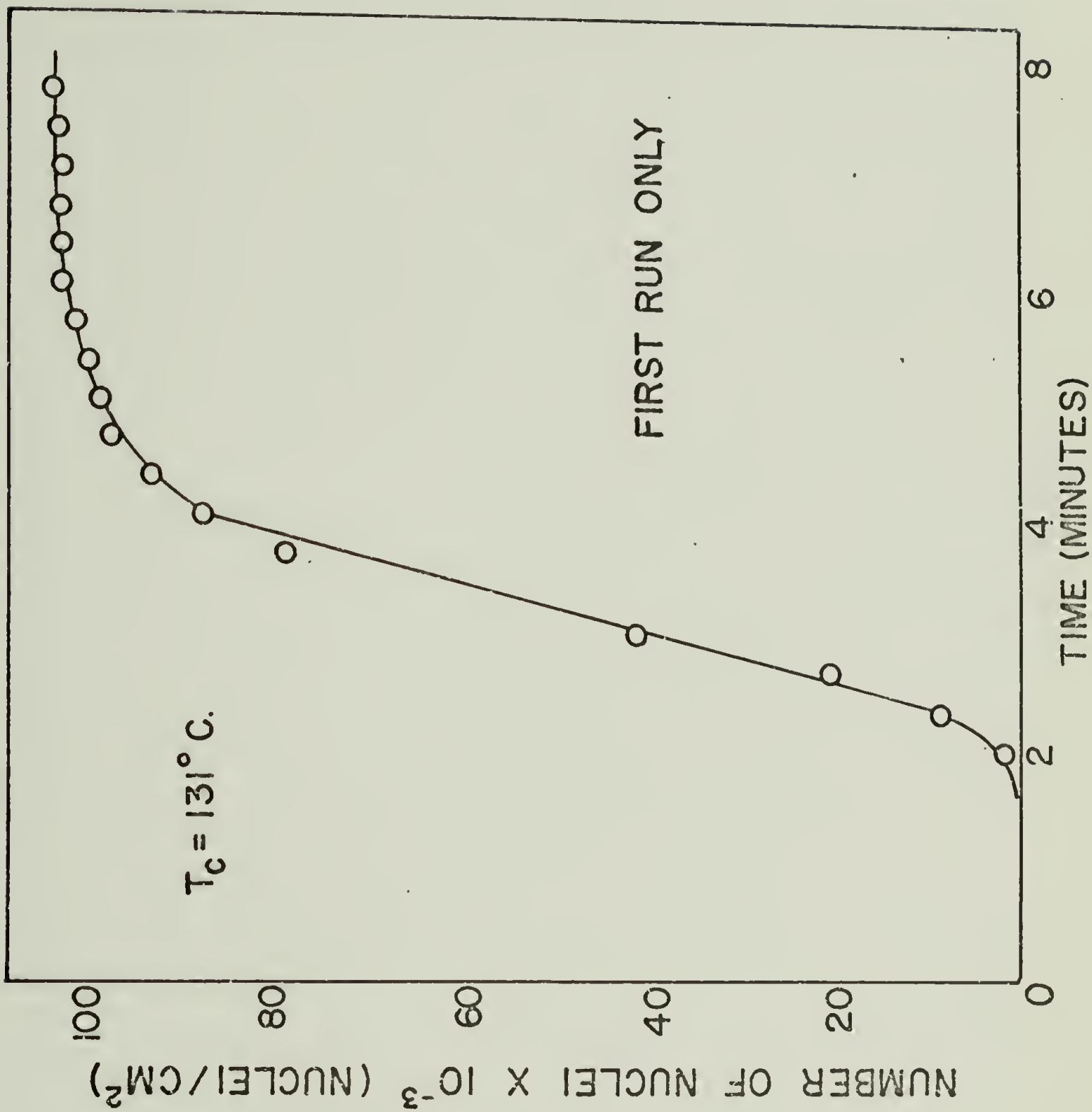


FIGURE 13

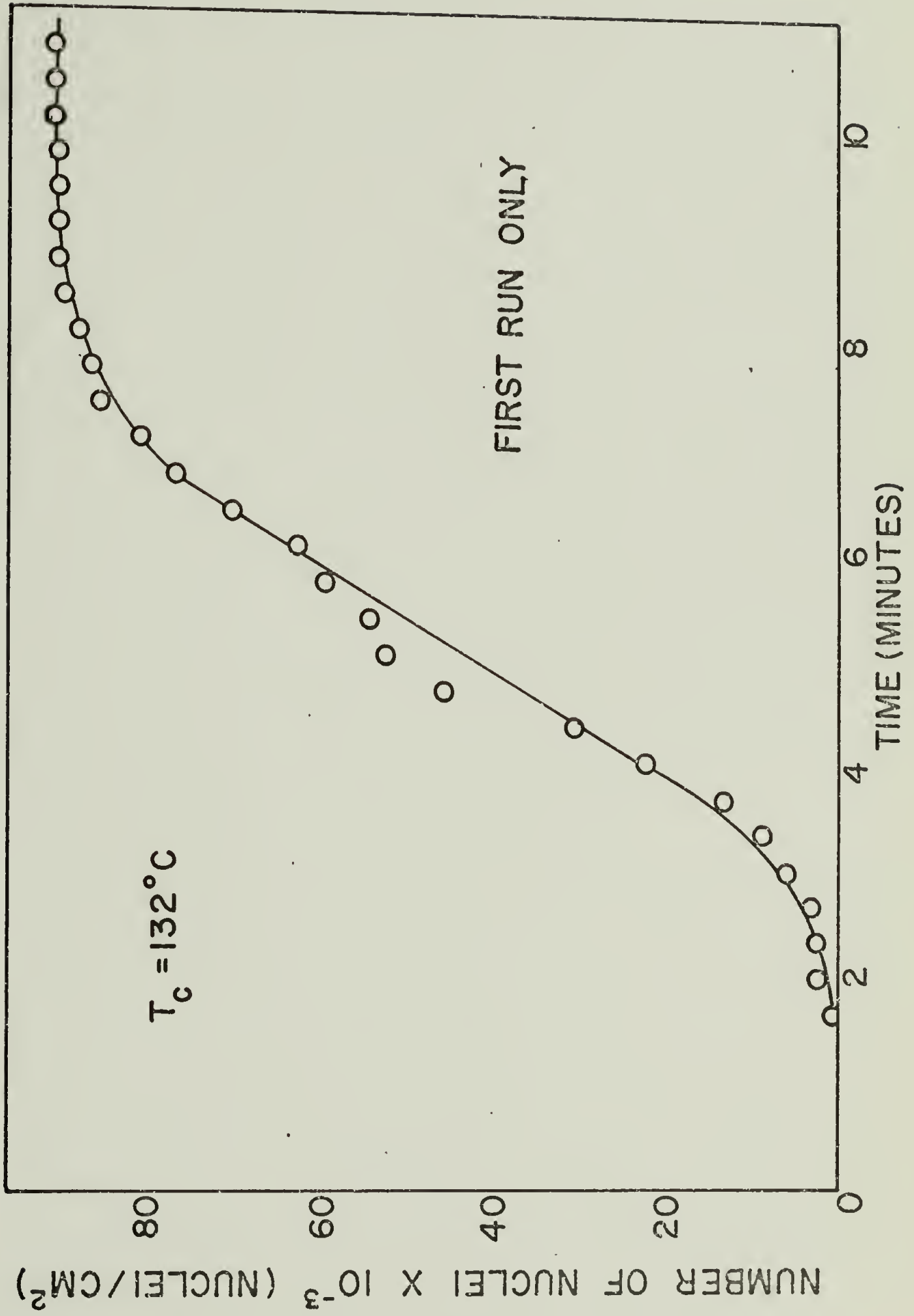


FIGURE 14

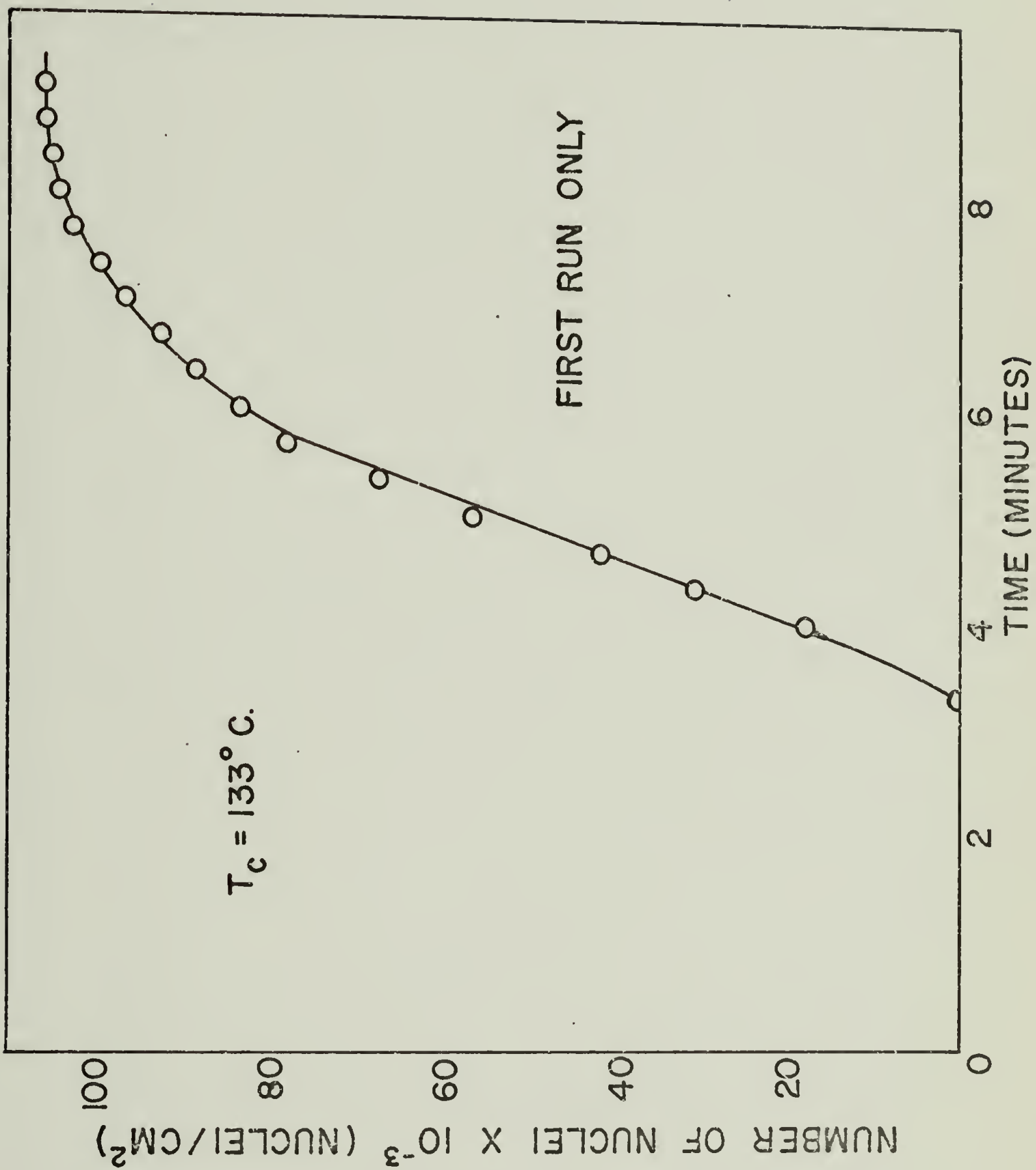


FIGURE 15

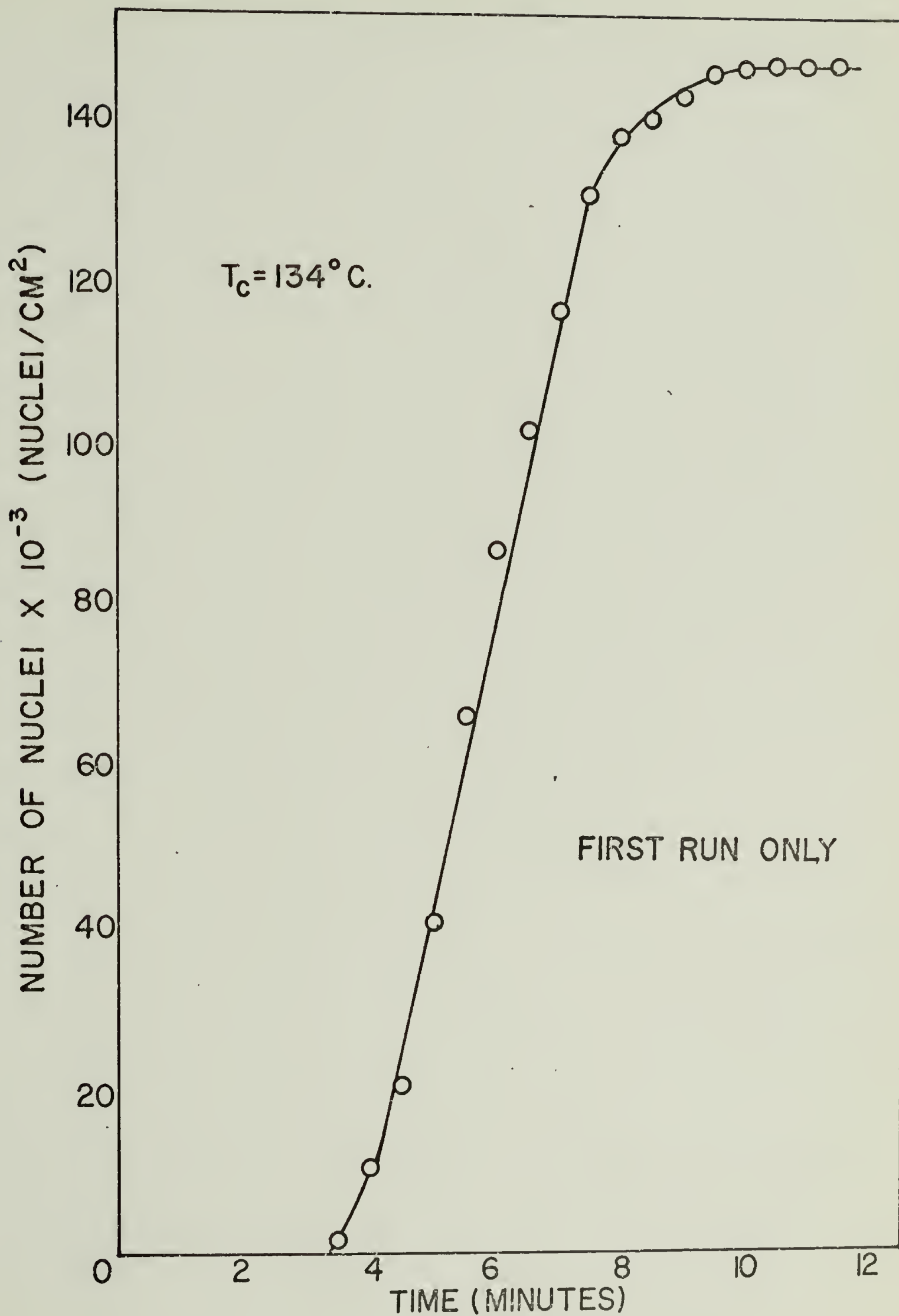


FIGURE 16

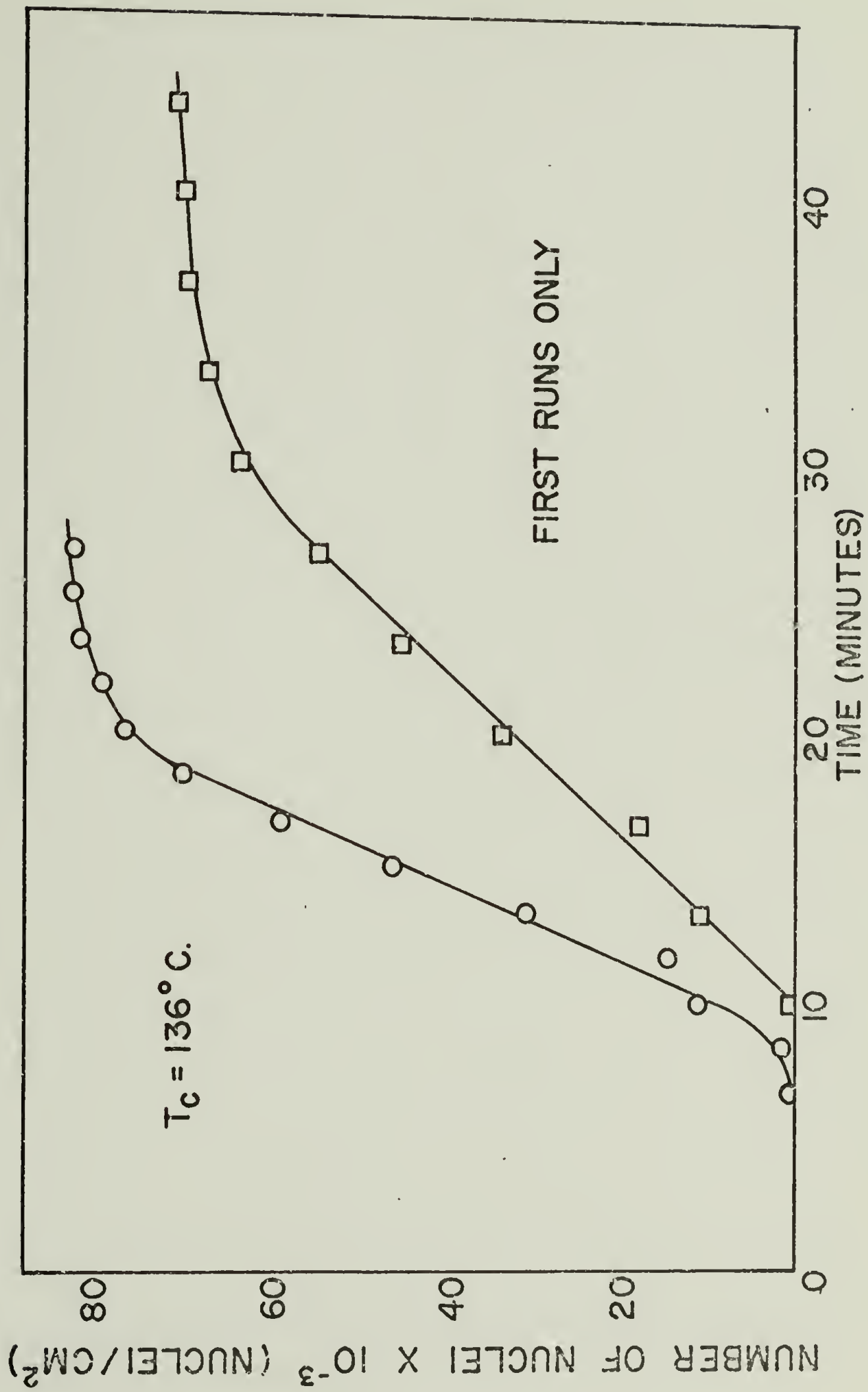


FIGURE 17

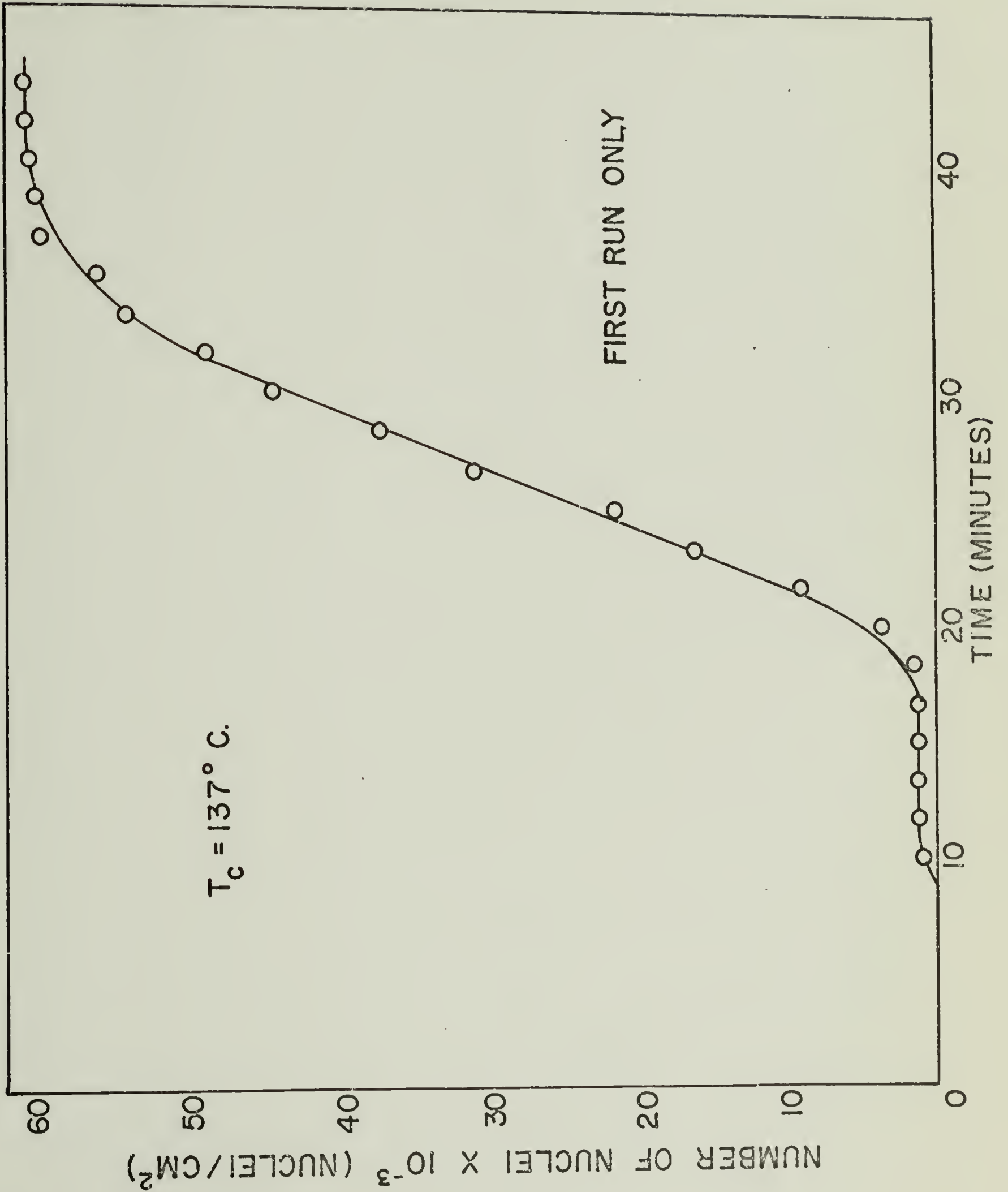


FIGURE 18

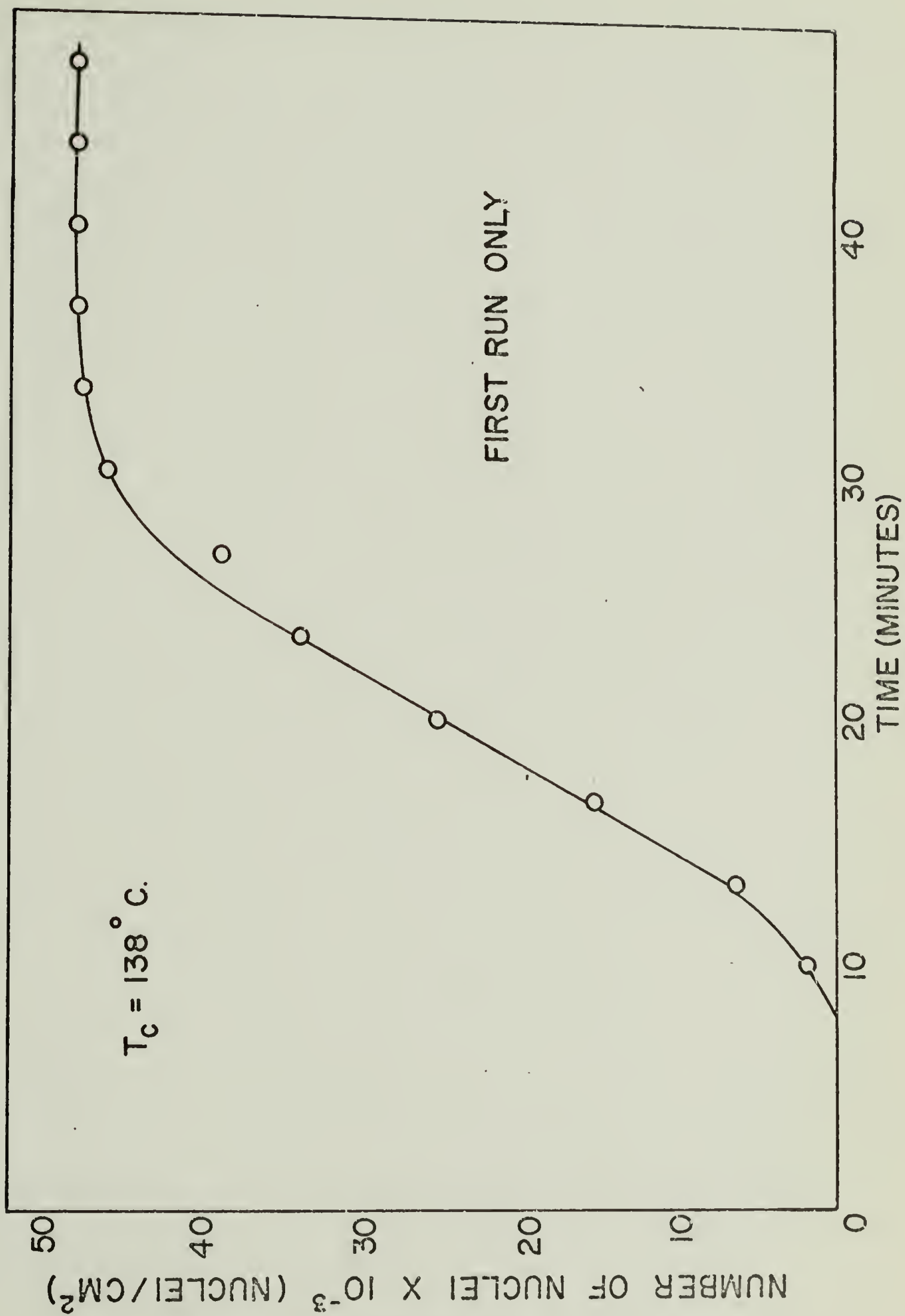


FIGURE 19

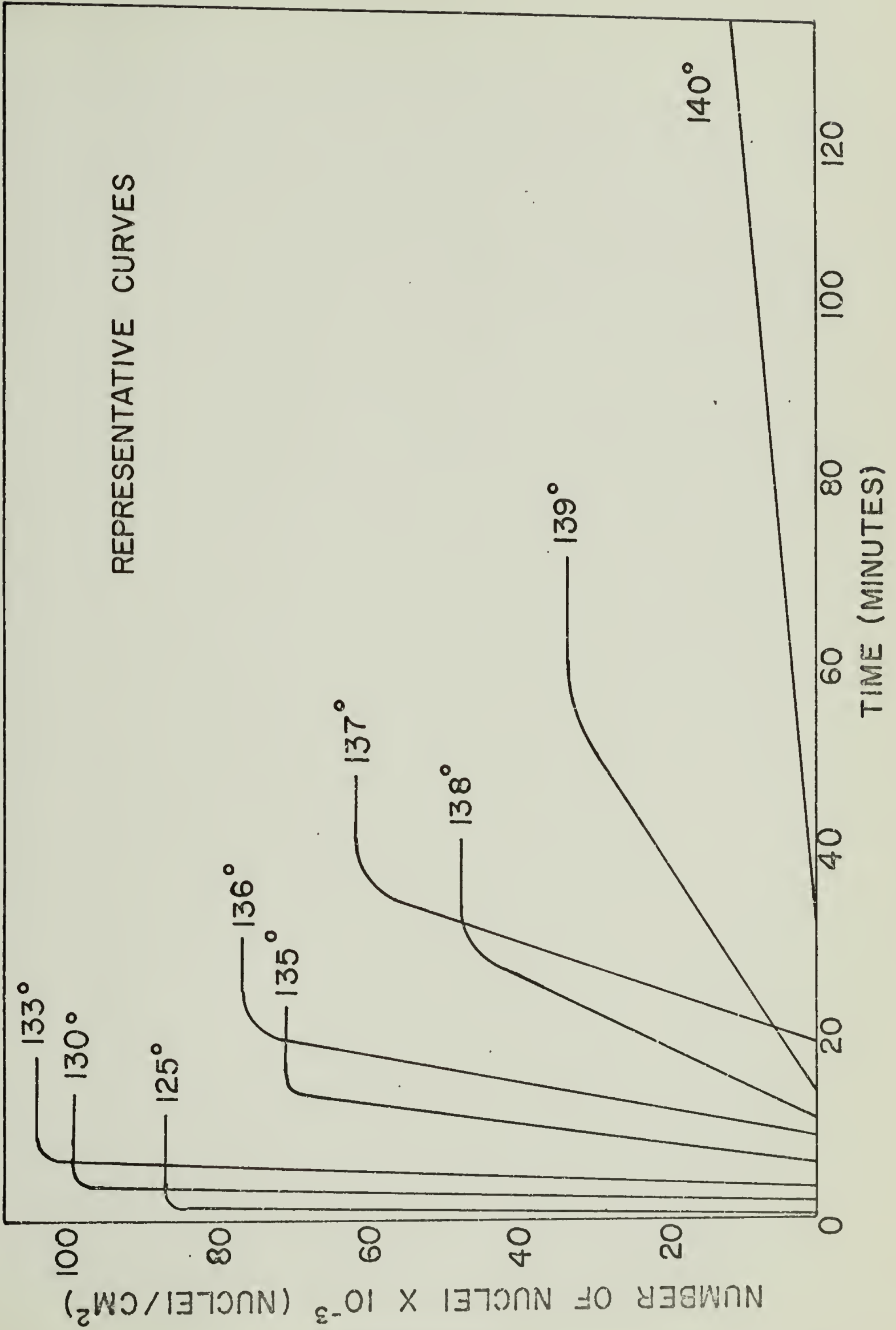


FIGURE 20

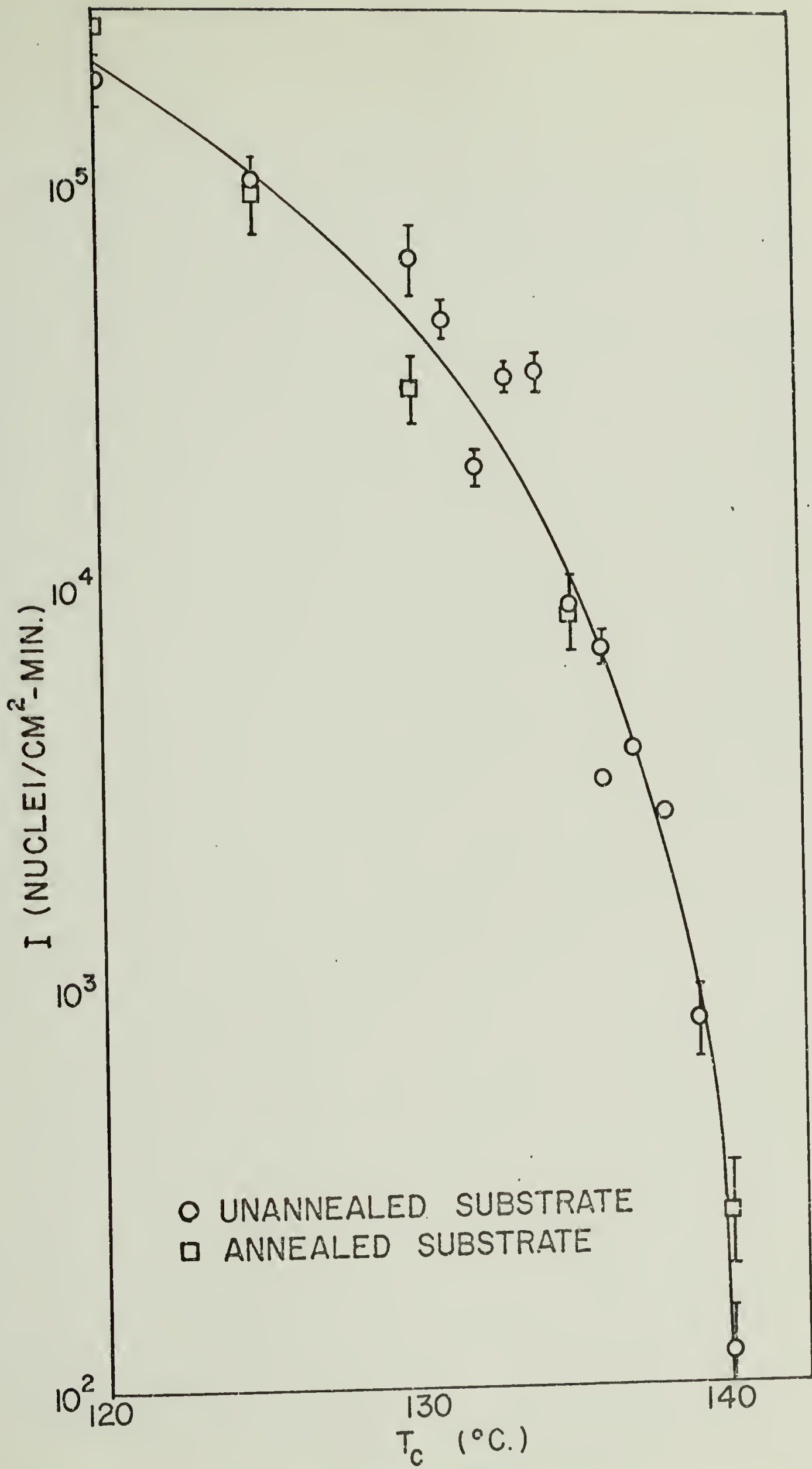


FIGURE 21

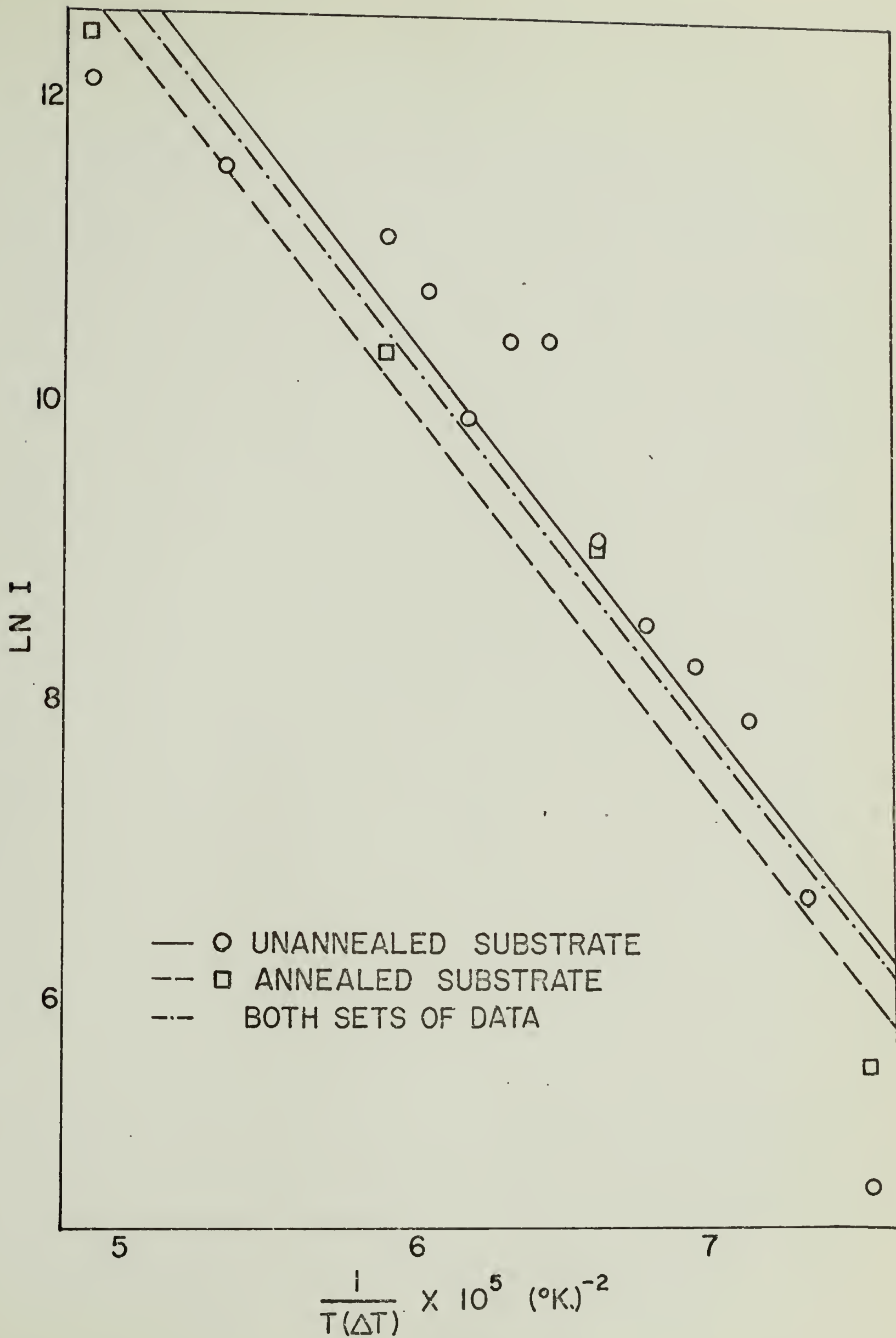


FIGURE 22

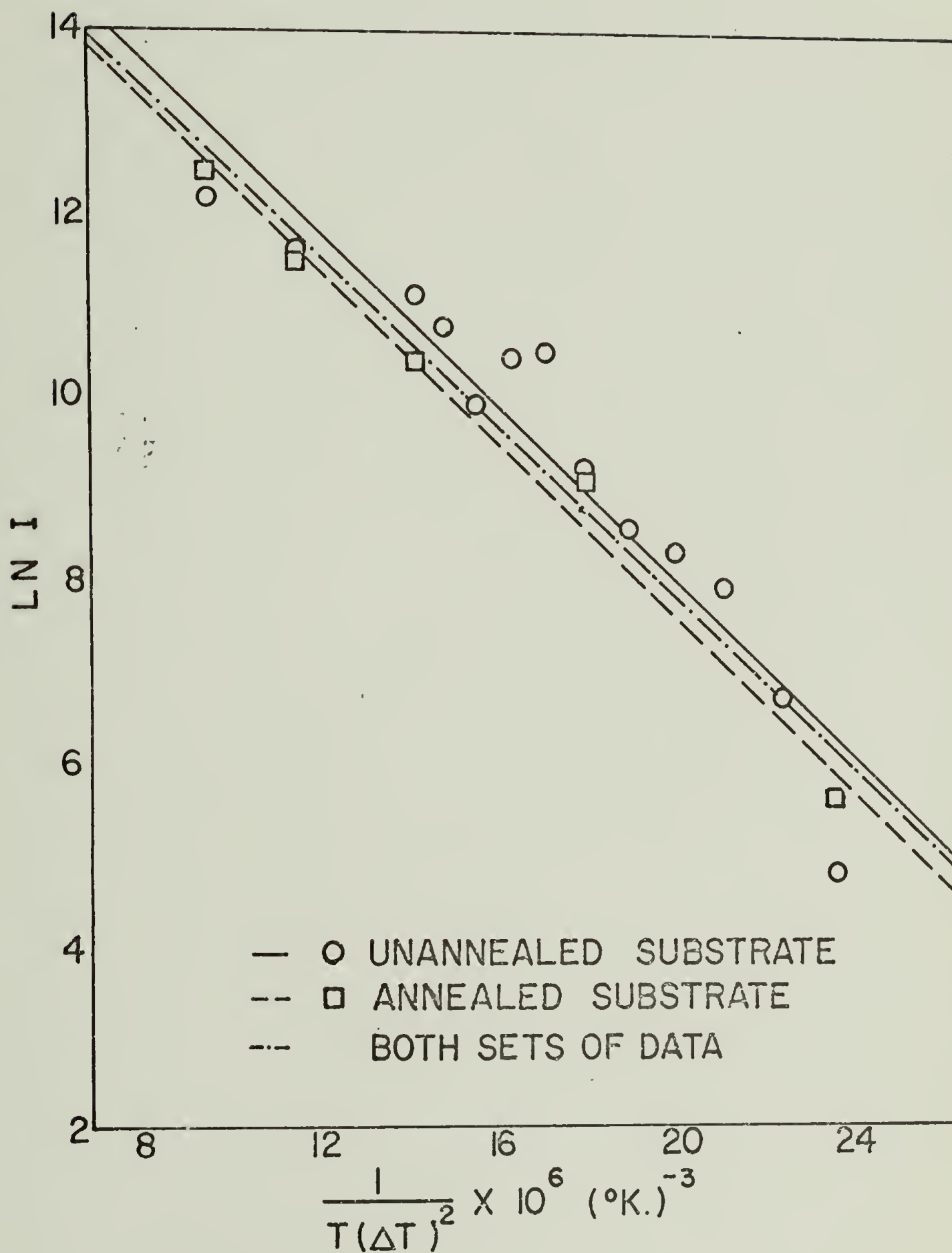


FIGURE 23

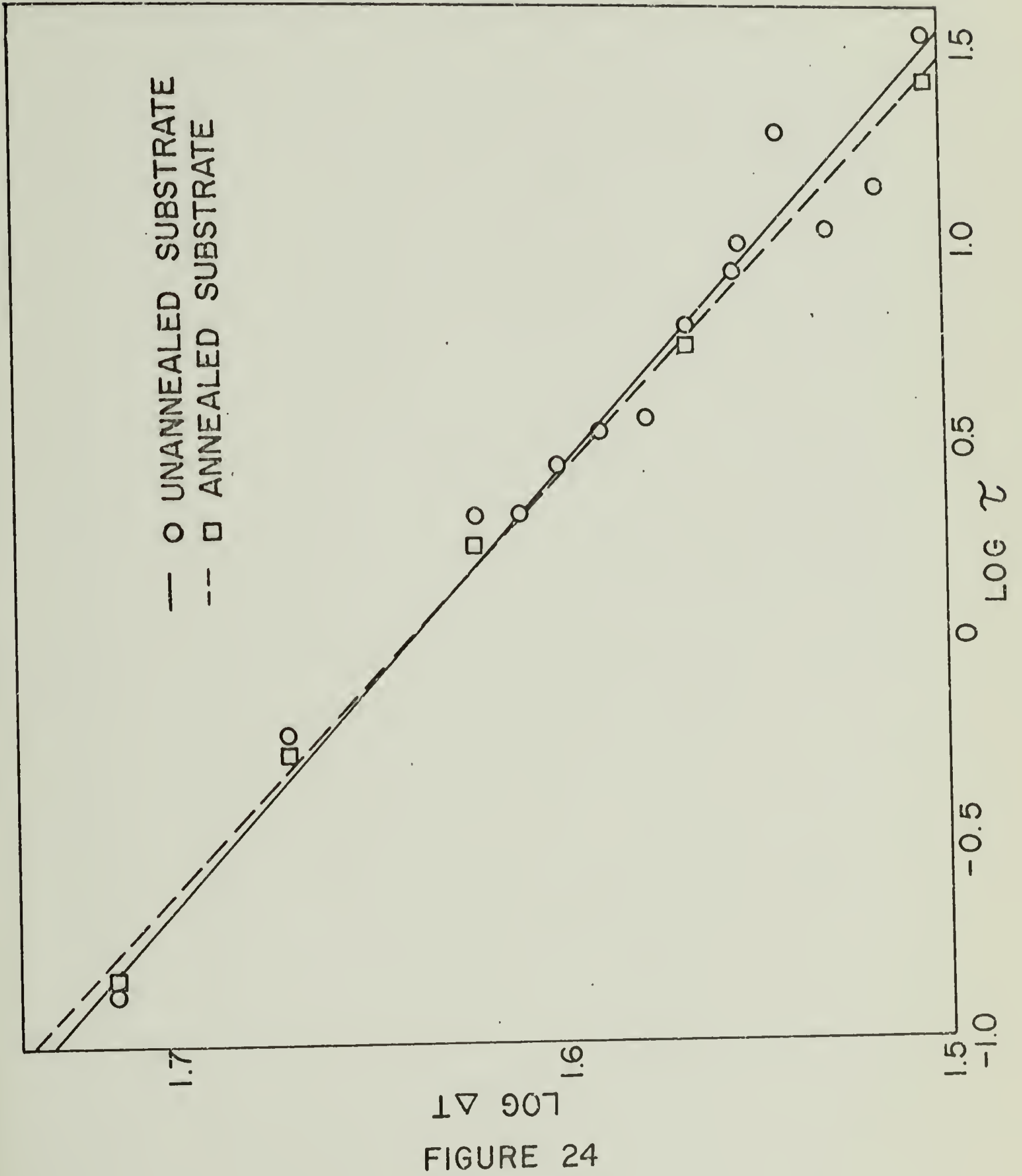


FIGURE 24

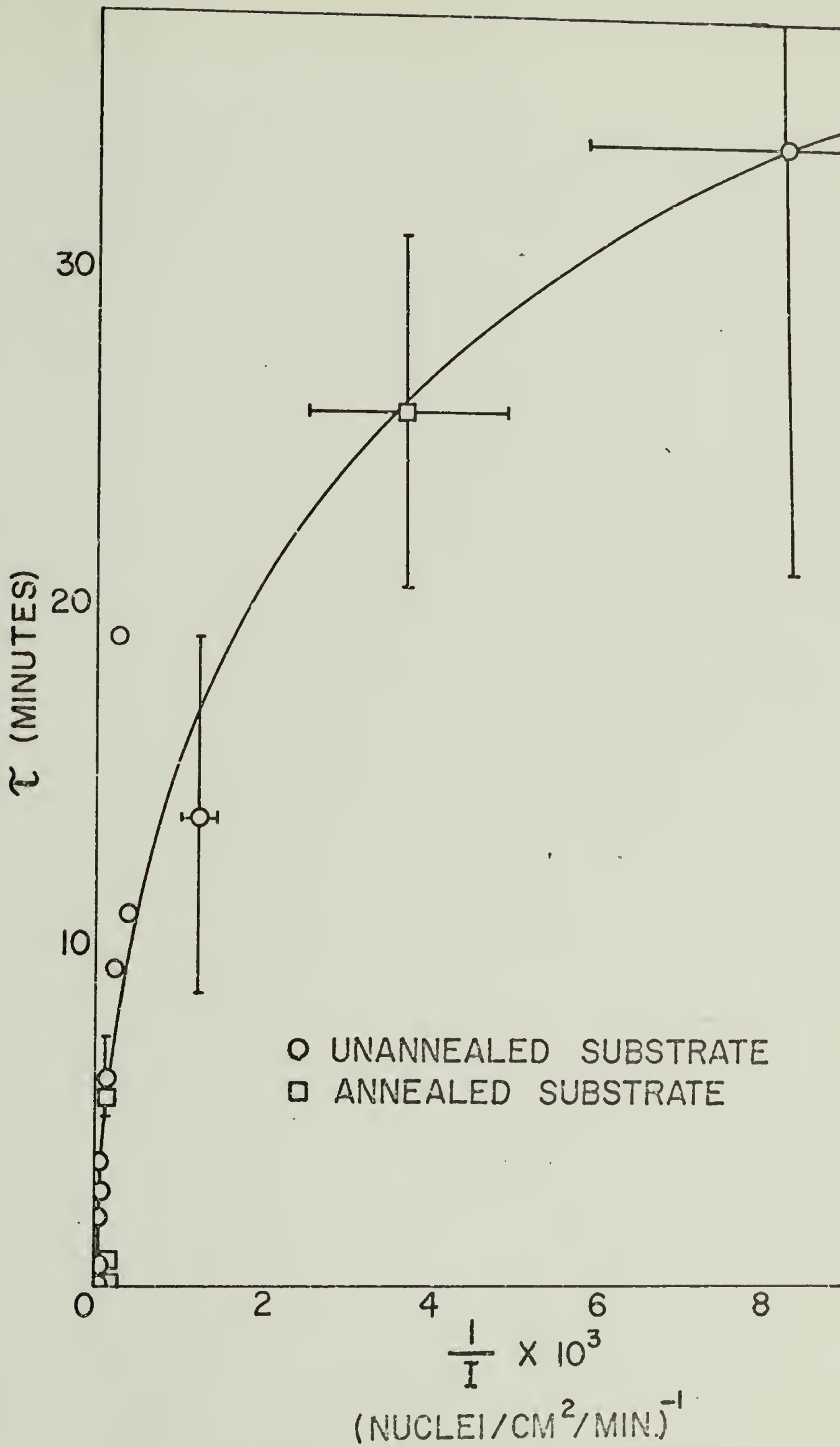


FIGURE 25

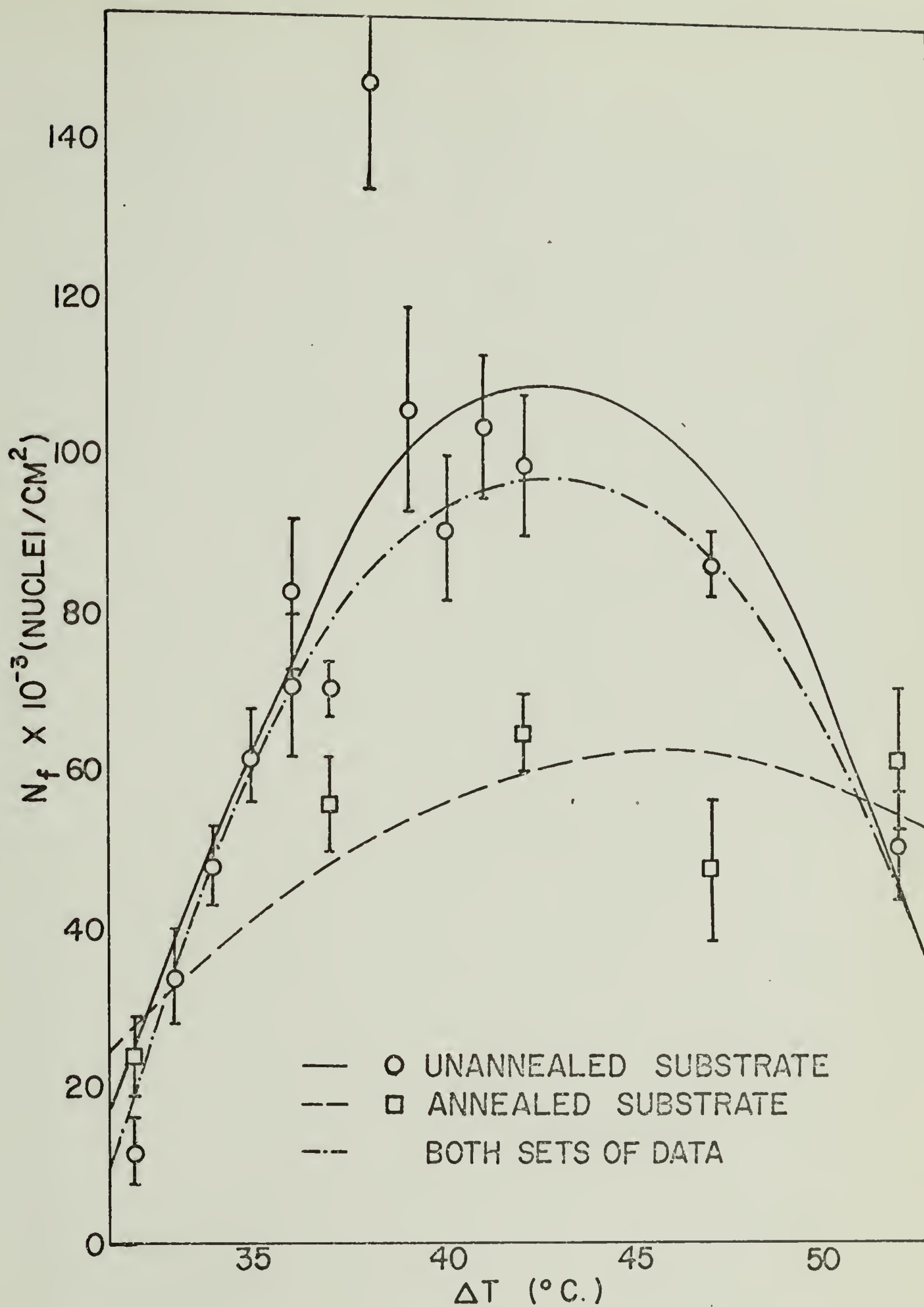
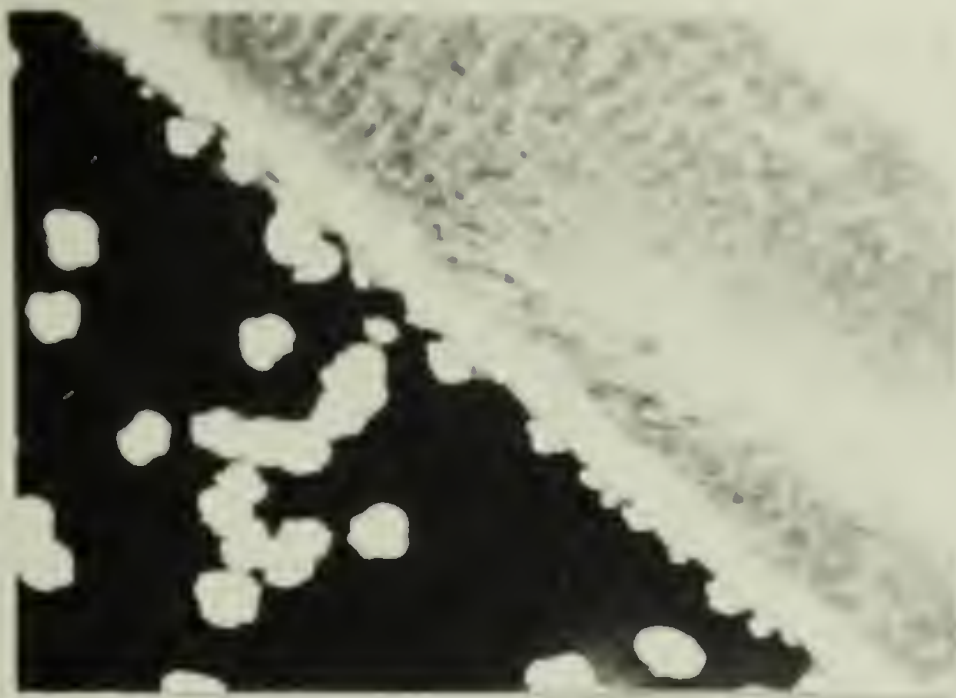
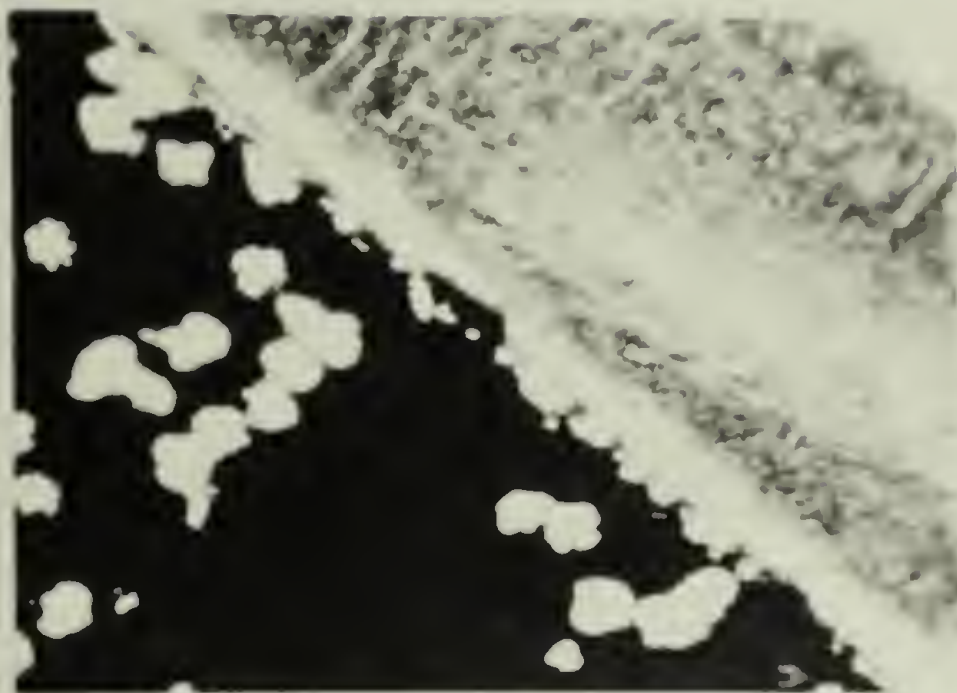


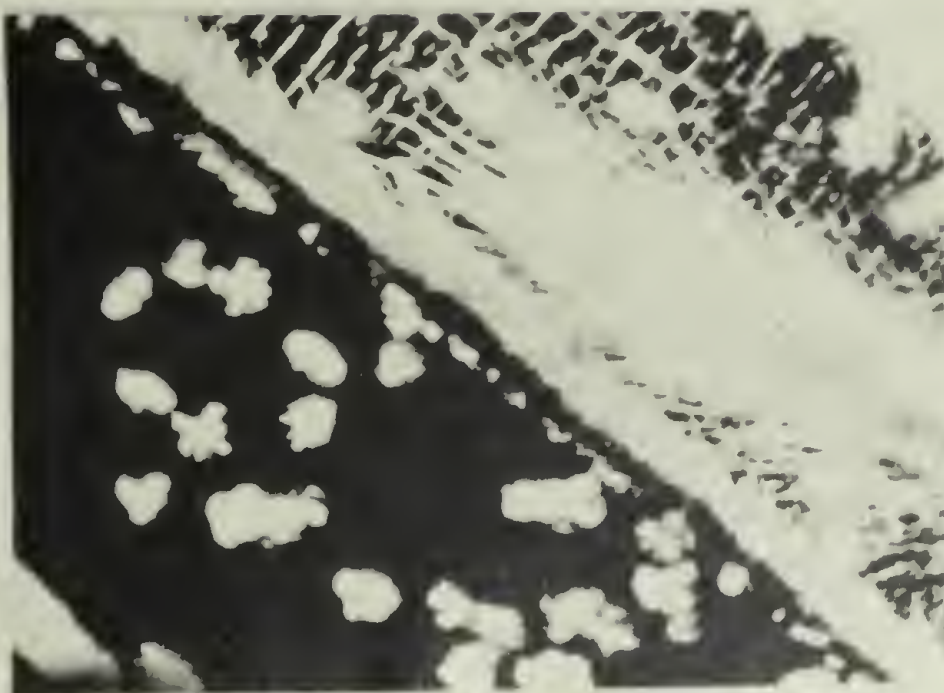
FIGURE 26



c

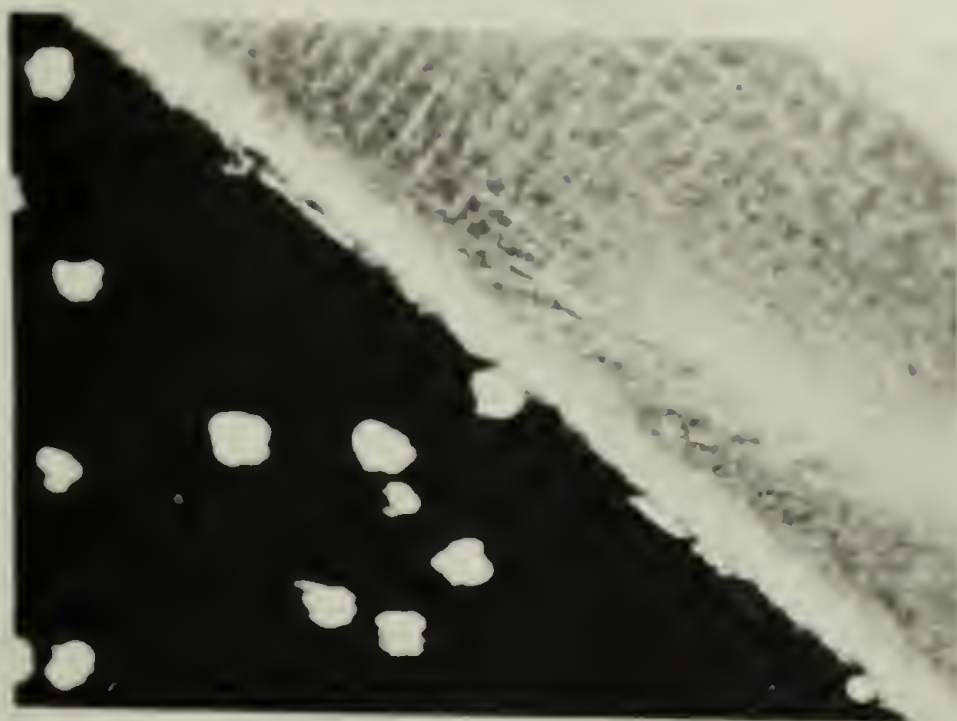


b

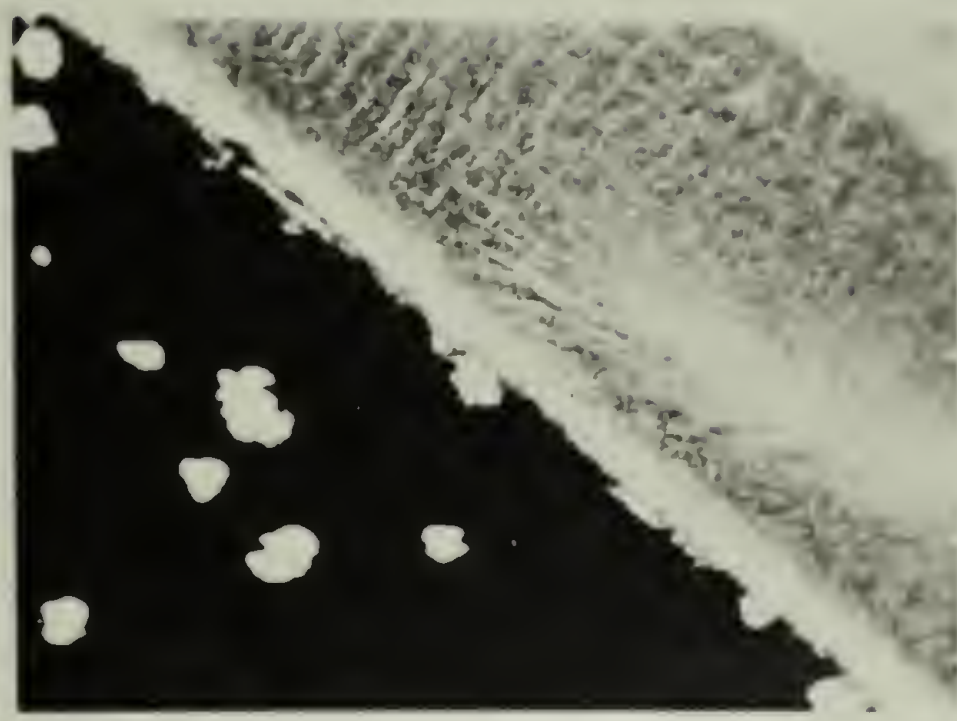


a

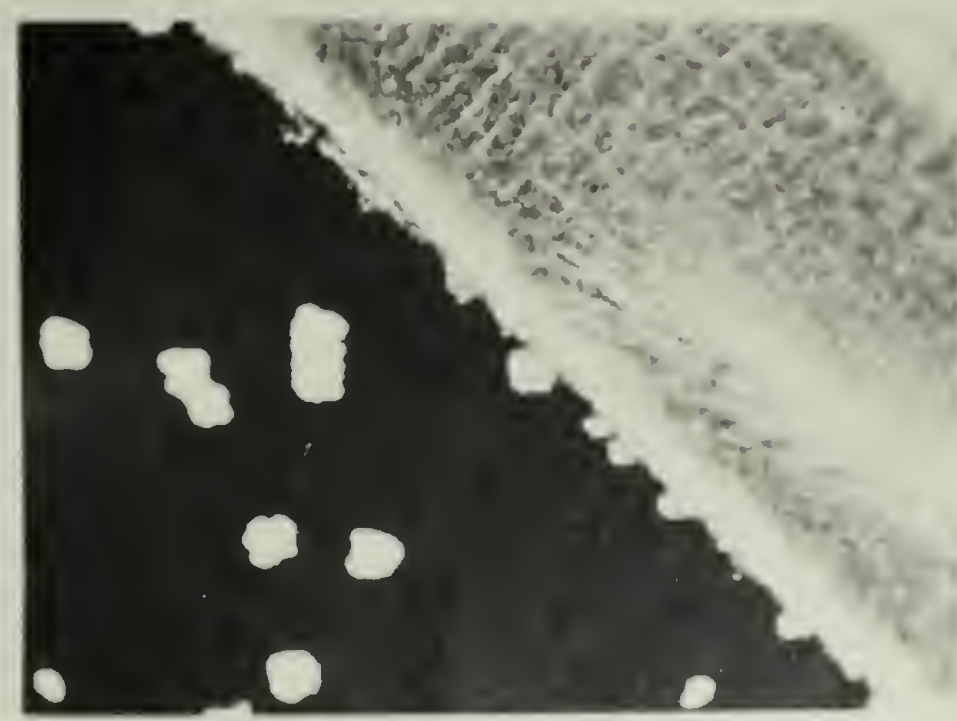
FIGURE 27



f



e



d

FIGURE 27

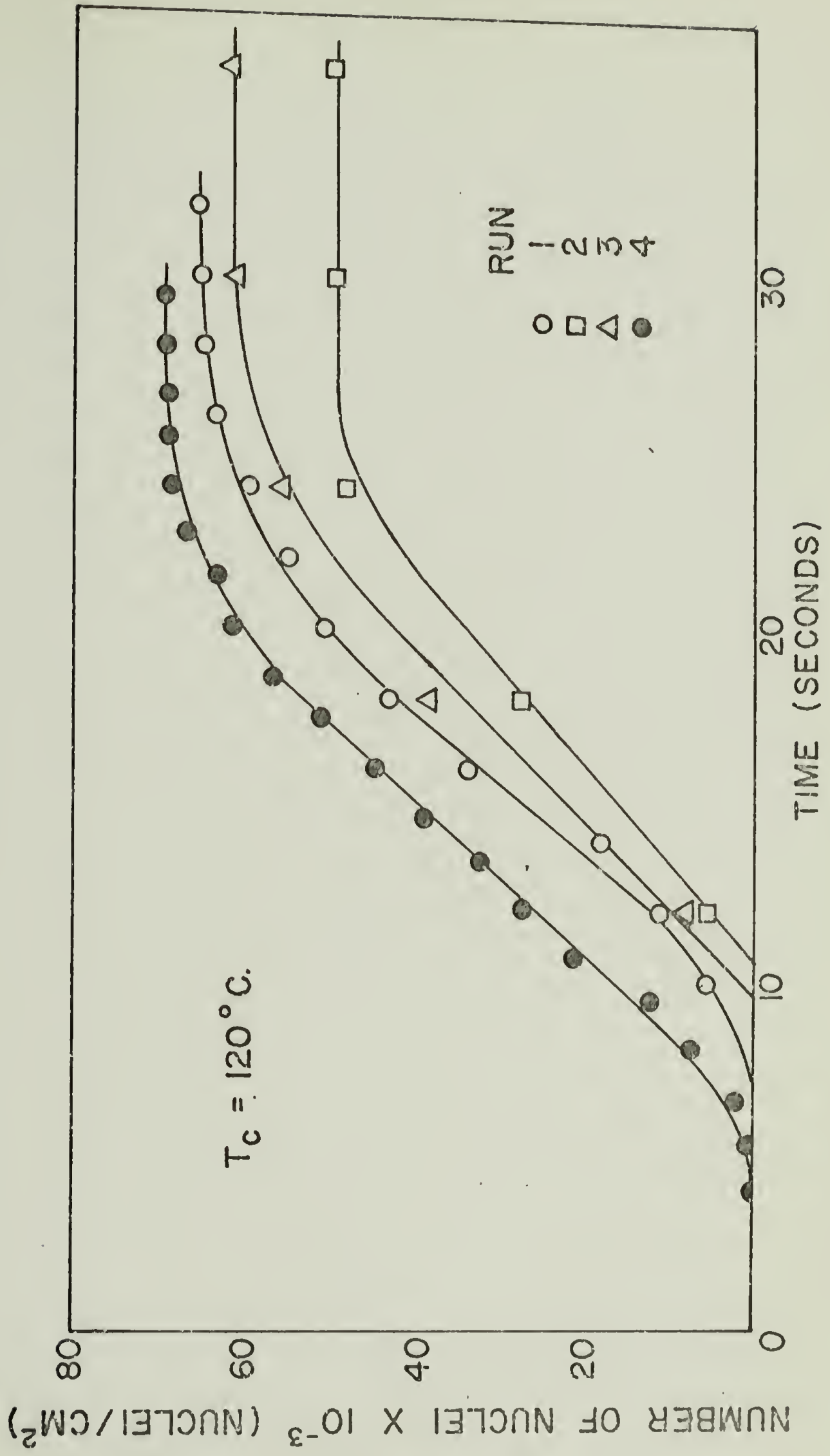


FIGURE 28

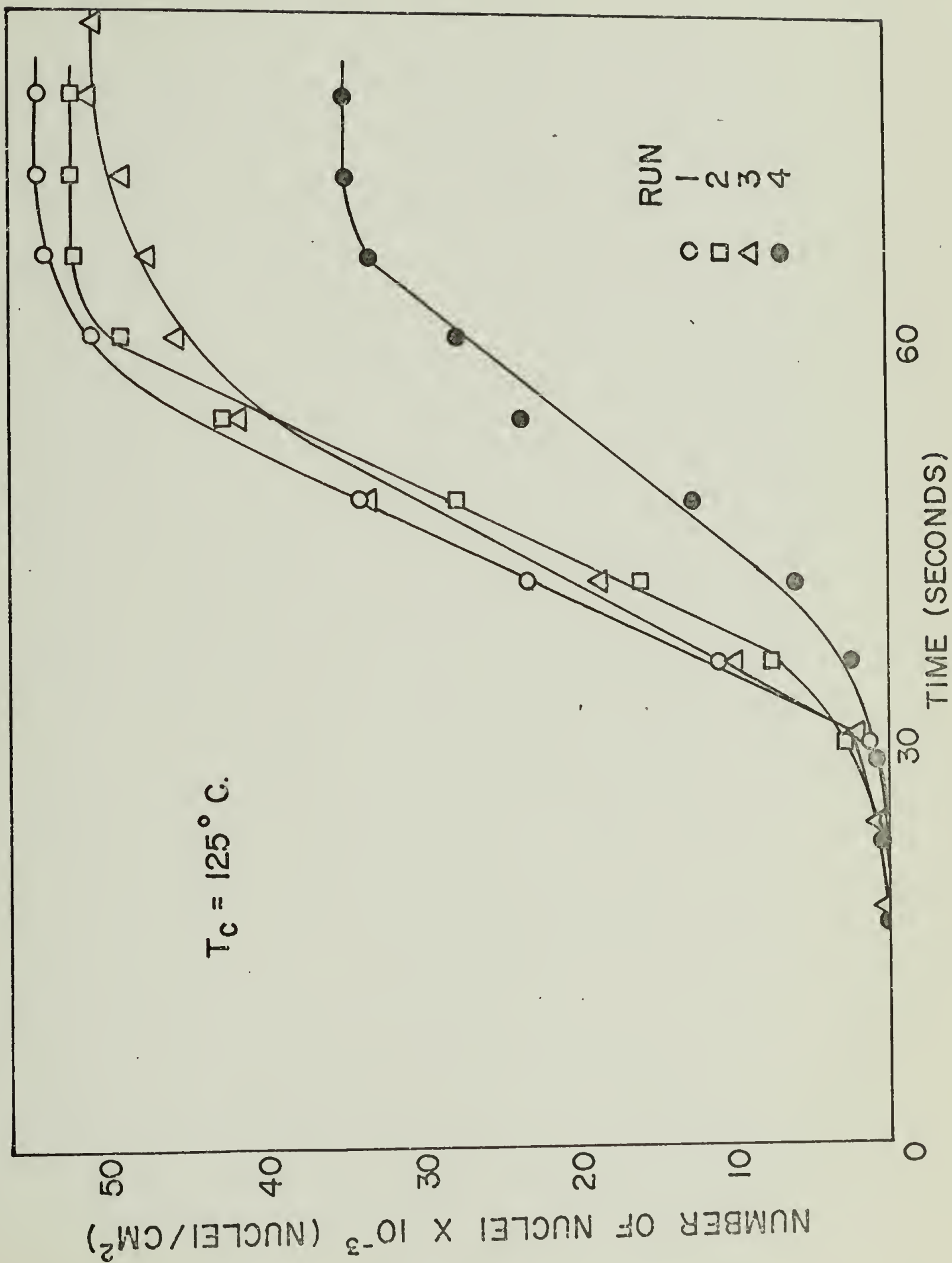


FIGURE 29

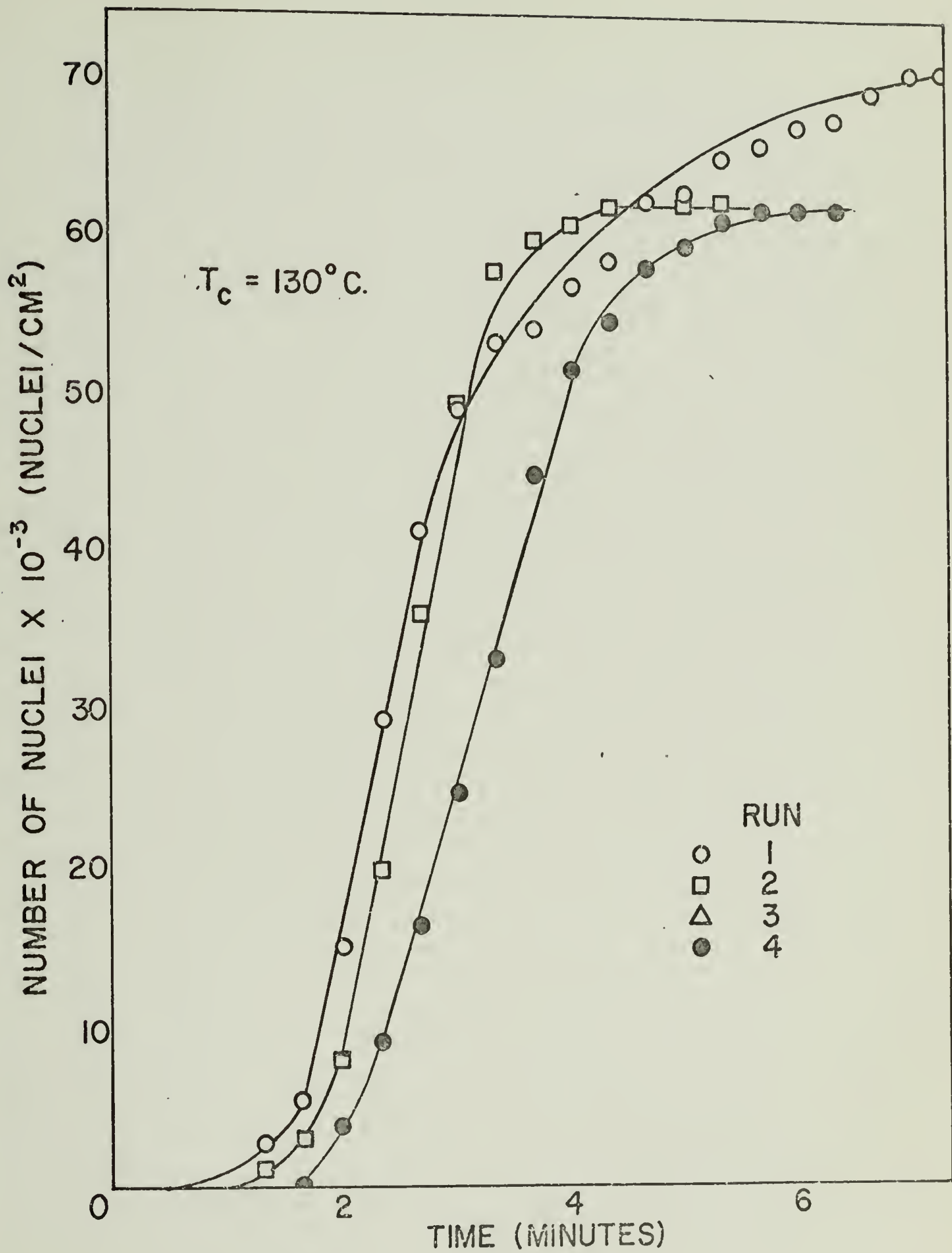


FIGURE 30

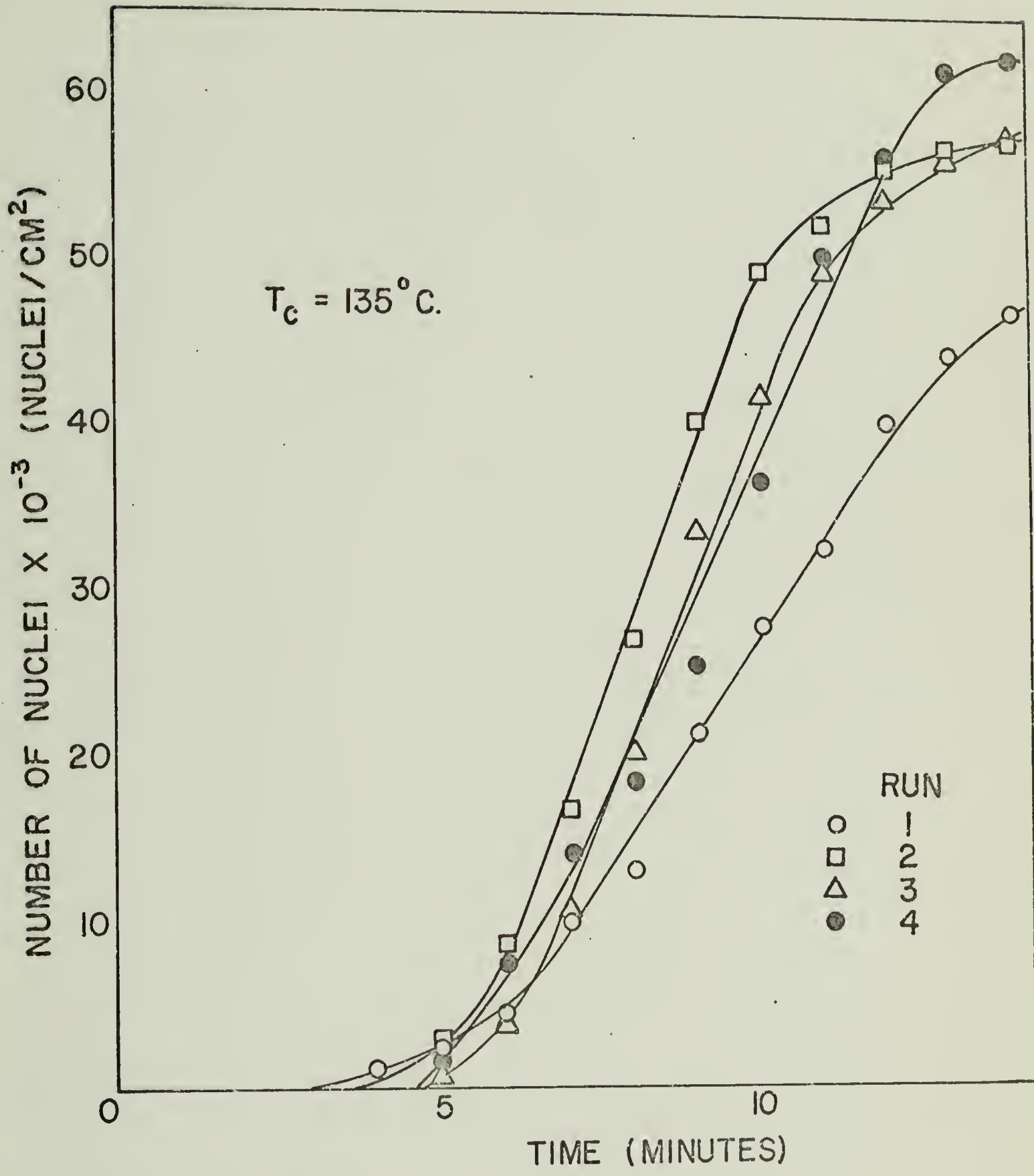


FIGURE 31

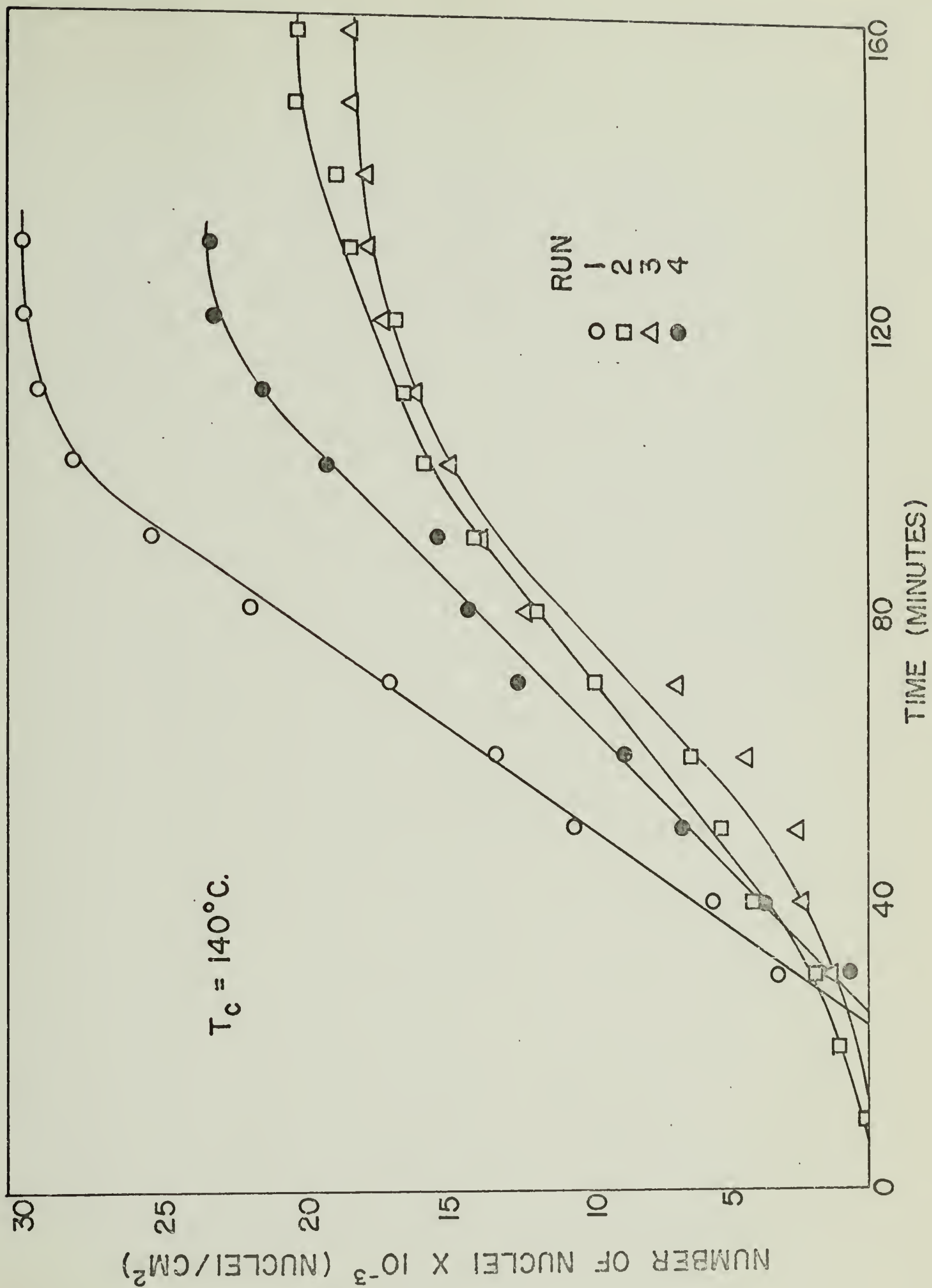


FIGURE 32

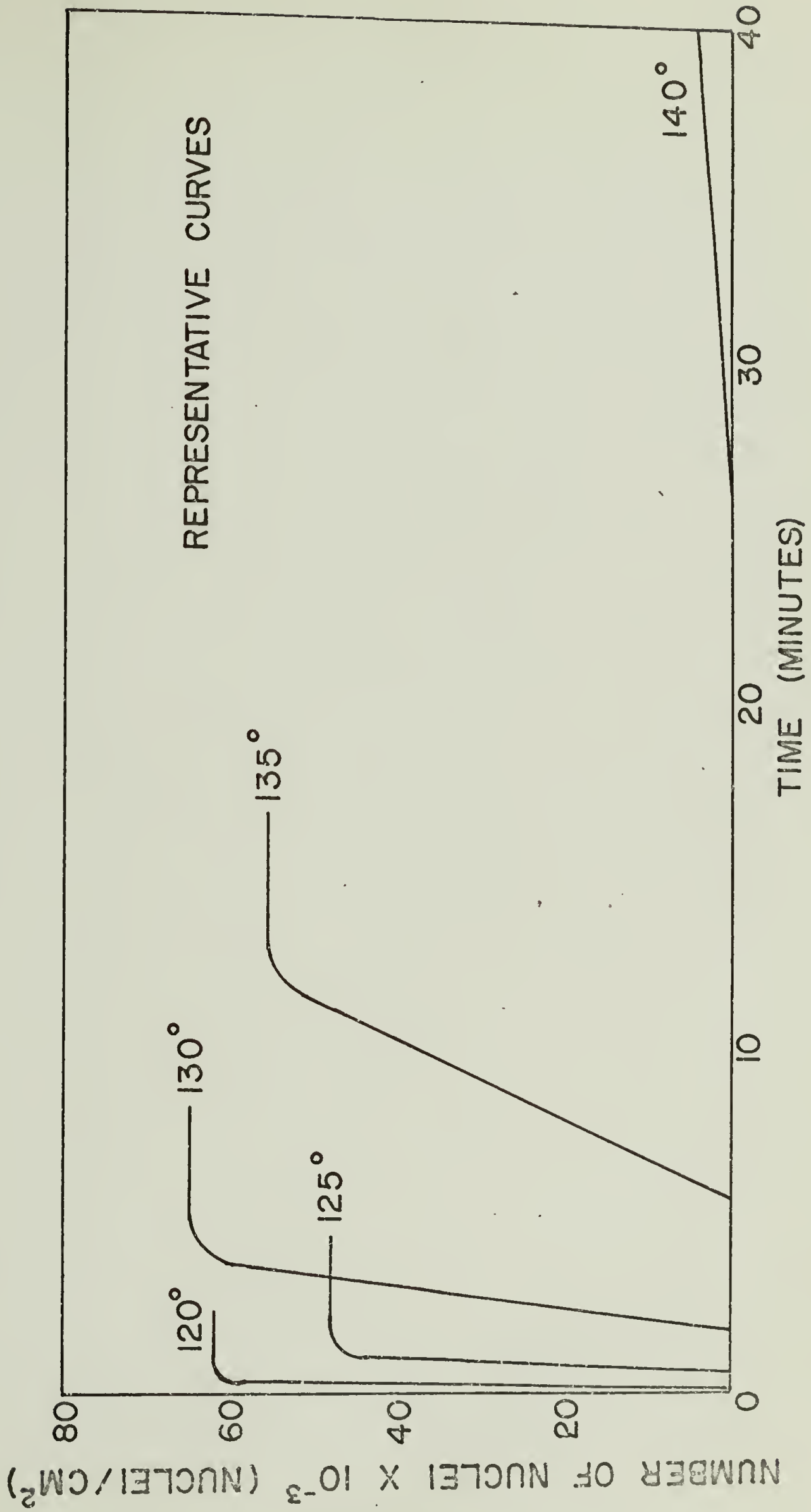


FIGURE 33

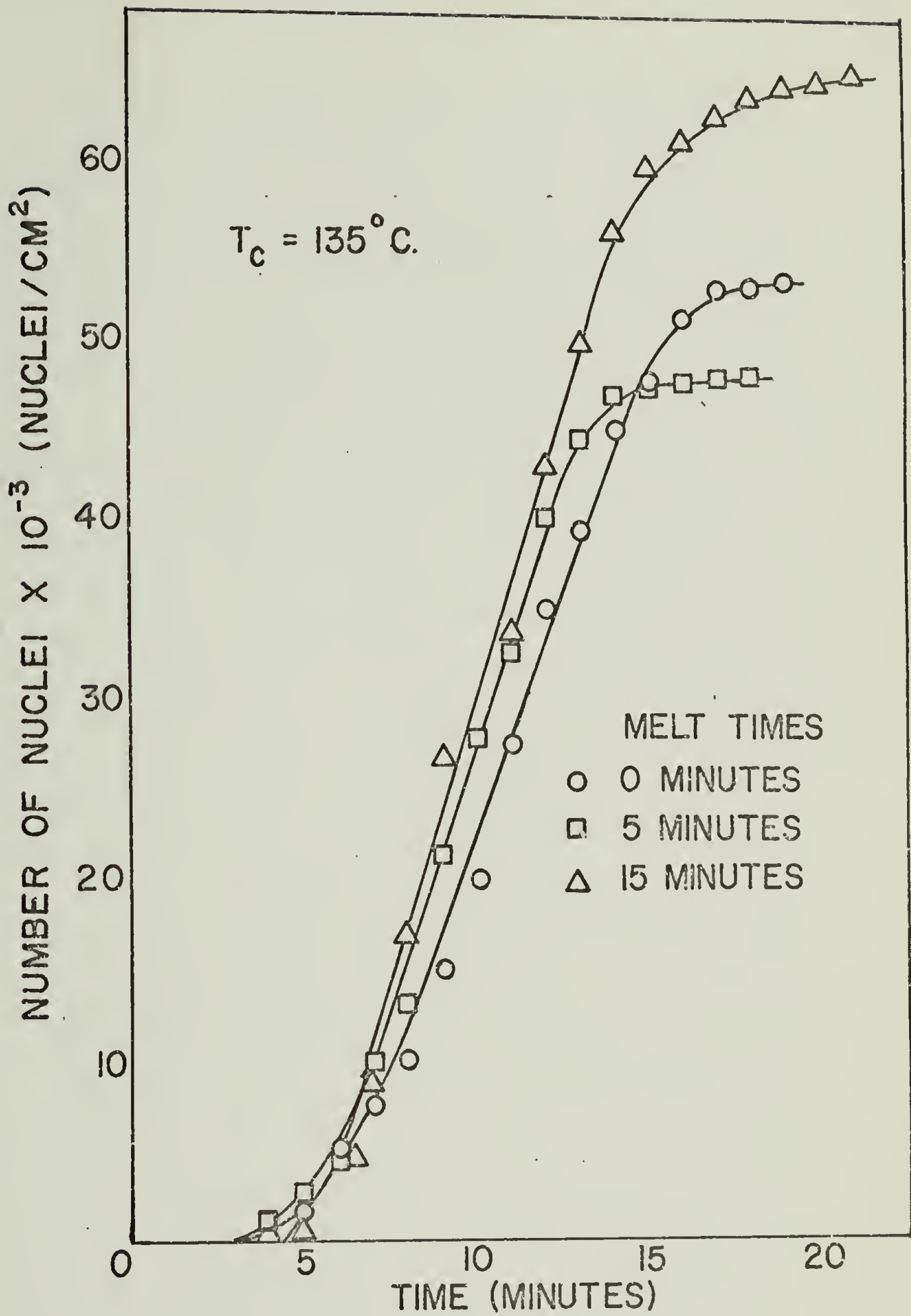


FIGURE 34

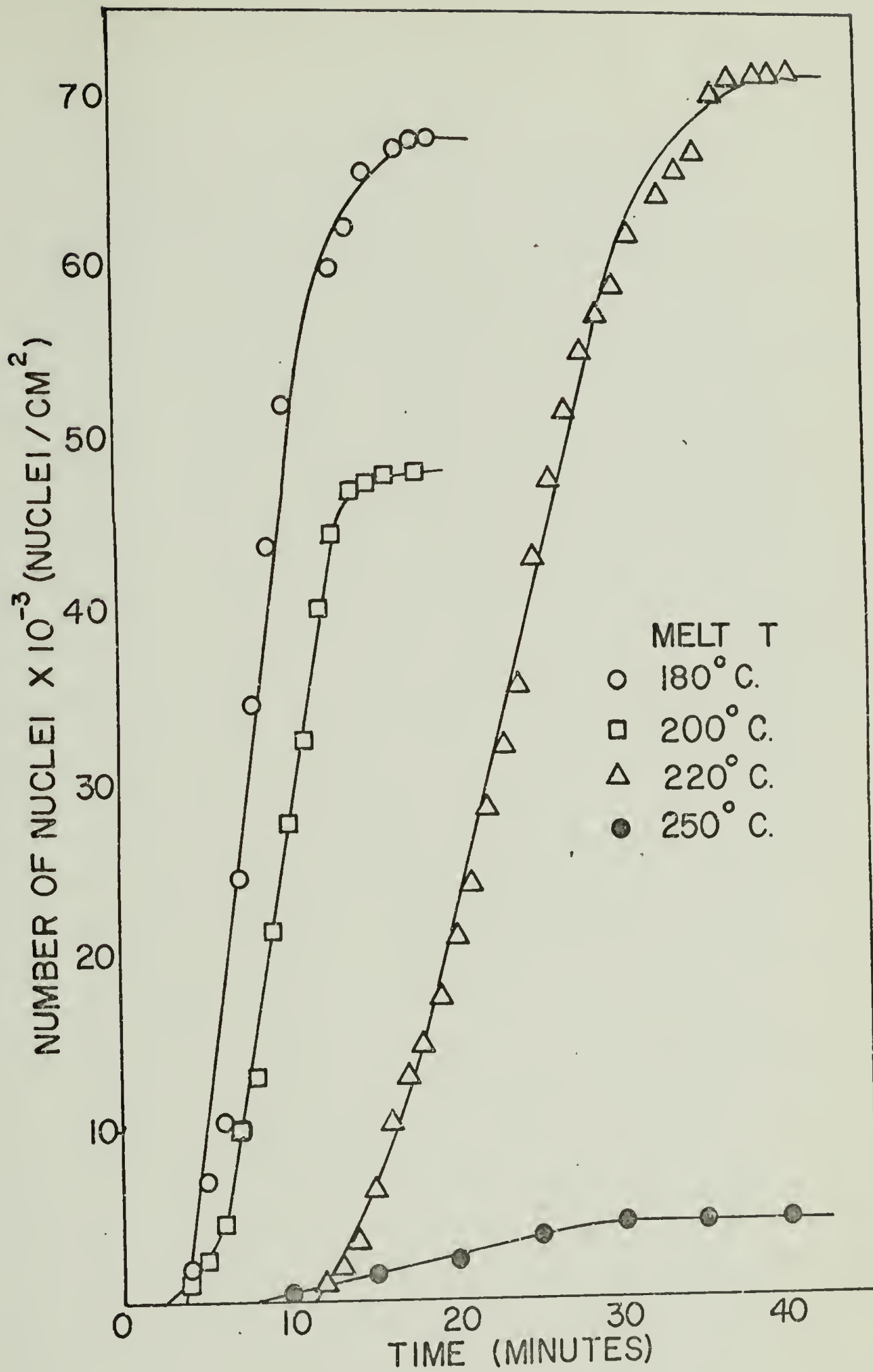
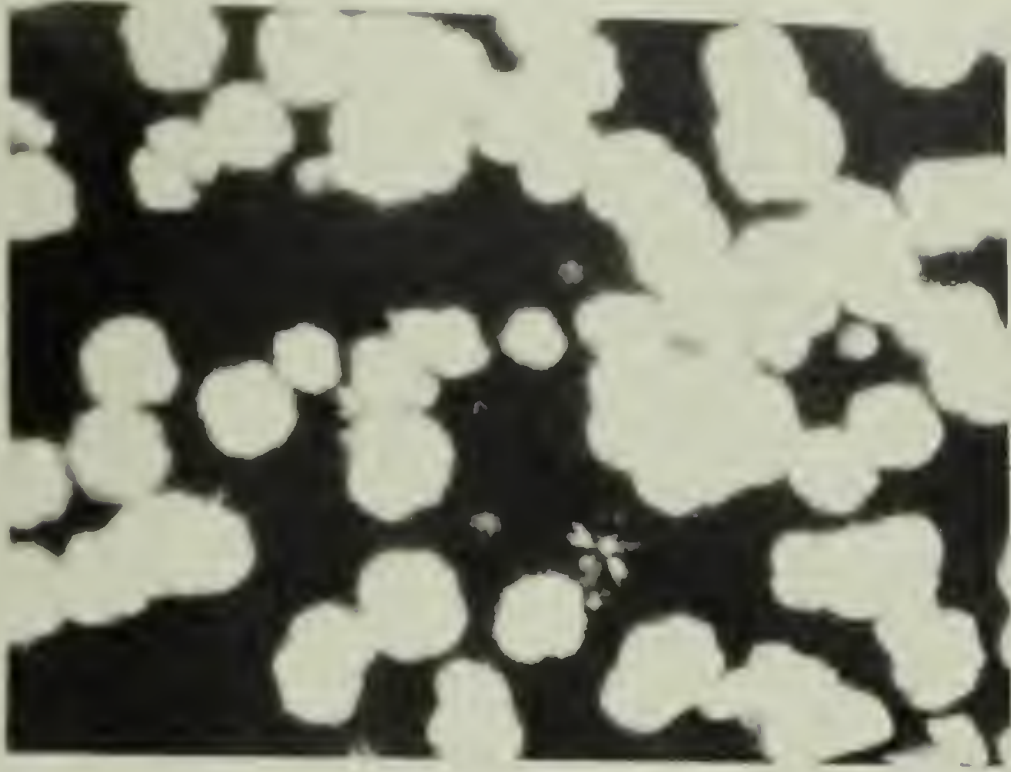
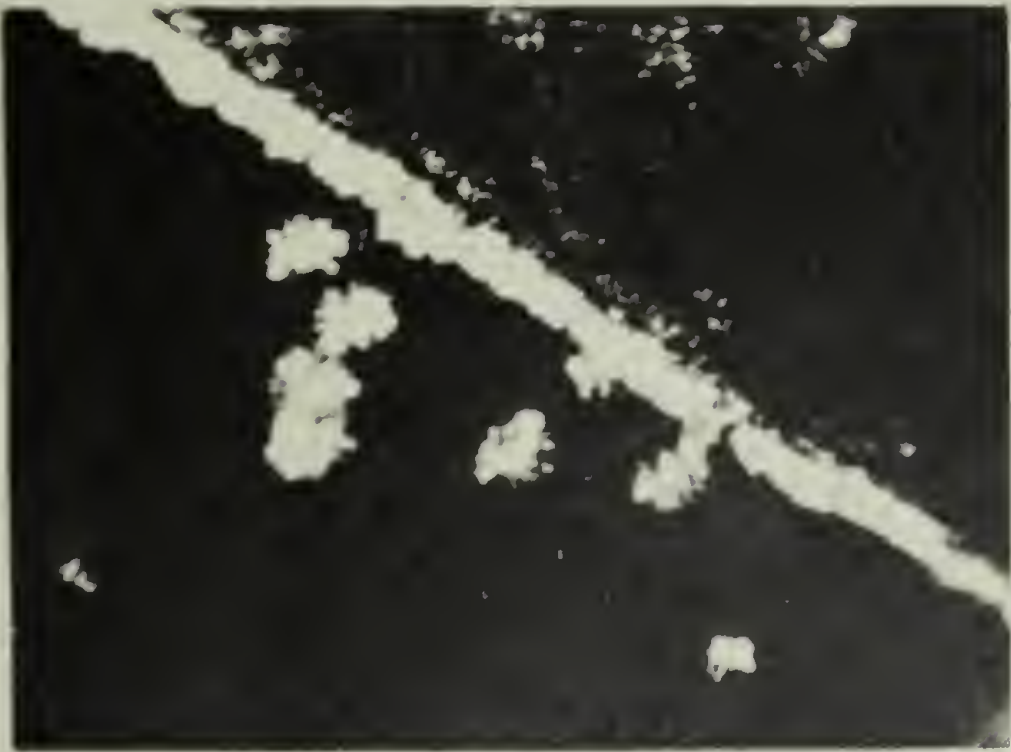


FIGURE 35



b



d

FIGURE 36

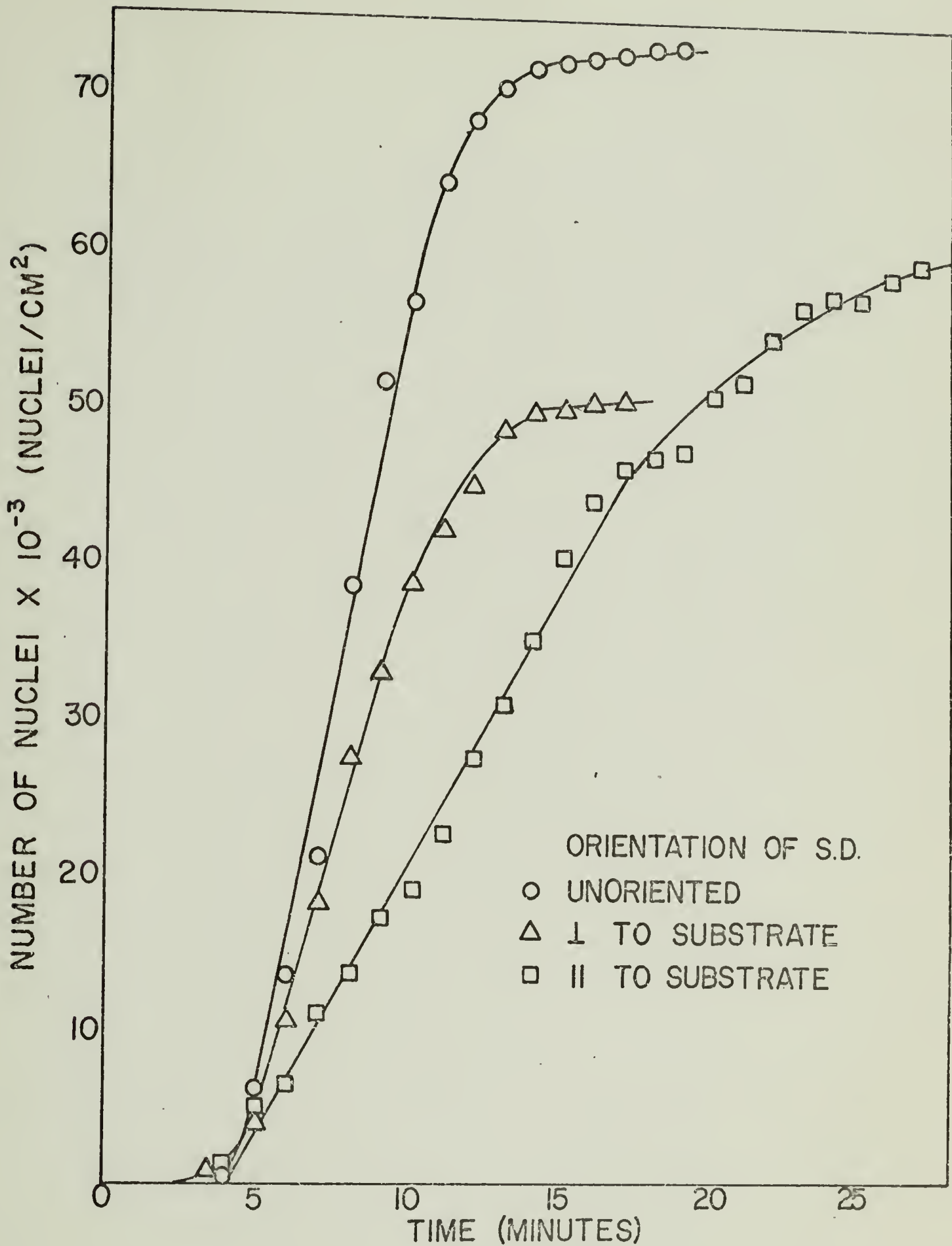


FIGURE 37

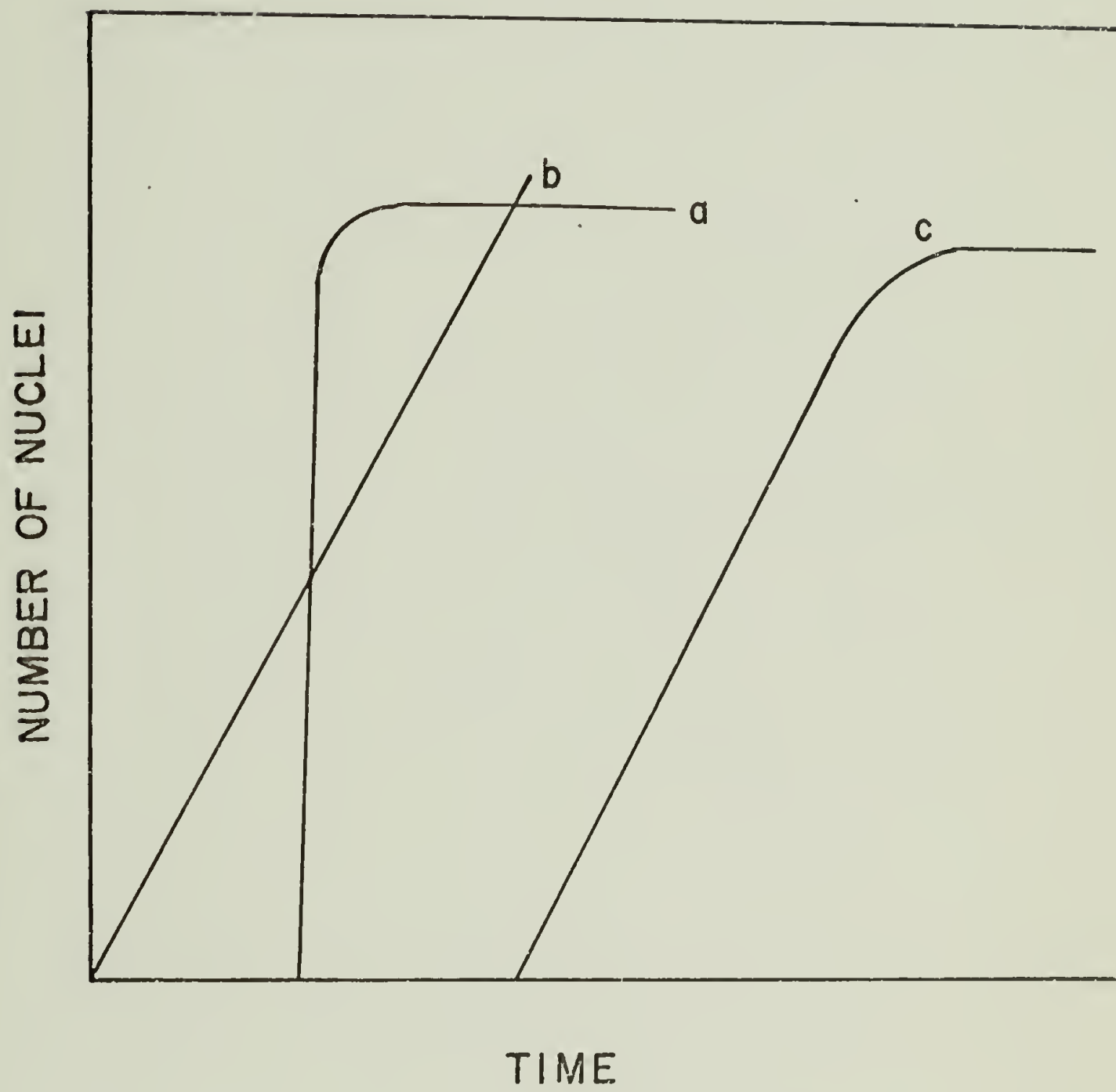


FIGURE 38

```
LIST
10 PROGRAM NUCLEI
20 INPUT, K, L, Z, W
35 DIMENSION N(40, 5), NS(40), S(40), AVE(40), ANORM(40), A(40, 5), C(40, 5)
36C, D(40, 5), E(40), STD(40), EL(40), DNORM(40)
40 PRINT 45
45 FORMAT(/, *AVERAGE N*, 6X, *NORMALIZED N*, 6X, *STANDARD DEVIATION*,
46C 6X, *PROBABLE ERROR*)
50 X=K-1
55 Y=K
60 I=0
70 I=I+1
80 READ, (N(I, J), J=1, K)
90 NS(I)=0
100 DO 120 J=1, K
110 NS(I)=NS(I)+N(I, J)
120 CONTINUE
125 S(I)=NS(I)
130 AVE(I)=S(I)/Y
131 ANORM(I)=AVE(I)/((Z*2.54)*(W/235.))
135 E(I)=0.
140 DO 190 J=1, K
150 A(I, J)=N(I, J)
160 C(I, J)=AVE(I)-A(I, J)
170 D(I, J)=C(I, J)**2
180 E(I)=E(I)+D(I, J)
190 CONTINUE
200 E(I)=E(I)/X
210 STD(I)=SQRT(E(I))
225 DNORM(I)=(STD(I)+.1*AVE(I))/((Z*2.54)*(W/235.))
226 EL(I)=DNORM(I)*.6745
230 PRINT 240, AVE(I), ANORM(I), STD(I), EL(I)
240 FORMAT(1X, F6.2, 10X, F6.2, 17X, F5.2, 17X, F5.2)
250 IF(I.EQ.L) 260, 70
260 END
270 EN
STOP
```